Scuola Internazionale Superiore di Studi Avanzati - Trieste

Exploring the space of many-flavor QED's in $2 < d < 6$

Candidate : Hrachya Khachatryan
Supervisors : Francesco Benini, Sergio Benvenuti

Academic Year 2018 – 2019

SISSA - Via Bonomea 265 - 34136 TRIESTE - ITALY

Abstract

We study many-flavor Quantum Electrodynamics (QED) in $2 < d < 6$. In the first chapter we review and summarise our results. In the second chapter we consider QED's in three dimensions, with N_f fermionic or bosonic flavors, allowing for interactions that respect the global symmetry $U(N_f/2)^2$. There are four bosonic and four fermionic fixed points, which we analyze using the large N_f expansion. We systematically compute, at order $O(1/N_f)$, the scaling dimensions of quadratic and quartic mesonic operators. We also consider three dimensional QED with minimal supersymmetry. In this case the large N_f scaling dimensions extrapolated at $N_f = 2$, agree quite well with the scaling dimensions of a dual supersymmetric Wess-Zumino model. This provides a quantitiative check of the conjectured duality.

In the third chapter, we analyze the fate of the non-supersymmetric QED's for small values of N_f. Large N_f arguments suggest that, lowering N_f, the fixed points collide pairwise, which leads the fixed points either to merge and to annihilate into the complex plane, or to pass through each other, exchanging their stability properties. In the bosonic QED's the merging happens around $N_f \sim 9 - 11$. In the fermionic QED's collision happens around $N_f \sim 3 - 7$. In the fermionic case, the fixed points with different symmetries are colliding.

In the last chapter we consider the $\mathbb{CP}^{(N_f-1)}$ Non-Linear-Sigma-Model in the dimension $4 < d < 6$. The critical behaviour of this model in the large N_f limit is reviewed. We propose a Higher Derivative Gauge (HDG) theory as an ultraviolet completion of the $\mathbb{CP}^{(N_f-1)}$ NLSM. Tuning mass operators to zero, the HDG in the IR limit reaches to the critical $\mathbb{CP}^{(N_f-1)}$. With partial tunings the HDG reaches either to the critical $U(N_f)$-Yukawa model or to the critical pure scalar QED (no Yukawa interactions).

We renormalize the HDG in its critical dimension $d = 6$. We study the fixed points of the HDG in $d = 6-2\epsilon$ and we calculate the scaling dimensions of various observables finding a full agreement with the order $O(1/N_f)$ predictions of the corresponding critical models.

The present PhD thesis is based on the following papers:

1. S. Benvenuti and H. Khachatryan, "Easy-plane QED_3's in the large N_f limit," JHEP **1905** (2019) 214 [arXiv:1902.05767].

2. S. Benvenuti and H. Khachatryan, "QED's in 2+1 dimensions: complex fixed points and dualities," [arXiv:1812.01544].

3. H. Khachatryan, "Higher Derivative Gauge theory in $d = 6$ and the $\mathbb{CP}^{(N_f-1)}$ NLSM," [arXiv:1907.11448].

Contents

1 Introduction and Summary **4**

2 Easy-plane QED$_3$'s in the large N_f limit **19**

2.1 Four bosonic QED fixed points in the large N_f limit 19

2.1.1 bQED (tricritical QED) 21

2.1.2 bQED$_+$ ($\mathbb{CP}^{N_f-1}$ model) 26

2.1.3 ep-bQED ("easy-plane" QED) 29

2.1.4 bQED$_-$ 32

2.2 Four fermionic QED fixed points in the large N_f limit 35

2.2.1 fQED 36

2.2.2 QED-GN$_+$ 37

2.2.3 QED-NJL 41

2.2.4 QED-GN$_-$ 44

2.3 Super-QED in the large N_f limit 45

2.3.1 Scaling dimension of low-lying mesonic operators 47

2.3.2 The duality $\mathcal{N}$=1 SQED with N_f=2 $\leftrightarrow$ 7-field Wess-Zumino model: a quantitative check 49

2.3.3 The $\mathcal{N}=1$ supersymmetric $O(N)$ sigma model and $\mathcal{N}=2$ SQED . . 50

3 QED's in $2+1$ dimensions and Complex CFT's **54**

3.1 Bosonic QED 55

3.2 Fermionic QED 61

4 Higher Derivative Gauge theory in $d = 6$ and the $\mathbb{CP}^{(N_f-1)}$ NLSM **66**

4.1 Large N_f expansion of the critical $\mathbb{CP}^{(N_f-1)}$ NLSM 66

4.2 Higher Derivative Gauge theory in $d = 6$ 71

4.3 Renormalization of fields and cubic vertices: anomalous dimensions of fields and beta functions 74

4.4 Renormalization of the mass parameters and the anomalous dimensions of the quadratic operators 84

A Bosonic QED's in the $4 - 2\epsilon$ expansion **89**

B Useful formulae **92**

C Feynman graphs **94**

D Scaling dimensions of monopole operators in $\mathcal{N} = 1$ SQED **97**

Chapter 1

Introduction and Summary

This thesis is organised into three chapters. Below we give a short summary and a review of each chapter.

Easy-plane QED$_3$'s in the large N_f limit

Quantum Electrodynamics (QED) in 2+1 dimensions, with fermionic and/or bosonic flavors, is a prime example of interacting Quantum Field Theory, with both theoretical and experimental relevance. We study QED's in the limit of large number of flavors, the large N_f limit, where perturbation theory allows to find quantitative results.

Our goal is to define and study models that admit a tractable large N_f expansion but at the same time might be realistic when the number of flavors is small. For this reason we consider an even number of flavors and allow for interactions that respect at least $U(N_f/2)^2$ global symmetry, instead of the usual $U(N_f)$. We use the name "easy plane" QED's because for N_f=2, one of the bosonic fixed points is the "easy-plane" $\mathbb{CP}^1$ model. Together with $SU(2)$-$\mathbb{CP}^1$ model it describes the Néel — Valence Bond Solid (VBS) quantum phase transition in the $SU(2)$ and XY antiferromagnets [1, 2, 3]. The Néel — VBS and the Superfluid — VBS phase transitions are examples of phenomena known as Deconfined Quantum Critical Points. The fermionic QED's with small flavor number are also important for physical applications. In particular the $N_f = 4$ pure fermionic QED[1] (no Yukawa interactions) describes the non-superconducting phase of the high-T_c superconducting cuprate compounds [4, 5]. Additionally non-trivial infrared dualities hold between the $N_f = 2$ fermionic and the $N_f = 2$ bosonic QED's [6, 7, 8].

[1] In the fermionic QED's by N_f we denote the number of 2-component Dirac fermions.

We find four bosonic (bQED, bQED$_+$, ep-bQED, bQED$_-$) and four fermionic (fQED, QED-GN$_+$, QED-NJL, QED-GN$_-$) fixed points[2]. The various models differ by the form of the quartic interactions, which in the large N_f limit are modelled introducing one or two Hubbard-Stratonovich scalar fields, see pages (19) and (35) for more details about the fixed points. In each of the 8 models we systematically compute the anomalous dimensions of all the scalar (mesonic) operators that at the leading order in N_f have small scaling dimension (Δ=1 or Δ=2). Some operators are quadratic or quartic in the charged fields, some are linear or quadratic in the Hubbard-Stratonovich fields. We work at the next-to-leading order in the large N_f expansion, $O(1/N_f)$, providing many details of the computations, including results for all individual Feynman diagrams.

Studying quantum field theories in the large N_f limit has been proved to be useful in different circumstances. In 2+1d the large N_f limit has recently been applied to calculate scaling dimensions of monopole operators, S^3 partition functions and central charges [9, 10, 11, 12, 13, 14, 15, 16]. We believe that it would be interesting to generalize these computations to the "easy-plane" models described in the chapter 2.

After discussing QED's with bosonic flavors in section 2.1 and QED's with fermionic flavors in section 2.2 we, move to QED with minimal supersymmetry, $\mathcal{N} = 1$. In section 2.3 we compute the scaling dimensions of bilinear and quartic mesonic operators. We also include the large N_f dimensions of monopole operators from [14]. $\mathcal{N} = 1$ QED with $N_f = 2$ is supposed to be dual to a supersymmetric Wess-Zumino model [17, 18], which can be studied quantitatively in the $4 - \epsilon$ expansion [18]. We compare the large N_f results on the gauge theory side of the duality with the $4 - \epsilon$ results on the supersymmetric Wess-Zumino side of the duality, and we find good quantitative agreement, providing a check of the conjectured $\mathcal{N} = 1$ duality.

As a prelude to chapter 2, here we discuss the large flavor limit of the $O(N)$ vector model. Although ultimately we are interested in gauge theories, the $O(N)$ vector model is a good laboratory to introduce some of the concepts and tools that we will need later for studying 3-dimensional gauge theories.

Let us introduce the $O(N)$ model with N real scalar fields ϕ_i in d-dimension

$$S_{O(N)} = \int d^d x \Big[\frac{1}{2} (\partial_\mu \phi_i)^2 + \lambda \big(\sum_{i=1}^{N} \phi_i^2 \big)^2 \Big] \ . \tag{1.1}$$

Notice that the mass term $\tau \sum_{i=1}^{N} \phi_i^2$ is tuned to zero or equivalently the temperature T is tuned

[2]In the literature the fixed point bQED$_+$ is known as Abelian Higgs or $\mathbb{CP}^{(N_f-1)}$ model, the bQED is known as tricritical scalar QED [48, 73, 74] and the QED-GN$_-$ is known simply as QED-GN [77, 89] .

to its critical value T_c ($\tau = \frac{T-T_c}{T_c} \to 0$). In $2 < d < 4$ the relevant quartic deformation (1.1) drives the theory to a Wilson-Fisher fixed point, where the physical observables are expected to have a power-law behaviour with some non-trivial critical exponents. In d=3, the following special cases: the $N = 1$ Ising model, the $N = 2$ XY magnet and the $N = 3$ Heisenberg magnet are very important in statistical physics in the context of phase transitions. For small values of N it is extremely difficult to analytically study the critical point (second order phase transition). However, as we will see, when N is large the $O(N)$ vector model becomes solvable.

First, with the help of Hubbard-Stratonovich (HS) transformation one is trading the quartic interaction with cubic and quadratic terms. The partition function of the vector model after HS transformation is as follows

$$\mathcal{Z}_{O(N)} = \int \big[\mathcal{D}\phi_i\big] e^{-S_{O(N)}} = \int \big[\mathcal{D}\phi_i \mathcal{D}\sigma\big] e^{-\int d^d x \left[\frac{1}{2}(\partial\phi_i)^2 + \sigma\phi_i^2 - \frac{\sigma^2}{4\lambda}\right]} \ . \tag{1.2}$$

Inside the exponent, summation over the flavor index i is assumed. The scalar field σ is known as a HS or a master field. Indeed integrating out the HS field in (1.2) we will obtain the partition function of the vector model[3]. So, we conclude that the vector model (1.1) can be described by an equivalent theory

$$S = \int d^d x \big[\frac{1}{2}(\partial\phi_i)^2 + \sigma\phi_i^2 - \frac{\sigma^2}{4\lambda}\big] \ . \tag{1.3}$$

We analyze the 2-point correlation function (i.e. the propagator) of the HS field in the limit $N \to \infty$. The graphs that contribute to the 2-point correlator are the bubble graphs in Fig. 1.1, all the other graphs are $1/N$ suppressed. For a single bubble graph we have

$$N \cdot 2 \int \frac{d^d q}{(2\pi)^d} \frac{1}{q^2 (p-q)^2} = N \frac{2\Gamma(\frac{d}{2}-1)^2 \Gamma(2-\frac{d}{2})}{(4\pi)^{d/2}\Gamma(d-2)} p^{d-4} = N A(d) p^{d-4} \ , \tag{1.4}$$

where the factor N is due to the N scalar flavors circulating inside the closed loop (1.1). The fraction in (1.4) is denoted by $A(d)$. To calculate the integral we used (B.8).

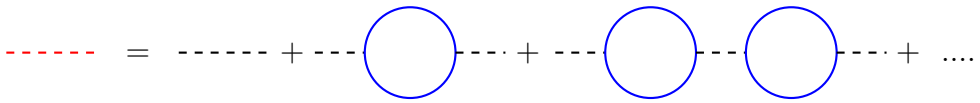

Figure 1.1: HS field σ effective propagator (red dashed line). The black dashed line stands for the tree level HS field propagator and the blue line stands for the scalar field ϕ_i propagator

[3]The path integral (1.2) over the HS field σ is performed along a contour parallel to the imaginary axis. This ensures that the path integral is convergent.

Summing geometric series of the bubble graphs in Fig. 1.1 we obtain

$$\begin{aligned}\langle\sigma(p)\sigma(-p)\rangle &= (-4\lambda) + (-4\lambda)NA(d)p^{d-4}(-4\lambda) + (-4\lambda)\big(NA(d)p^{d-4}(-4\lambda)\big)^2 + ... \\ &= (-4\lambda)\frac{1}{1+4\lambda NA(d)p^{d-4}} \ . \end{aligned} \tag{1.5}$$

Using (1.5), we find in $2 < d < 4$, the effective propagator of the HS field in the IR limit

$$\langle\sigma(p)\sigma(-p)\rangle|_{p\to 0} = (-4\lambda)\frac{1}{1+4\lambda NA(d)p^{d-4}}\bigg|_{p\to 0} = -\frac{p^{4-d}}{NA(d)} \ , \tag{1.6}$$

where in the right hand side we kept only the leading term after expanding at small momentum. We conclude that when the number of flavors is large, in the IR limit the scalar HS field has a scaling dimension $\Delta[\sigma] = 2$. Therefore at the critical point, the σ^2 operator has a scaling dimension equal to 4 and it is an irrelevant operator. We remind that irrelevant, marginal and relevant operators are defined with scaling dimensions $\Delta > d, \Delta = d, \Delta < d$ respectively. The critical $O(N)$ model is described by the following effective action

$$S_{eff} = \int d^dx\big[\frac{1}{2}(\partial\phi_i)^2 + \sigma\phi_i^2\big] \ . \tag{1.7}$$

with an HS propagator defined in (1.6). Using the effective action we can proceed to the next step, which is to find the order $O(1/N)$ corrections to the scaling dimensions of various observables. In Fig. 1.2 we show the relevant graphs that appear in the 2-point functions of the scalar fields ϕ_i and the HS field σ. Each HS field propagator carries a $1/N$ factor (1.6) and each closed loop, with N scalar flavors circulating inside, gives a factor N. Therefore the last three graphs in the 2-point function of the HS field are of order $1/N$, relative to the leading order effective propagator (1.6). Also notice that, unlike to standard perturbative expansions, the $1/N$ expansion has a peculiar property that at a given order in $1/N$ in each graph the number of loops will not be necessarily the same for all the graphs. The non-tree level graphs in Fig. 1.2 are actually divergent (if we specialise in $d = 3$ then the three loop graph, also known as Aslamazov-Larkin graph, turns to be finite). The divergent parts of these graphs (after appropriately regularizing the corresponding integrals) is all we need for finding order $O(1/N)$ corrections to the scaling dimensions. There are various approaches for calculating such integrals. Especially it is easy to work in a position space and to identify the regions from where the potential UV divergencies might raise. We do not provide any further details here, since all these and other similar graphs will be treated in the chapter 2 and in the appendix C. There we specialise in $d = 3$, however one might think about generalizing our results to arbitrary dimension.

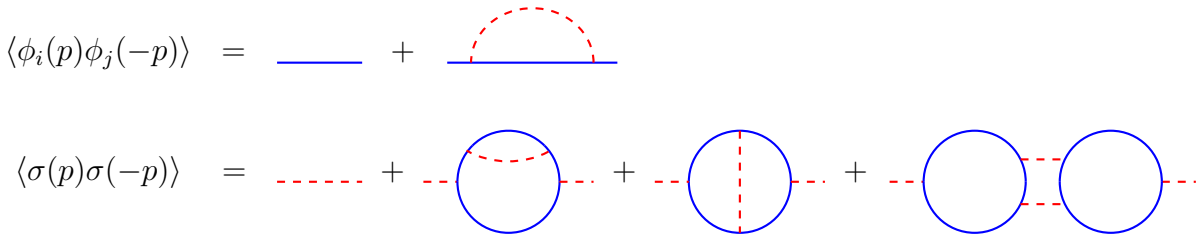

Figure 1.2: $1/N$ corrections to the 2-point functions

Below we give the scaling dimensions of the basic fields [19] at the order $O(1/N)$

$$\Delta[\phi] = \frac{d-2}{2} + \frac{1}{2}\frac{\eta_1}{N} + O\Big(\frac{1}{N^2}\Big) \ , \tag{1.8}$$

$$\text{where} \quad \eta_1 \equiv -\frac{4a\big(2-\frac{d}{2}\big)a\big(\frac{d}{2}-1\big)}{a(2)\Gamma\big(\frac{d}{2}+1\big)} \quad \text{and} \quad a(z) \equiv \frac{\Gamma(d/2-z)}{\Gamma(z)} \ , \tag{1.9}$$

$$\Delta[\sigma] = 2 + \frac{2(d-1)(d-2)}{d-2}\frac{\eta_1}{N} + O\Big(\frac{1}{N^2}\Big) \ . \tag{1.10}$$

In the physically interesting dimension $d = 3$ one obtains

$$\Delta[\phi] = \frac{1}{2} + \frac{4}{3\pi^2 N} + O\Big(\frac{1}{N^2}\Big) \ , \tag{1.11}$$

$$\Delta[\sigma] = 2 - \frac{32}{3\pi^2 N} + O\Big(\frac{1}{N^2}\Big) \ . \tag{1.12}$$

The critical $O(N)$ model can be studied near 4 dimensions with the help of the epsilon-expansion. The IR stable fixed point of the $O(N)$ vector model in $d = 4 - 2\epsilon$, known as a Wilson-Fisher fixed point, describes the critical regime of the $O(N)$ model which so far we have been examining with large N methods. Indeed plugging $d = 4 - 2\epsilon$ in (1.8, 1.10), expanding for small ϵ and comparing the results versus epsilon expansion predictions, one finds total agreement. In other words the large N expansion and the epsilon expansion being quite different approaches to the problem, are useful for cross-checking each other. The non-triviality of this check stems from the fact that in the $1/N$ expansion the critical $O(N)$ model (1.7) is renormalized, while in the epsilon expansion the $O(N)$ model with (UV) action (1.1) is perturbatively renormalized.

Finally, we comment about the relation between the d-dimensional $O(N)$ vector model and the d-dimensional $O(N)$ Non-Linear-Sigma-Model (NLSM). The latter is defined with a standard kinetic term for the scalar flavor fields, plus a constraint $\sum_{i=1}^{N} \phi_i^2 = 1$. It can be proved (for instance using the large N methods) that these models lie in the same universality class, i.e. have the same critical behaviour. Additionally the $O(N)$ NLSM admits an interacting UV fixed point near 2 dimensions, which can be studied with the help of epsilon expansions in $d = 2 + 2\epsilon$.

QED's in $2+1$ dimensions and Complex CFT's

The fixed points[4] of many-flavor fermionic and many-flavor bosonic QED's, which we examine in the chapter 2, are examples of unitary conformal field theories. Lowering values of N_f the RG flow might experience a first order phase transition: a runaway RG flow in the bosonic QED's (see the discussion on pages 11-12) and a dynamical chiral symmetry breaking (DχSB) in the fermionic QED's. The DχSB has been a subject of many theoretical studies, see for instance [21, 22, 23, 24, 25, 26, 27, 28, 29, 30, 31, 32, 33] and the references therein. Lattice simulations in $N_f = 2$ fQED, bQED$_+$ and ep-bQED suggest second order or weakly first order phase transitions[5] with certain critical exponents [34, 35, 36, 37, 38]. However the numerical bootstrap [39, 40, 41, 42, 43] shows that there are no 3d unitary CFT's with those critical exponents. Question arises: for which values of N_f the transition ceases to be second order, and what is the mechanism behind the weakness of the first order transitions in these theories?

In the chapter 3, using the $O(1/N_f)$ scaling dimensions of various mesonic operators, we argue that lowering N_f, at some critical value N_f^* the bosonic fixed points collide in the following pattern: bQED$_+$ with bQED (both have $U(N_f)$ symmetry), and ep-bQED with bQED$_-$ (both have $U(N_f/2)^2$ symmetry). The large N_f formulas allow us to estimate $N_f^* \sim 9-11$. We interpret these collisions as "merging and annihilation" of the fixed points: two (real) fixed points annihilate into each other and become a pair of complex conjugate fixed points or complex CFT's [44, 45, 46]. The RG flow preserves unitarity and doesn't hit those complex fixed points, instead it slows down while passing between the complex fixed points[6]. For $N_f \lesssim N_f^*$ the IR physics is not described by a second order phase transition, but by a weakly first order phase transition. The merging and annihilation between the bQED$_+$ and bQED was also discussed in [47, 48, 49, 50, 51].

In the case of the fermionic QED's, the large N_f formulas suggest the following collisions: $U(N_f)$ fQED with $U(N_f/2)^2$ QED-GN$_-$, and $U(N_f)$ QED-GN$_+$ with $U(N_f/2)^2$ QED-NJL. The collisions happen at $N_f^* \sim 3-7$. Notice that the fixed points with different symmetries collide with each other! For this reason, it is not obvious whether these collisions can

[4] We remind that the stable solutions of the RG beta functions, known as fixed points, are associated with the second order phase transitions [20]. At those fixed points the couplings do not run and there is a scale invariance. The absence of a stable fixed point predicts a 1st order phase transition between the disordered and ordered phases.

[5] First order phase transitions with huge (compared to the lattice spacing) correlation length are known as weak first order transitions.

[6] This behaviour of the RG flow is also known as "walking", and it was introduced in the context of 4d gauge theories, see [46] and references therein. In walking gauge theories the gauge coupling runs slowly for a broad range of energies and the theory is approximately scale invariant.

be interpreted as merging and annihilation into the complex plane[7]. Another possibility is that the fixed points with different symmetries, lowering N_f to N_f^*, do not disappear into the complex plane but instead "pass through each other" and exchange their stability properties[8]. Unfortunately this scenario (exchange of stability between fermionic QED's following the pattern above) doesn't predict a first order phase transition and DχSB, and so the N_f^* will not be associated with the critical number of flavors (N^c) below which a DχSB takes place. However it is an interesting phenomenon by itself, and its importance has been discussed in the context of vector models with cubic anisotropy. The "passing through each other" scenario is useful for understanding whether a given theory with a bigger symmetry is stable or unstable under the symmetry breaking deformations. In the paper [6] we claimed a merging and annihilation between the fermionic QED's and we supported it with IR dualities, instead in this thesis we will study the collision patterns using the large N_f techniques, without specifying the fate of the fermionic QED's after the collisions.

Let us explain the rationale behind the collisions from the large-N_f perspective. Let us consider the scaling dimensions of the quartic operators in tricritical bosonic QED and in fQED, at order $O(1/N_f)$:

$$\text{Tricritical bosonic QED: } \Delta[|\Phi|^4_{[2,0,...,0,2]}] = 2 - \frac{128}{3\pi^2 N_f} \ , \tag{1.13}$$

$$\Delta[|\Phi|^4_{singlet}] = 2 + \frac{256}{3\pi^2 N_f} \ . \tag{1.14}$$

$$\text{fQED: } \Delta[|\Psi|^4_{[0,1,0,...,0,1,0]}] = 4 - \frac{192}{3\pi^2 N_f} \ , \tag{1.15}$$

$$\Delta[\{(|\Psi|^2_{singlet})^2, F^{\mu\nu}F_{\mu\nu}\}] = 4 + \frac{64(2 \pm \sqrt{7})}{3\pi^2 N_f} \ , \tag{1.16}$$

where we explicitly mentioned the Dynkin labels under $SU(N_f)$. Decreasing N_f continuously, in bQED the singlet operator approaches from below $\Delta = 3$. The physical interpretation is that tricritical bosonic QED merges with the $\mathbb{CP}^{N_f-1}$ model. In the fermionic QED instead, it is the $SU(N_f)$-$[0, 1, 0, ..., 0, 1, 0]$ (symmetry breaking) operator that approaches $\Delta = 3$ from above. A simple, estimate of the collision points is then easy to obtain:

$$N^*_{bQED} \sim \frac{256}{3\pi^2} \simeq 8.6 \ , \qquad N^*_{fQED} \sim \frac{192}{3\pi^2} \simeq 6.5 \ . \tag{1.17}$$

In the chapter 3 we provide various estimates of N_f^* in all the four collisions, by studying the operators that hit $\Delta = 3$ (marginality crossing equation) at the collision points. These operators are quartic in the flavors or quadratic in the Hubbard-Stratonovich fields. We consistently find that in the bosonic QED's $N_f^* \sim 9-11$, while in fermionic QED's $N_f^* \sim 3-7$.

[7]See however, [25] and [45] where the merging and annihilation between fQED and QED-GN$_-$ was discussed.

[8]This scenario for the relativistic fermion theories was discussed in [52] using the functional RG technique.

Let us close this discussion comparing with other large N_f 2+1d models. In $O(N)$ models or $O(N)$-Gross-Neveu models, the 1st order corrections to the singlet operators are smaller, $\sim\frac{32}{3\pi^2 N}$, and there is a unitary CFT for all $N \geq 1$. Yukawa and quartic scalar interactions are weaker than gauge interactions. In the minimally supersymmetric QED with N_f flavors the order $O(1/N_f)$ correction to the $SU(N_f)$-singlet quadratic operator, instead of being large as in non supersymmetric QED's, is zero. There is no indication of merging and annihilation into the complex fixed points in the supersymmetric case. Additionally, the duality between the $N_f = 2$ super-QED and the Wess-Zumino model (which is checked in the section 2.3.3) suggests that the $\mathcal{N} = 1$ super-QED doesn't experience DχSB even for $N_f = 2$, but instead in the IR flows to a CFT. On the other hand, it is natural to expect that non supersymmetric gauge theories with non-Abelian gauge groups, and possibly Chern-Simons interactions, display a qualitative behavior similar to QED. The large-N_f expansion might be useful for instance to improve our understanding of the quantum phase scenarios of [53, 54, 55].

Main tool used in the chapter 3 (besides the order $O(1/N_f)$ scaling dimensions) is the marginality crossing equation applied to various mesonic operators. In order to introduce the concept, below we give two examples. The first example (Abelian Higgs model) is actually very relevant for the discussion of merging and annihilation between the bQED$_+$ and the bQED. It shows the merging mechanism of these fixed points near 4 dimensions (instead in the chapter 3 we study the merging in the physical d=3 dimension). The second example illustrates the "passing through each other" mechanism in the $O(N) \times O(N)$ vector model. In the chapter 3 we will briefly discuss this model as an ungauged version of the easy-plane bosonic gauge theories.

The Abelian Higgs model in Euclidean metric is defined as follows

$$\mathcal{L} = \frac{1}{4}F^{\mu\nu}F_{\mu\nu} + \sum_{i=1}^{N_f} |D_\mu \Phi_i|^2 + \lambda\Big(\sum_{i=1}^{N_f} |\Phi_i|^2\Big)^2 + (\text{gauge fixing term}) \ , \tag{1.18}$$

where $D_\mu = \partial_\mu + ieA_\mu$ and Φ^i, $i = 1, ..., N_f$ are complex scalars. Theory has a global symmetry $SU(N_f)$. The one-loop beta functions in $d = 4 - 2\epsilon$ for the gauge and quartic couplings are

$$\beta_e = \frac{de}{dl} = \epsilon e - \frac{1}{(4\pi)^2}\frac{2N_f e^3}{6} \ , \tag{1.19}$$

$$\beta_\lambda = \frac{d\lambda}{dl} = 2\epsilon\lambda - \frac{1}{(4\pi)^2}\big[16(N_f+4)\lambda^2 - 12\lambda e^2 + \frac{3}{2}e^4\big] \ , \tag{1.20}$$

where the beta functions are defined as derivatives of running couplings with respect to the logarithm of the length scale, which we denote by l [9]. For positive ϵ theory in the UV

[9] We will use this definition in the Introduction, chapters 2 and 3. In the chapter 4, the beta functions

limit is asymptotically free. When the number of flavors is larger than some critical value $N_f > N_f^* \approx 183$ the theory has a charged (non-zero gauge coupling) Wilson-Fisher fixed point besides the standard uncharged WF point [56] [10]. Actually two such fixed points exist, stable (bQED$_+$) and unstable (bQED). In the range $N_f < N_f^*$ the beta functions do not have real solutions, instead the RG flow runs toward the negative coupling and the quartic potential becomes unstable. This runaway behaviour can be interpreted as a fluctuation driven first-order phase transition, between the Coulomb and the Higgs phases.

Now, let us more carefully examine the fixed points. Usually one is interested in real solutions of (1.19, 1.20) which can be interpreted as unitary CFT's, however for our purposes we will not discard the complex solutions. The one-loop beta functions are quadratic in the variables (e^2, λ), and they always have solutions, either real or complex. For convenience we rescale the couplings $e^2 \to (4\pi)^2 e^2,\ \lambda \to (4\pi)^2\lambda$. Solving (1.19, 1.20) one finds

$$e_*^2 = \frac{3}{N_f}\epsilon \ , \tag{1.21}$$

$$\lambda_* = \frac{N_f + 18 \pm \sqrt{N_f^2 - 180N_f - 540}}{16N_f(N_f+4)}\epsilon \ . \tag{1.22}$$

The scaling dimension of the quartic operator $\Phi^4 \equiv \big(\sum_{i=1}^{N_f} |\Phi_i|^2\big)^2$, at this fixed points is related to the slope of the quartic coupling beta function

$$\Delta[\Phi^4] = d - \frac{d\beta_\lambda}{d\lambda}\bigg|_{(\lambda=\lambda_*, e^2=e_*^2)} = d \pm 2\epsilon\frac{\sqrt{N_f^2 - 180N_f - 540}}{N_f} \ . \tag{1.23}$$

From (1.23) we conclude that for $N_f > N_f^*$ the fixed point with a plus sign (1.21, 1.22) is stable (i.e. $\Delta[\Phi^4] > d$) and we identify it with bQED$_+$, and the other solution is unstable and we identify it with bQED (the tricritical bosonic QED).

Lowering the number of flavors we observe that the solutions (1.21, 1.22) are approaching to each other. Meanwhile the scaling dimension of the Φ^4 operator (1.23), converges from above (at bQED$_+$) and from below (at bQED) to its marginal value d. When N_f hits the critical value $N_f^* \approx 183$ the fixed points merge and the scaling dimension of the quartic operator becomes exactly equal to d: $\Delta[\Phi^4] = d$. The last equation is the "marginality crossing equation" [45]. Let us continue lowering further the number of flavors $N_f < N_f^*$. Then the λ_* becomes complex and the scaling dimension of the Φ^4 equals to the marginal

are defined as derivatives of couplings with respect to the energy scale.

[10] It seems that including the higher loop corrections and performing Padé resummations significantly reduces the value of N_f^* obtained in [56], see [57, 58, 59, 60].

value d plus a pure imaginary correction

$$\Delta[\Phi^4] = d \pm i\delta,\ \delta \equiv 2\epsilon \frac{\sqrt{540 + 180N_f - N_f^2}}{N_f},\ N_f < N_f^* \ . \tag{1.24}$$

Let us decompose the quartic coupling into real and imaginary parts $\lambda = x + iy$, then using (1.20) we can write the RG flow equations for each component. This leads to the following system of coupled differential equations

$$\frac{de^2}{dl} = 2\epsilon e^2 - \frac{2N_f e^4}{3} \ , \tag{1.25}$$

$$\frac{dx}{dl} = 2\epsilon x - [16(N_f + 4)(x^2 - y^2) - 12xe^2 + \frac{3}{2}e^4] \ , \tag{1.26}$$

$$\frac{dy}{dl} = 2\epsilon y - [32(N_f + 4)xy - 12ye^2] \ . \tag{1.27}$$

Notice that the "beta" function of the y is proportional to y. This means that if we start the flow with y tuned to zero, then it will stay zero along the flow. This is not surprising since the RG flow preserves unitarity.

In the Fig. 1.3 we draw the RG flow in the (x, y) plane (i.e. in the complex λ plane) at fixed $e_*^2 = \frac{3\epsilon}{N_f}$. The complex fixed points are indicated by red dots. From Fig. 1.3 we see that the RG flow lines never cross the axis x, in accordance with the discussion above. The beta functions near the fixed points can be treated in a linear approximation

$$\beta_\lambda = \frac{d\lambda}{dl} \approx \pm i\delta \cdot (\lambda - \lambda_*) \ . \tag{1.28}$$

The equation (1.28) can be easily solved to give

$$\lambda(l) - \lambda_* \sim l^{\pm i\delta} \ . \tag{1.29}$$

This explains why the RG flow lines are circles around the fixed points Fig. 1.3. It also explains why the circles are oppositely directed.

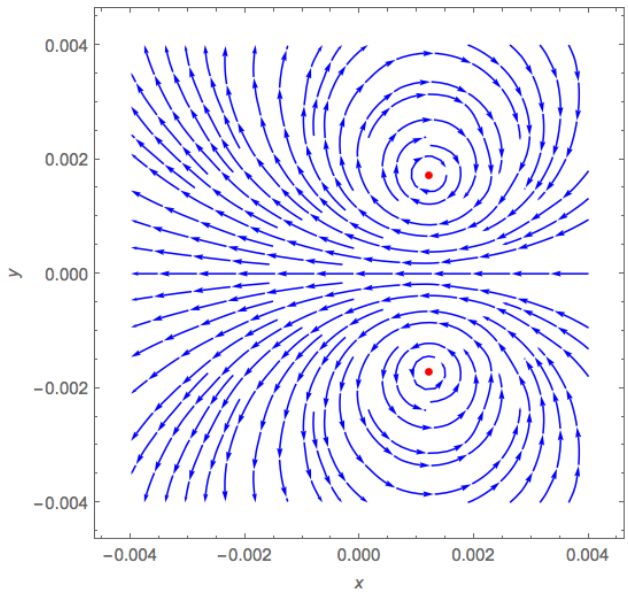

Figure 1.3: Runaway RG flow in the (x, y) plane for $N_f = 35$.

Let us finally study what happens when the number of flavors is less but very close to the critical number. In this case the complex fixed points are located very close to the real axis and the imaginary part of the scaling is

$$\delta \sim 2\epsilon \left(\sqrt{N_f^* - N_f}\right), \quad N_f \to N_f^* \ . \tag{1.30}$$

The unitary RG flow passes between those complex fixed points and slows down. To understand the last point, we rewrite the beta function in the following form

$$\frac{d(\lambda - A)}{dl} = -16(N_f + 4)\left[(\lambda - A)^2 + \frac{\delta^2}{32^2(N_f + 4)^2}\right], \quad A \equiv \frac{N_f + 18}{16(N_f + 4)N_f}\epsilon \ . \tag{1.31}$$

If we interpret the RG scale l as a time, then we can ask how long it takes for the RG flow to pass from $\lambda = \lambda_0$ to $\lambda = -\lambda_0$ (shifting $\lambda \to \lambda + A$ in advance)

$$\Delta l = -\int_{\lambda_0}^{-\lambda_0} \frac{d\lambda}{16(N_f + 4)\left[\lambda^2 + \frac{\delta^2}{32^2(N_f+4)^2}\right]} \sim \frac{2\pi}{\delta} = \frac{\pi}{\epsilon\left(\sqrt{N_f^* - N_f}\right)} \ . \tag{1.32}$$

The integral was evaluated in the limit $N_f \to N_f^*$, i.e. for small δ (1.30). Equation (1.32) proves that, closer the number of flavors is to its critical value slower becomes the RG flow: $\Delta l \sim \frac{1}{\sqrt{N_f^* - N_f}}$. In conclusion the merging and annihilation scenario explains the weakness of the first order phase transition in this example. The scaling behaviour (1.32) is known as a Miransky scaling. It was discovered in the context of the conformal phase transitions in 4d gauge theories, see [61, 62, 63].

The $O(N)\times O(N)$ vector model (see [64] and the references therein) is defined with the following action

$$\mathcal{L}=\frac{1}{2}\sum_{i=1}^{N}|\partial_\mu\phi_i|+\frac{1}{2}\sum_{i=1}^{N}|\partial_\mu\tilde{\phi}_i|^2+\lambda_{ep}\Big(\big(\sum_{i=1}^{N}|\phi_i|^2\big)^2+\big(\sum_{i=1}^{N}|\tilde{\phi}_i|^2\big)^2\Big)+\lambda\sum_{i=1}^{N}|\phi_i|^2\sum_{j=1}^{N}|\tilde{\phi}_j|^2\ . \quad (1.33)$$

The scalar fields ϕ_i ($\tilde{\phi}_i$) transform as a vector under the left (right) factor of the symmetry group $O(N)\times O(N)$. Beta functions for the quartic couplings (λ_{ep},λ) are

$$\beta_{\lambda_{ep}}=\frac{d\lambda_{ep}}{dl}=2\epsilon\lambda_{ep}-\left[8(N+8)\lambda_{ep}^2+2N\lambda^2\right]\ , \quad (1.34)$$

$$\beta_{\lambda}=\frac{d\lambda}{dl}=2\epsilon\lambda-\left[16\lambda^2+16(N+2)\lambda\lambda_{ep}\right]\ . \quad (1.35)$$

The system of equations $(\beta_{\lambda_{ep}}=0,\beta_\lambda=0)$ has four solutions, i.e. four fixed points

$$\text{Gaussian}\ :\ \lambda_{ep}=0,\ \lambda=0\ , \quad (1.36)$$

$$O(2N):\quad \lambda_{ep}=\frac{\epsilon}{8(4+N)},\ \lambda=2\lambda_{ep}\ , \quad (1.37)$$

$$\text{Decoupled}\ :\ \lambda_{ep}=\frac{\epsilon}{4(8+N)},\ \lambda=0\ , \quad (1.38)$$

$$\text{Model3}\ :\quad \lambda_{ep}=\frac{\epsilon N}{8(8+N^2)},\ \lambda=\frac{\epsilon(4-N)}{4(8+N^2)}\ . \quad (1.39)$$

At the $O(2N)$ fixed point the symmetry is $O(2N)$ since $\lambda=2\lambda_{ep}$. At the decoupled fixed point the coupling $\lambda=0$. Since this coupling mediates interactions between ϕ_i and $\tilde{\phi}_i$, then at the Decoupled fixed point we simply have two decoupled copies of the $O(N)$ model. The fixed point Model3 carries a symmetry $O(N)\times O(N)$.

For large values of N, more precisely when $N>4$ the RG flow diagram is as in the left panel of Fig. 1.4. In this region, the decoupled fixed point is fully stable, while the $O(2N)$ fixed point is only stable along the deformations that preserve $O(2N)$ symmetry and is unstable under the symmetry breaking deformations $O(2N)\to O(N)\times O(N)$. For $2<N<4$ the Model3 is the fully stable fixed point[11]: when $N\to 4^+$ it moves clockwise and collides with the Decoupled fixed point and passes through it by exchanging its stability. The central panel of Fig. 1.4 shows the RG plot in the region $2<N<4$. Continuing to

[11] See also the discussion at the beginning of the section (3.1), which disagrees with the statements above, if those are extrapolated to $d=3$. This is not surprising since here we are using a one-loop approximation, which is not so good for extrapolation. In [98], the $O(N)\times O(N)$ model is analyzed using the 5-loop order beta functions. Since these beta functions are no longer quadratic in the quartic couplings, then there are more than 4 fixed points. The analysis becomes more involved than what we have discussed above. The fixed points no longer collide while lowering N. However for small value of N some of the fixed points exchange their stability properties. More precisely: for $N>1$ the decoupled fixed point is fully stable and for $N=1$ the $O(2N=2)$ model becomes fully stable.

lower N, for $N < 2$ the $O(2N)$ model becomes the fully stable fixed point (right panel of Fig. 1.4): when $N \to 2^+$ the Model3 moving clockwise collides with the $O(2N)$ model (symmetry enhancement) and passes through it exchanging the stability. The $O(2N)$ model is stable under both $O(2N)$ symmetry preserving and symmetry breaking $O(2N) \to O(N) \times O(N)$ deformations. We want to stress that the collisions of various fixed points in this particular example cannot be interpreted as "merger and annihilation", and no complex CFT's appear while lowering N.

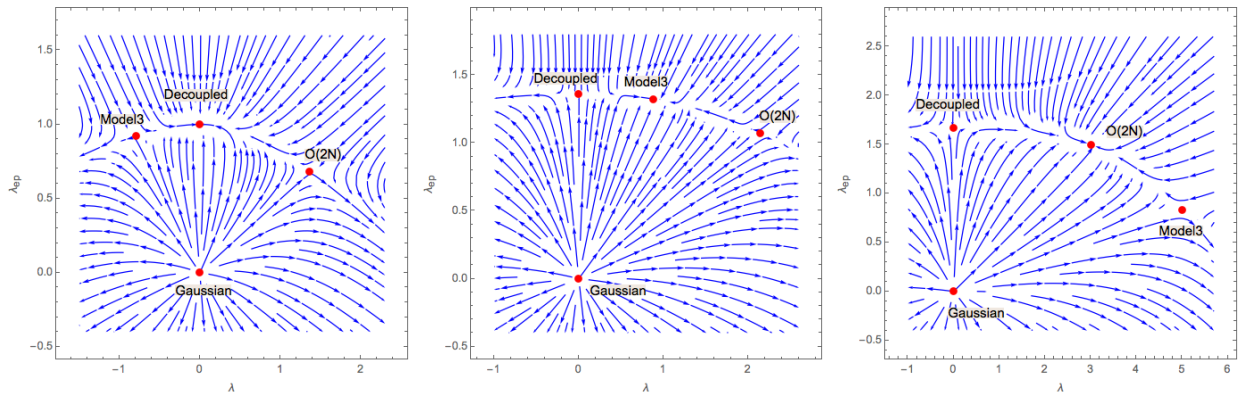

(a) $N > 4$ (b) $2 < N < 4$ (c) $N < 2$

Figure 1.4: RG flow diagram of the $O(N) \times O(N)$ model.

To conclude, we provide the scaling dimensions of quartic operators at the fixed points $O(2N)$ and Model3.

$$O(2N) : \Delta_1 = 4, \ \Delta_2 = 4 - 2\epsilon - \frac{2\epsilon(N-2)}{N+4} \ , \tag{1.40}$$

$$\text{Model3: } \Delta_1 = 4, \ \Delta_2 = 4 - 2\epsilon - \frac{2\epsilon(N^2 - 6N + 8)}{N^2 + 8} \ . \tag{1.41}$$

The scaling dimension Δ_1 is associated with the $O(2N)$ invariant quartic operator and it follows from (1.40, 1.41) that both fixed points are stable with respect to this deformation ($\Delta_1 > d = 4 - 2\epsilon$). The scaling dimension Δ_2 is associated with the $O(2N) \to O(N) \times O(N)$ symmetry breaking quartic operator. We see that the marginality crossing equation $\Delta_2 = d$ holds when these fixed points collide at $N = 2$. However for $N < 2$, Δ_2 doesn't acquire an imaginary part but stays real as the fixed points pass through each other. This is qualitatively different behaviour than what we observed in the "merger and annihilation" scenario (1.24).

Higher Derivative Gauge theory in $d = 6$ and the $\mathbb{CP}^{(N_f-1)}$ NLSM

In the paper [65], Fei, Giombi and Klebanov studied the $O(N)$ vector model in the dimension $4 < d < 6$. When $d > 4$ the ϕ^4 operator is an irrelevant deformation, and the existence of a UV interacting fixed point was conjectured[12]. The $O(N)$ vector model was engineered in the form (1.3), introducing a scalar HS field σ. Notice that in contrast to the case $d < 4$, in $d > 4$ in the large N limit the operator σ^2 is a relevant operator at the critical point (since it has a scaling dimension 4).

The theory (1.3) was UV completed in $4 < d < 6$: including in the action a kinetic term $(\partial_\mu \sigma)^2$ and a cubic term σ^3 [65]. Because of the presence of a "Yukawa" type interaction $\sigma\phi^2$, we will refer to this model as $O(N)$-Yukawa. It is very crucial to observe that these ultraviolet completion in the dimension $4 < d < 6$ has a relevant operator σ^2, which must be tuned to zero (the mass term ϕ^2 needs to be tuned to zero as well) in order to reach the IR critical point. The IR critical $O(N)$-Yukawa model was identified with the UV interacting fixed point of the $O(N)$ vector model in $4 < d < 6$.

Additionally, the $O(N)$-Yukawa model was examined [65] near its critical dimension $d = 6$ (the critical dimension of a given theory is defined as the dimension where the interactions in the action become marginal). In its critical dimension the theory was renormalized at one loop (later 3-loop [67] and 4-loop [68] analysis have been carried out). It was proved that the IR stable interacting fixed point at $d = 6 - 2\epsilon$ coincides with the critical $O(N)$ vector model[13].

Motivated with this discussion, in the chapter 4 we study the $\mathbb{CP}^{(N_f-1)}$ NLSM with N_f complex scalar fields Φ_i in $4 < d < 6$. This model will be engineered with the help of two master fields: the vector A_μ and the scalar σ. Notice that the operators $(\sigma^2, F^2_{\alpha\beta})$ are relevant at the critical point in the large N_f limit, since both have scaling dimension $4 > d$.

The $\mathbb{CP}^{(N_f-1)}$ model engineered with the help of two master fields, will be UV completed including in the action the "kinetic terms": $(\partial_\mu \sigma)^2, (\partial_\mu F_{\alpha\beta})^2$ and the interaction terms: $\sigma^3, \sigma F^2_{\alpha\beta}$. Notice that the kinetic term of the gauge field contains 4-derivatives, instead the term $F^2_{\alpha\beta}$ plays a role of a gauge invariant mass term for the gauge field. For this reason we will refer to the UV completion as a Higher Derivative Gauge (HDG) theory. In this theory the mass terms $(\sigma^2, F^2_{\alpha\beta})$ are relevant deformations, and we need to tune both of them to zero in order to reach in the IR limit the critical $\mathbb{CP}^{(N_f-1)}$. If we choose to not tune the σ^2

[12] See however [66], where the authors using the functional RG seem to rule out existence of such a UV interacting fixed point, with bounded critical potential.

[13] See also [69, 70, 71, 72], where the vector model, tensor models, fermionic QED and fermionic QCD are studied in the dimension $4 < d < 6$.

term, then we end up on another interesting critical point: the critical pure scalar QED in $4 < d < 6$ (no Yukawa interactions of type $\sigma\Phi^2$). Notice that in the dimension $4 < d < 6$ the operator Φ^4 is irrelevant, and therefore to reach the IR critical scalar QED, there will be no need to tune that operator to zero (this was not the case in $2 < d < 4$, where for instance to reach the tricritical point we had to tune to zero the quartic operator). Instead if we do not tune the term $F^2_{\alpha\beta}$, then we will end on the critical $O(N)$-Yukawa, which has already been discussed in [65].

Most importantly we renormalize the HDG in its critical dimension $d = 6$. In the dimension $d = 6 - 2\epsilon$ (taking N_f large) we find two IR interacting fixed points (besides the ungauged fixed point which corresponds to the critical $O(N)$-Yukawa). We prove that these fixed points coincide with the critical $\mathbb{CP}^{(N_f-1)}$ and the critical pure scalar-QED.

The chapter 4 is organized as follows. First we review the model $\mathbb{CP}^{(N_f-1)}$ and its critical properties in the large N_f limit in $4 < d < 6$ using [73]. In particular we provide scaling dimensions of various operators at the order $O(1/N_f)$ in d-dimension. We also discuss the critical pure scalar-QED in the large N_f limit. The large N_f limit of this model has not been studied yet in the literature, we provide scaling dimensions of some operators without giving the details of the computations. Second, we renormalize the UV action in $d = 6$ by constructing the one-loop beta functions, one-loop anomalous dimensions of the fields and of the mass operators (mass renormalization). The beta functions are solved in the large N_f limit and the fixed points are classified. At all the fixed points the scaling dimensions of the fields and of the mass operators are explicitly provided. Finally, these results are checked versus the large N_f predictions of the critical models.

Chapter 2

Easy-plane QED$_3$'s in the large N_f limit

2.1 Four bosonic QED fixed points in the large N_f limit

In this section we study bosonic QED with large N_f complex scalar fields, imposing at least $U(N_f/2)^2$ global symmetry. There are four different fixed points, two fixed points have $U(N_f)$ global symmetry, two fixed points have $U(N_f/2)^2$ global symmetry.

We start by considering the following UV (Euclidean) lagrangian

$$\mathcal{L} = \frac{1}{4e^2}F_{\mu\nu}F^{\mu\nu} + \sum_{i=1}^{N_f/2}(|D\Phi_i|^2 + |D\tilde{\Phi}_i|^2) + \lambda\sum_{i,j=1}^{N_f/2}|\Phi_i|^2|\tilde{\Phi}_j|^2$$
$$+ \lambda_{ep}\left((\sum_{i=1}^{N_f/2}|\Phi_i|^2)^2 + (\sum_{i=1}^{N_f/2}|\tilde{\Phi}_i|^2)^2\right) + \frac{N_f}{32(1-\xi)}\int d^3y\frac{\partial_\mu A^\mu(x)\partial_\nu A^\nu(y)}{2\pi^2|x-y|^2}\ , \tag{2.1}$$

where $F_{\mu\nu} = \partial_\mu A_\nu - \partial_\nu A_\mu$, and $D_\mu = \partial_\mu + iA_\mu$ is the covariant derivative with respect to the $U(1)$ gauge field A_μ. The complex scalar fields $(\Phi_i, \tilde{\Phi}_i)$ $(i = 1, .., N_f/2)$ carry charge $+1$ under the gauge group. Continuous global symmetry group of the action (2.1) is $SU(N_f/2)\times SU(N_f/2)\times U(1)_b\times U(1)_{top}$. The scalars Φ_i $(\tilde{\Phi}_i)$ transform in the fundamental representation under the left (right) factor of the symmetry group $SU(N_f/2)\times SU(N_f/2)$. Under $U(1)_b$, Φ_i and $\tilde{\Phi}_i$ carry charge $+1$ and -1, respectively. $U(1)_{top}$ is the topological symmetry, it is associated with the conserved flux current $\sim \epsilon_{\mu\nu\sigma}\partial_\nu A_\sigma$. There are also discrete symmetries, such as parity, charge conjugation and exchange symmetry $\Phi_i \leftrightarrow \tilde{\Phi}_i$.

The conformal gauge fixing is defined by the last term in (2.1). Choosing the gauge fixing parameter to be zero ($\xi = 0$) simplifies the calculations a lot, however we prefer to

keep ξ arbitrary (notice that in this parametrization $\xi = 1$ is the Landau gauge). Calculating correlation functions of gauge invariant operators, we will see that some Feynman graphs depend on ξ, but the sum (at a given order in $1/N_f$) doesn't as expected. This is a useful check of the calculations. In the following, we will always assume conformal gauge fixing for all the QED actions, but will not write it explicitly.

The quartic potential in (2.1) is a relevant deformation of the free theory. Depending on the form of the quartic couplings $\{\lambda_{ep}, \lambda\}$ there are four different fixed points[1]:

- bQED (tricritical), defined by vanishing quartic potential ,
- bQED$_+$ ($\mathbb{CP}^{N_f-1}$ model), defined by $V \sim (\sum |\Phi_i|^2 + |\tilde{\Phi}_i|^2)^2$,
- ep-bQED ("easy-plane"), defined by $V \sim (\sum |\Phi_i|^2)^2 + (\sum |\tilde{\Phi}_i|^2)^2$,
- bQED$_-$, defined by $V \sim (\sum |\Phi_i|^2 - |\tilde{\Phi}_i|^2)^2$.

In appendix A we study the RG flow diagram and the fixed points of the model (2.1) using the epsilon expansion technique. The zeros of the beta functions support the existence of precisely these four RG fixed points. See Introduction and chapter 3 for discussions about the ungauged fixed points and the RG flow.

We study the critical behaviour of the fixed points in the large N_f limit. For this purpose we engineer the quartic interactions in terms of cubic and quadratic interactions via the Hubbard-Stratonovich trick. Introducing two HS fields σ and $\tilde{\sigma}$, we get an expression equivalent to (2.1)

$$\begin{aligned}\mathcal{L} =& \frac{1}{4e^2} F_{\mu\nu}F^{\mu\nu} + \sum_{i=1}^{N_f/2} (|D\Phi_i|^2 + |D\tilde{\Phi}_i|^2) + \sigma \sum_{i=1}^{N_f/2} |\Phi_i|^2 + \tilde{\sigma} \sum_{i=1}^{N_f/2} |\tilde{\Phi}_i|^2 \\ & - \frac{\eta_1}{2}(\sigma^2 + \tilde{\sigma}^2) - \eta_2 \sigma\tilde{\sigma} \ . \end{aligned} \tag{2.2}$$

Integrating out σ and $\tilde{\sigma}$, one recovers the quartic potential in (2.1) with couplings $\{\lambda_{ep}, \lambda\}$ expressed in terms of $\{\eta_1, \eta_2\}$:

$$\lambda_{ep} = \frac{\eta_1}{2(\eta_1^2 - \eta_2^2)} \ , \tag{2.3}$$

$$\lambda = -\frac{\eta_2}{\eta_1^2 - \eta_2^2} \ . \tag{2.4}$$

It is sometimes convenient to work with the following HS fields

$$\begin{aligned}\sigma_+ &= \frac{\sigma + \tilde{\sigma}}{2} \ , \\ \sigma_- &= \frac{\sigma - \tilde{\sigma}}{2} \ . \end{aligned} \tag{2.5}$$

[1] We tune all the mass terms to zero.

With the choice (2.5) there is no mixed quadratic term between σ_+ and σ_-.

$$\mathcal{L} = \frac{1}{4e^2}F_{\mu\nu}F^{\mu\nu} + \sum_{i=1}^{N_f/2}(|D\Phi_i|^2 + |D\tilde{\Phi}_i|^2) + \sigma_+ \sum_{i=1}^{N_f/2}(|\Phi_i|^2 + |\tilde{\Phi}_i|^2) + \sigma_- \sum_{i=1}^{N_f/2}(|\Phi_i|^2 - |\tilde{\Phi}_i|^2)$$
$$- (\eta_1 + \eta_2)\sigma_+^2 - (\eta_1 - \eta_2)\sigma_-^2 \ . \tag{2.6}$$

2.1.1 bQED (tricritical QED)

The bQED is reached tuning to zero both the mass terms and the quartic interactions. For this reason another name for it is tricritical bosonic QED. The large N_f effective action is described by N_f copies of complex scalars Φ_i (we collected all the scalars $(\Phi, \tilde{\Phi})$ into a single field and denoted it by Φ) minimally coupled to the effective photon

$$\mathcal{L}_{eff} = \sum_{i=1}^{N_f} |D_\mu \Phi_i|^2 \ . \tag{2.7}$$

The effective photon propagator is obtained by summing geometric series of bubble diagrams such as Fig. 2.1 [2].

$$\langle A_\mu(x)A_\nu(0)\rangle_{\text{eff}} = \frac{8}{\pi^2 N_f |x|^2}\Big((1-\xi)\delta_{\mu\nu} + 2\xi\frac{x_\mu x_\nu}{|x|^2}\Big) \ . \tag{2.8}$$

The feynman rules for the bQED action (2.7) are summarised in Tab. 2.1.

The faithful global symmetry is

$$\Big(\frac{SU(N_f)}{\mathbb{Z}_{N_f}} \times U(1)_{\text{top}}\Big) \rtimes \mathbb{Z}_2^{\mathcal{C}} \ , \tag{2.9}$$

where $\mathbb{Z}_{N_f}$ is the center of $SU(N_f)$, generated by $e^{2\pi i/N_f}\mathbb{I} \in SU(N_f)$, which is a gauge transformation, so the actual global symmetry is $PSU(N_f) = \frac{SU(N_f)}{\mathbb{Z}_{N_f}}$ instead of $SU(N_f)$ (the gauge invariant local operators transform in $SU(N_f)$ representations with zero N_f-ality). $\mathbb{Z}_2^{\mathcal{C}}$ is the charge-conjugation symmetry $\Phi_i \to \Phi_i^*, A_\mu \to -A_\mu$. There is also parity symmetry.

[2] It is easier to construct the effective photon propagator in momentum space first. Summing the geometric series in (2.1) gives $\langle A_\mu(p)A_\nu(-p)\rangle_{\text{eff}} = D_{\mu\rho}(1-\Pi D)^{-1}_{\rho\nu}\big|_{p\to 0}$, where $D_{\mu\rho}(p) = \frac{e^2}{p^2}\big(\delta_{\mu\rho} - \frac{p_\mu p_\rho}{p^2}\big) + \frac{16(1-\xi)}{N_f|p|}\frac{p_\mu p_\rho}{p^2}$ is the tree level propagator (it is derived from the action (2.1)) and $\Pi_{\alpha\beta}(p) = N_f \int \frac{d^3q}{(2\pi)^3}\frac{(p+2q)_\alpha(p+2q)_\beta}{q^2(p+q)^2} = -\frac{N_f|p|}{16}\big(\delta_{\alpha\beta} - \frac{p_\alpha p_\beta}{p^2}\big)$ is the one loop integral in Fig. 2.1. Since we are interested in the IR behaviour of the propagator, we take the limit $|p| \to 0$, and after some algebra one obtains $\langle A_\mu(p)A_\nu(-p)\rangle_{\text{eff}} = \frac{16}{N_f|p|}\big(\delta_{\mu\nu} - \xi\frac{p_\mu p_\nu}{p^2}\big) + O(\frac{p^2}{e^2})$. Fourier transforming to position space we obtain (2.8).

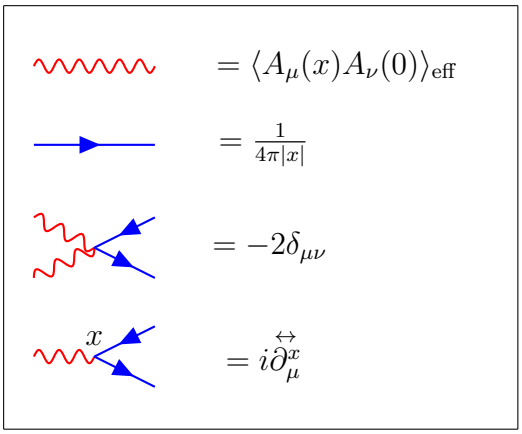

Table 2.1: bQED Feynman rules.

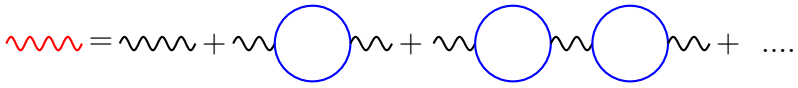

Figure 2.1: Effective photon propagator (red wavy line). The black wavy line stands for tree level photon propagator.

Using the Feynman rules Tab. 2.1, we compute anomalous dimensions of gauge-invariant operators at order $O(1/N_f)$. For this purpose, first we calculate the 2-point correlation function for a given operator, then using it we extract anomalous contribution to the scaling. It might happen that for a given model there are several gauge invariant operators that have the same scaling dimensions at the order $O(N_f^0)$ and carry the same quantum numbers. These operators can mix by quantum corrections at order $O(1/N_f)$ and one needs to study the matrix of mixed 2-point correlation functions in order to correctly identify the eigenbasis of mixed operators and their anomalous dimensions.

Scaling dimension of low-lying scalar operators

Bilinear mesonic operators At the quadratic level, there are N_f^2 operators of the form $\Phi_i^* \Phi^j$. They transform in the adjoint plus singlet representations of $SU(N_f)$:

$$|\Phi|^2_{adj} = \Phi_i^* \Phi^j - \frac{\delta_i^j}{N_f} \sum_k \Phi_k^* \Phi^k \ , \tag{2.10}$$

$$|\Phi|^2_{sing} = \frac{1}{\sqrt{N_f}} \sum_k \Phi_k^* \Phi^k \ . \tag{2.11}$$

[3] When it is not crucial for the graph evaluation, we drop the arrows from propagators.

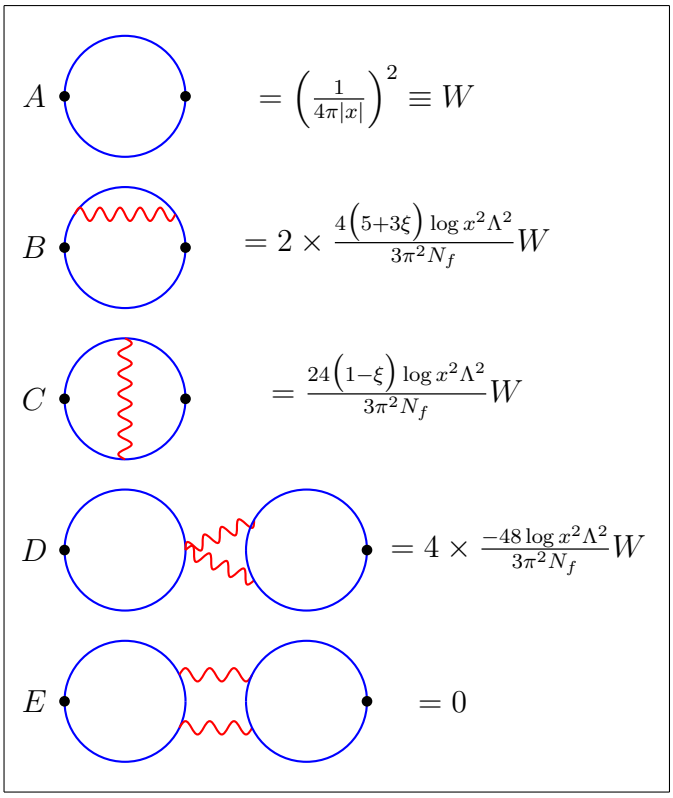

Table 2.2: (bQED) Results for individual Feynman graphs appearing in the 2-point correlation function of the scalar-bilinear operators. The graph D has a vanishing contribution in the 2-point function of the adjoint operator (see the explanation after eq. (2.11)).[3]

The 2-point correlation function for the adjoint operator is the sum of the graphs A,B,C Tab. 2.2. Each scalar loop assumes tracing over the flavor indices and the trace with an adjoint operator insertion is identically zero, this is because the adjoint operator defined in (2.10) is traceless. Therefore we conclude that for the adjoint operator the graphs D and E have a vanishing contribution. All the divergent graphs are regularized by putting an UV cutoff Λ on the momentum integrals. Check the appendix C for more details of the loop calculations.

$$\begin{aligned}\langle|\Phi|^2_{adj}(x)|\Phi|^2_{adj}(0)\rangle &= \Big(\frac{1}{4\pi|x|}\Big)^2 + \frac{8\big(5+3\xi\big)\log x^2\Lambda^2}{3\pi^2 N_f}\Big(\frac{1}{4\pi|x|}\Big)^2 + \frac{24\big(1-\xi\big)\log x^2\Lambda^2}{3\pi^2 N_f}\Big(\frac{1}{4\pi|x|}\Big)^2 \\ &= \Big(\frac{1}{4\pi|x|}\Big)^2\Big[1-\Big(-\frac{64}{3\pi^2 N_f}\Big)\log x^2\Lambda^2\Big] \\ &= \Big(\frac{1}{4\pi|x|}\Big)^2\Big(\frac{1}{x^2\Lambda^2}\Big)^{\Delta^{(1)}_{adj}} , \end{aligned} \tag{2.12}$$

where we defined anomalous dimension of adjoint operator $\Delta^{(1)}_{adj}$, so $\Delta^{(1)}_{adj} = -\frac{64}{3\pi^2 N_f}$. We extract the anomalous dimension for the singlet operator in a similar way. Notice that for the singlet operator there is an additional order $O(1/N_f)$ contribution coming from the graph D in Tab. 2.2 (in the singlet case each loop in the graphs D and E gives a factor N_f). The 3-loop graphs of type D and E are known as Aslamazov-Larkin (AL) graphs. Notice how big is the contribution of AL graph compared to the contributions of the other graphs in Tab. (2.2). Below we give the final results

$$\Delta[|\Phi|^2_{adj}] = 1 - \frac{64}{3\pi^2 N_f} + O(1/N_f^2) , \tag{2.13}$$

$$\Delta[|\Phi|^2_{sing}] = 1 + \frac{128}{3\pi^2 N_f} + O(1/N_f^2) . \tag{2.14}$$

Quartic mesonic operators Next we consider scalar quartic operators

$$T^{ij}_{kl} \equiv \Phi^i\Phi^j\Phi^*_k\Phi^*_l . \tag{2.15}$$

T^{ij}_{kl} is a gauge invariant operator, symmetric in its upper and lower indices. The following decomposition of T into irreducible representations under the $SU(N_f)$ group is useful for discussion of their scaling dimensions

$$\begin{aligned} T^{ij}_{kl} =& \frac{1}{N_f(N_f+1)}\big[\delta^{(i}_k\delta^{j)}_l T^{mn}_{mn}\big] + \frac{1}{N_f+2}\big[\delta^{(j}_{(l}T^{i)n}_{k)n} - \frac{2}{N_f}\delta^{(j}_l\delta^{i)}_k T^{mn}_{mn}\big] \\ &+ \big[T^{ij}_{kl} - \frac{1}{N_f+2}\delta^{(j}_{(l}T^{i)n}_{k)n} + \frac{1}{(N_f+1)(N_f+2)}\delta^{(j}_l\delta^{i)}_k T^{mn}_{mn}\big] . \end{aligned} \tag{2.16}$$

The first, second and third terms in the right hand side of (2.16) are correspondingly singlet, adjoint and adjoint-2 (Dynkin labels $[2,0,\ldots,0,2]$) quartic operators. All of them have

scaling dimension 2 at leading order, it remains to calculate order $O(1/N_f)$ corrections.

Let us consider quartic adjoint-2 operator defined by the last term of (2.16). It is enough to study the two-point correlation function for only one component of the adjoint-2 representation, which we choose to be

$$T^{12}_{34} = \Phi^1\Phi^2\Phi^*_3\Phi^*_4 \ . \tag{2.17}$$

All the relevant graphs for extracting the anomalous dimension of the operator (2.17) are collected in Tab. 2.3 (the last graph doesn't contribute). It receives contribution from the anomalous dimensions of the Φ_i fields (there are 4 such graphs) plus graphs with a photon connecting two different legs ("kite"-graphs, there are 6 "kite"-graphs). In 2 "kite"-graphs the photon connects the scalar propagators with arrows going in the same direction, while in the other 4 "kite"-graphs the photon connects propagators with arrows going in the opposite direction. The contribution of a "kite"-graph where the photon connects arrows going in the same direction is equal to minus the contribution of a "kite"-graph where the photon connects arrows going in the opposite direction. So effectively we are left with the contribution of 2 such "kite"-graphs[4].

For the quartic adjoint operator the last graph in Tab. 2.3 contributes at order $O(1/N_f)$. For the singlet quartic operator the last graph contributes twice as much as for the quartic adjoint operator. We list the quartic operators and their scaling dimensions

$$\Delta[|\Phi|^4_{adj-2}] = 2\Delta[|\Phi|^2_{adj}] + O(1/N_f^2) = 2 - \frac{128}{3\pi^2 N_f} + O(1/N_f^2) \ , \tag{2.18}$$

$$\Delta[|\Phi|^4_{adj}] = \Delta[|\Phi|^2_{adj}] + \Delta[|\Phi|^2_{sing}] + O(1/N_f^2) = 2 + \frac{64}{3\pi^2 N_f} + O(1/N_f^2) \ , \tag{2.19}$$

$$\Delta[|\Phi|^4_{sing}] = 2\Delta[|\Phi|^2_{sing}] + O(1/N_f^2) = 2 + \frac{256}{3\pi^2 N_f} + O(1/N_f^2) \ . \tag{2.20}$$

[4]One can consider degree-$2k$ operators which transform in the adjoint-k representation (Dynkin labels $[k, 0, \ldots, 0, k]$). These operators do not mix with other operators. The anomalous dimension of a degree-$2k$ adjoint-k operator, at order $O(1/N_f)$, receives contribution from the anomalous dimensions of the Φ_i fields (there are $2k$ such graphs) plus the contribution of "kite" graphs (there are $\binom{2k}{2} = 2k^2 - k$ "kite"-graphs). In $2 \cdot \binom{k}{2} = k^2 - k$ "kite"-graphs the photon connects fields with arrows going in the same direction, while in the other k^2 "kite"-graphs the photon connects fields with arrows going in the opposite direction. These two groups of "kite"-graphs contribute with opposite signs, so effectively we are left with the contribution of $k^2 - (k^2 - k) = k$ such "kite"-graphs. Therefore the scaling dimension of the degree-$2k$ adjoint-k operator is

$$\Delta[|\Phi|^{2k}_{adj-k}] = k\Delta[|\Phi|^2_{adj}] + O(1/N_f^2) = k - \frac{64k}{3\pi^2 N_f} + O(1/N_f^2) \ .$$

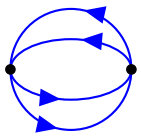	$= W^2$
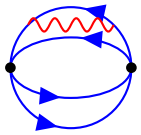	$= 4 \times \frac{4\left(5+3\xi\right)\log x^2\Lambda^2}{3\pi^2 N_f} W^2$
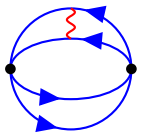	$= 2 \times \frac{-24\left(1-\xi\right)\log x^2\Lambda^2}{3\pi^2 N_f} W^2$
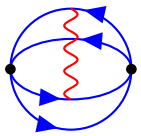	$= 4 \times \frac{24\left(1-\xi\right)\log x^2\Lambda^2}{3\pi^2 N_f} W^2$
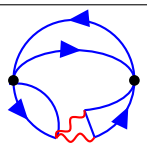	$= 4 \times \frac{-48\log x^2\Lambda^2}{3\pi^2 N_f} W^2$

Table 2.3: (bQED) adjoint-2 and adjoint quartic operator renormalization.

2.1.2 bQED$_+$ ($\mathbb{CP}^{N_f-1}$ model)

The bQED$_+$ fixed point is reached with $SU(N)_f$ invariant quartic deformation $V \sim (\sum |\Phi_i|^2 + |\tilde{\Phi}_i|^2)^2$ and by tuning the mass term to zero. In the literature this model is also known as Abelian Higgs model or $\mathbb{CP}^{N_f-1}$ model. The large N_f effective action is described by N_f copies of complex scalars Φ_i (we collected all the scalars $(\Phi, \tilde{\Phi})$ into a single field and denoted it by Φ), minimally coupled to an effective photon and interacting with a single Hubbard-Stratonovich field σ_+ via a cubic interaction:

$$\mathcal{L}_{eff} = \sum_{i=1}^{N_f} |D_\mu \Phi_i|^2 + \sigma_+ \sum_{i=1}^{N_f} |\Phi_i|^2 \,. \tag{2.21}$$

The effective photon propagator is the same as in (2.8) and the effective propagator for the HS field is obtained from summing geometric series of the bubble diagrams in Fig. 2.2.

$$\langle \sigma_+(x)\sigma_+(0)\rangle_{eff} = \frac{8}{\pi^2 N_f |x|^4} \,. \tag{2.22}$$

The global symmetry is the same as in bQED (2.9).

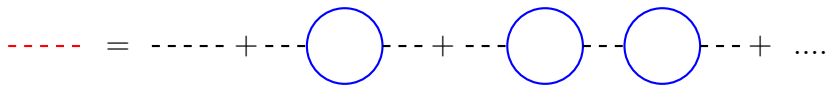

Figure 2.2: (bQED$_+$) HS field σ_+ effective propagator (red dashed line). The black dashed line stands for tree level HS field propagator.

Scaling dimension of low-lying scalar operators

The N_f^2 gauge invariant operators $\Phi_i^*\Phi^j$ transform in the adjoint plus singlet of $SU(N_f)$. The singlet operator is set to zero by the equation of motion of the Hubbard-Stratonovich field σ_+.[5] So we consider the scaling dimension of σ_+ instead. The scaling dimensions of these operators can be readily extracted using the Feynman graphs in Tab. 2.4

$$\Delta[|\Phi|^2_{adj}] = 1 - \frac{48}{3\pi^2 N_f} + O(1/N_f^2) \ , \tag{2.23}$$

$$\Delta[\sigma_+] = 2 - \frac{144}{3\pi^2 N_f} + O(1/N_f^2) \ . \tag{2.24}$$

The formulas above have already been discussed in [56, 74, 73, 75]. The scaling dimensions (2.23, 2.24) are related to traditional critical exponents by

$$\eta_N = 2\Delta[|\Phi|^2_{adj}] - 1 = 1 - \frac{96}{3\pi^2 N_f} + O(1/N_f^2) \ , \tag{2.25}$$

$$\nu^{-1} = 3 - \Delta[\sigma_+] = 1 + \frac{144}{3\pi^2 N_f} + O(1/N_f^2) \ , \tag{2.26}$$

where η_N is the anomalous scaling dimension of the adjoint scalar-bilinear operator also known as Néel field [75].

[5] As a simple check of this statement, one can explicitly check that the two point function $\langle |\Phi|^2_{sing}(x)|\Phi|^2_{sing}(0)\rangle$ is zero at order $O(N_f^0)$.

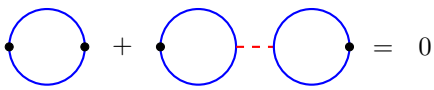

The 1-loop diagram cancels with a 2-loop diagram given by two bubbles connected by a σ_+ propagator (normalizing the singlet operator as $\frac{1}{\sqrt{N_f}}\sum_k \Phi_k^*\Phi^k$, both such graphs are of order 1 at large N_f). We thank to Silviu Pufu for clarifying this point.

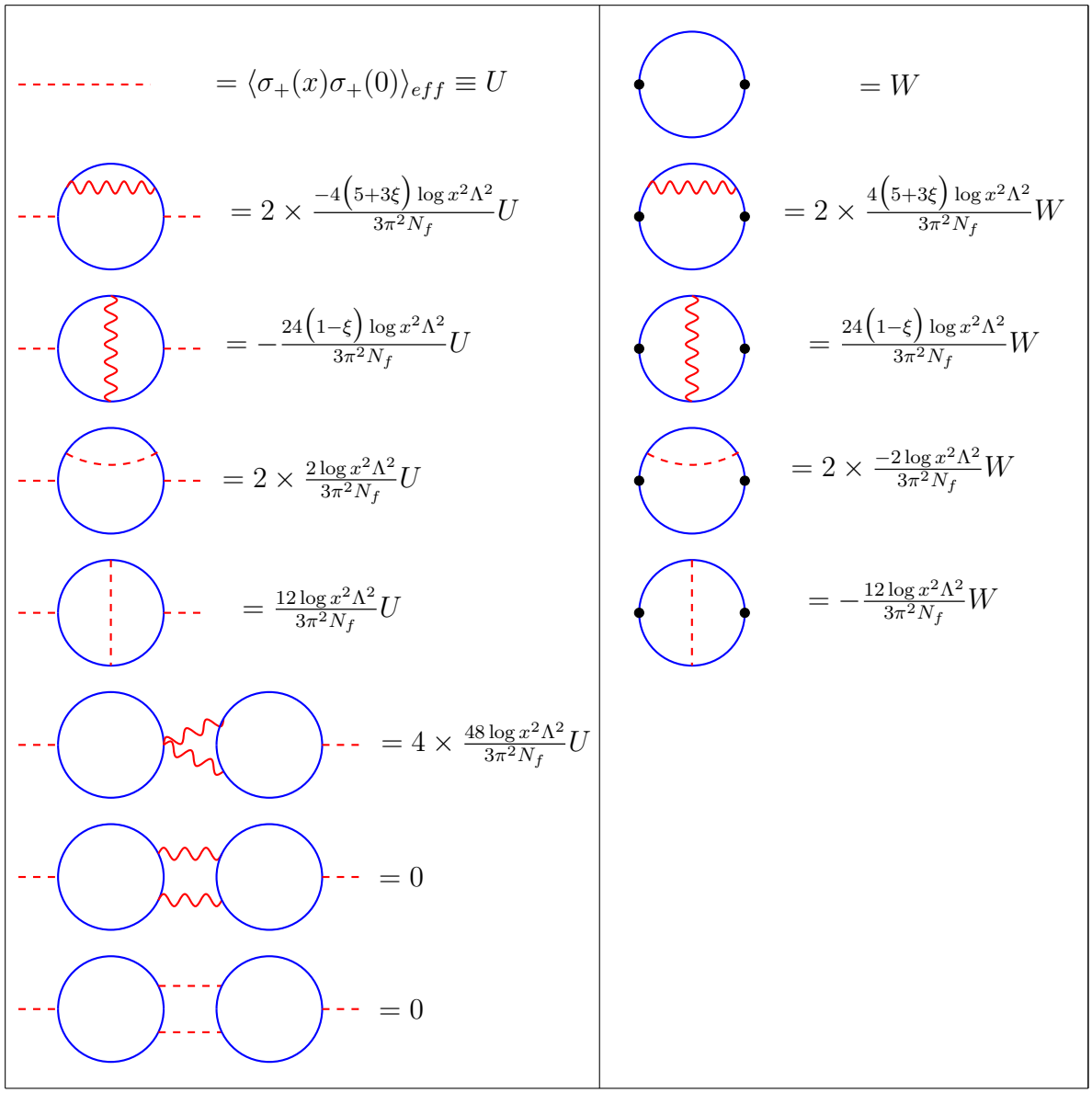

Table 2.4: (bQED$_+$) Results for the individual Feynman graphs appearing in the 2-point correlation functions $\langle\sigma_+(x)\sigma_+(0)\rangle$ (left column)[6] and $\langle|\Phi|^2_{adj}(x)|\Phi|^2_{adj}(0)\rangle$ (right column).

Next we discuss scaling dimension of the quartic adjoint-2 operator (with Dynkin labels $[2, 0, ..., 0, 2]$). This operator is in the spectrum and has scaling dimension 2 at order $O(N_f^0)$. The graphs that contribute to its 2-point correlation function at the order $O(1/N_f)$ are the ones in Tab. 2.3 (already discussed in the context of bQED), supplemented with the list of graphs in Tab. 2.5. There are 4 graphs with HS field connecting a leg with itself and 6 kite graphs with the HS field joining two different legs. Summing all the contributions we can

[6]The last two graphs have no logarithmic divergences.

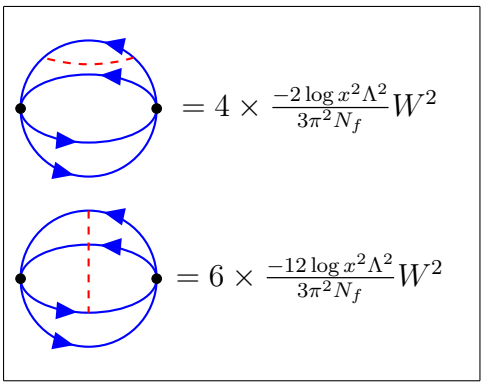

Table 2.5: (bQED$_+$) quartic adjoint-2 renormalization. (contribution from graphs with HS prop.)

extract anomalous dimension of the quartic adjoint-2 operator[7]

$$\Delta[|\Phi|^4_{adj-2}] = 2 - \frac{48}{3\pi^2 N_f} + O(1/N_f^2) \ . \tag{2.27}$$

2.1.3 ep-bQED ("easy-plane" QED)

The ep-bQED fixed point is reached with the quartic potential $V \sim (\sum_{i=1}^{N_f/2} |\Phi_i|^2)^2 + (\sum_{i=1}^{N_f/2} |\tilde{\Phi}_i|^2)^2$ and by tuning the mass terms to zero. The large N_f effective action is described by complex scalar fields $(\Phi_i, \tilde{\Phi}_i)$ minimally coupled to the effective photon and interacting with two HS fields via cubic interactions

$$\mathcal{L}_{eff} = \sum_{i=1}^{N_f/2} (|D\Phi_i|^2 + |D\tilde{\Phi}_i|^2) + \sigma \sum_{i=1}^{N_f/2} |\Phi_i|^2 + \tilde{\sigma} \sum_{i=1}^{N_f/2} |\tilde{\Phi}_i|^2 \, . \tag{2.28}$$

The effective propagator for the photon is the same as in (2.8), and the effective propagators for the HS fields are

$$\langle \sigma(x)\sigma(0)\rangle = \langle \tilde{\sigma}(x)\tilde{\sigma}(0)\rangle = \frac{8}{\pi^2 (N_f/2)|x|^4} \ . \tag{2.29}$$

The photon "sees" all the N_f flavors, σ and $\tilde{\sigma}$ only "see" $N_f/2$ flavors. In the Feynman graphs, we use red dashed (double dashed) line for σ ($\tilde{\sigma}$) and blue (double blue) line for Φ ($\tilde{\Phi}$).

[7]The quartic adjoint and the quartic singlet operators are out of the spectrum, because of the equations of motion of σ_+. In their place, one could consider the operators $\sigma_+|\Phi|^2_{adj}$ and σ_+^2. At order $O(N_f^0)$, these operators have scaling dimensions 3 and 4, respectively. The operator σ_+^2 mixes with $F_{\mu\nu}F^{\mu\nu}$ at order $O(1/N_f)$. The corresponding mixing matrix and anomalous dimensions were computed in [73].

The global symmetry of the effective action (2.28) is

$$\Big(\frac{SU(N_f/2)\times SU(N_f/2)\times U(1)_b\rtimes\mathbb{Z}_2^e}{\mathbb{Z}_{N_f}}\times U(1)_{top}\Big)\rtimes\mathbb{Z}_2^C\ . \tag{2.30}$$

The $U(1)_b$ acts: $\{\Phi_i\to e^{i\alpha}\Phi_i,\tilde\Phi_i\to e^{-i\alpha}\tilde\Phi_i\}$. The $\mathbb{Z}_2^e$ acts: $\{\Phi_i\leftrightarrow\tilde\Phi_i,\ \sigma\leftrightarrow\tilde\sigma\}$. There is also parity invariance.

Scaling dimension of low-lying scalar operators

The N_f^2 quadratic gauge invariant operators transform as two adjoints, two singlets and two bifundamentals of $SU(N_f/2)^2$. More precisely, in the reducible representation

$$(\mathbf{adj},\mathbf{1})\oplus(\mathbf{1},\mathbf{adj})\oplus(\bar{\mathbf{F}},\mathbf{F})\oplus(\mathbf{F},\bar{\mathbf{F}})\oplus\mathbf{2}\cdot(\mathbf{1},\mathbf{1})\ , \tag{2.31}$$

where by $\mathbf{F}$ we denoted the fundamental representation of $SU(N_f/2)$.

Feynman graphs that contribute to the anomalous scaling dimension of $|\Phi|^2_{adj}$ are the graphs in the right column of Tab. 2.4. One has to keep in mind that the photon "sees" all the flavors, while each sigma field "sees" only half of them, therefore the contribution of graphs that involve an HS propagator is twice as big as the contribution of the corresponding graphs in bQED$_+$. For the adjoint operator $|\tilde\Phi|^2_{adj}$ one has the same set of graphs, but the blue lines are exchanged by blue double lines and red dashed lines are exchanged by red dashed double lines. On the other hand, the scaling dimension of the bifundamental operators $(\Phi_i\tilde\Phi_j^*,\Phi_i^*\tilde\Phi_j)$ is corrected by graphs similar to those in the right column of Tab. 2.4, except that the last graph is absent. The two scalar-bilinear singlets are set to zero by the equations of motion of the HS fields σ and $\tilde\sigma$.

The 2-point correlation function $\langle\sigma(x)\sigma(0)\rangle$ is corrected by the left column graphs in Tab. 2.4, and similar graphs stand for $\langle\tilde\sigma(x)\tilde\sigma(0)\rangle$. It is preferable to denote by U the effective propagator of the HS field σ (2.29), then the graphs involving single photon contribute as in bQED$_+$, the graphs involving HS propagator contribute 2 times the corresponding graphs in bQED$_+$, the graph involving two photons contributes twice less than the same graph in bQED$_+$. So we conclude that the $O(1/N_f)$ corrected propagator for the HS σ field is

$$\langle\sigma(x)\sigma(0)\rangle=\Big(1+\frac{64\log x^2\Lambda^2}{3\pi^2N_f}\Big)\Big(\frac{8}{\pi^2(N_f/2)|x|^4}\Big)\ . \tag{2.32}$$

It turns out that already at order $O(1/N_f)$ there is a mixing between HS fields σ and $\tilde\sigma$ Fig. 2.3.

$$\langle\sigma(x)\tilde\sigma(0)\rangle=\frac{96\log x^2\Lambda^2}{3\pi^2N_f}\Big(\frac{8}{\pi^2(N_f/2)|x|^4}\Big)\ . \tag{2.33}$$

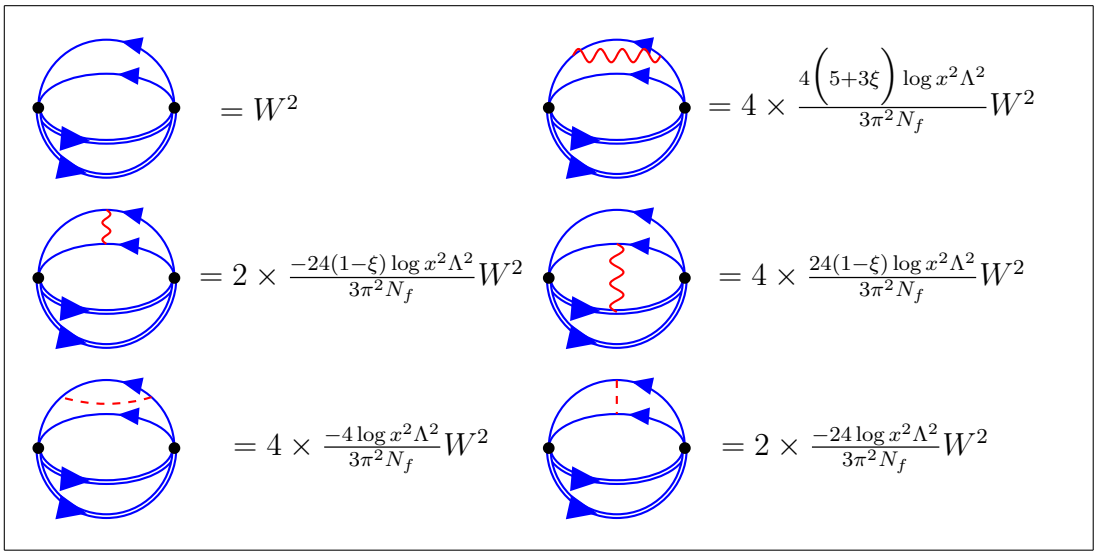

Table 2.6: Renormalization of the $(\overline{\mathbf{sym}}, \mathbf{sym})$ quartic operator.

The HS fields $\sigma_\pm$ defined in (2.5) are the eigenvectors of the mixing matrix. Using (2.32, 2.33) one readily extracts anomalous dimensions of those fields (2.37, 2.38).

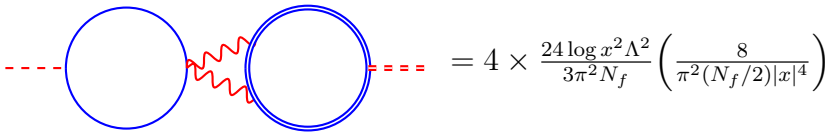

Figure 2.3: Diagram responsible for mixing $\langle\sigma(x)\tilde{\sigma}(0)\rangle$.

The N_f^4 quartic gauge invariant operators transform as reducible representation of $SU(N_f/2)^2$ with the following decomposition into irreducible blocks

$$\begin{aligned}
&(\mathbf{adj_2}, \mathbf{1}) \oplus (\mathbf{1}, \mathbf{adj_2}) \oplus (\overline{\mathbf{sym}}, \mathbf{sym}) \oplus (\mathbf{sym}, \overline{\mathbf{sym}}) \\
\oplus&(\mathbf{adj}, \mathbf{adj}) \oplus (\mathbf{R}, \bar{\mathbf{F}}) \oplus (\bar{\mathbf{R}}, \mathbf{F}) \oplus (\bar{\mathbf{F}}, \mathbf{R}) \oplus (\mathbf{F}, \bar{\mathbf{R}}) \\
\oplus&\mathbf{2} \cdot (\mathbf{adj}, \mathbf{1}) \oplus \mathbf{2} \cdot (\mathbf{1}, \mathbf{adj}) \oplus \mathbf{2} \cdot (\mathbf{F}, \bar{\mathbf{F}}) \oplus \mathbf{2} \cdot (\bar{\mathbf{F}}, \mathbf{F}) \oplus \mathbf{3} \cdot (\mathbf{1}, \mathbf{1}) \ ,
\end{aligned} \tag{2.34}$$

where by $\mathbf{R}$ we denote the representation of $SU(N_f/2)$ with Dynkin labels $[2, 0, ..., 0, 1]$. All the irreducible blocks in the third row of (2.34) contain a singlet quadratic factor and therefore they are out of spectrum. In the Tab. 2.6 we collected all the relevant graphs for extracting the anomalous scaling dimension of the operator $(\overline{\mathbf{sym}}, \mathbf{sym}) = \Phi_i^* \Phi_j^* \tilde{\Phi}_k \tilde{\Phi}_l$. One can make similar tables for the other quartic operators which are in the spectrum.

The scaling dimensions are as follows

$$\Delta[|\Phi|^2_{adj}] = \Delta[|\tilde{\Phi}|^2_{adj}] = 1 - \frac{32}{3\pi^2 N_f} + O(1/N_f^2) \ , \tag{2.35}$$

$$\Delta[\Phi_i \tilde{\Phi}^*_j] = \Delta[\Phi^*_i \tilde{\Phi}_j] = 1 - \frac{56}{3\pi^2 N_f} + O(1/N_f^2) \ , \tag{2.36}$$

$$\Delta[\sigma_-] = 2 + \frac{32}{3\pi^2 N_f} + O(1/N_f^2) \ , \tag{2.37}$$

$$\Delta[\sigma_+] = 2 - \frac{160}{3\pi^2 N_f} + O(1/N_f^2) \ , \tag{2.38}$$

$$\Delta[|\Phi|^4_{adj-2}] = \Delta[|\tilde{\Phi}|^4_{adj-2}] = 2 + \frac{32}{3\pi^2 N_f} + O(1/N_f^2) \ , \tag{2.39}$$

$$\Delta[\tilde{\Phi}^*_l (\Phi_i \Phi_j \Phi^*_k)_{[2,0,\ldots,0,1]}] = \Delta[\tilde{\Phi}_l (\Phi_k \Phi^*_i \Phi^*_j)_{[1,0,\ldots,0,2]}] = 2 - \frac{40}{3\pi^2 N_f} + O(1/N_f^2) \ , \tag{2.40}$$

$$\Delta[\Phi^*_l (\tilde{\Phi}_i \tilde{\Phi}_j \tilde{\Phi}^*_k)_{[2,0,\ldots,0,1]}] = \Delta[\Phi_l (\tilde{\Phi}_k \tilde{\Phi}^*_i \tilde{\Phi}^*_j)_{[1,0,\ldots,0,2]}] = 2 - \frac{40}{3\pi^2 N_f} + O(1/N_f^2) \ , \tag{2.41}$$

$$\Delta[|\Phi|^2_{adj} |\tilde{\Phi}|^2_{adj}] = 2 - \frac{64}{3\pi^2 N_f} + O(1/N_f^2) \ , \tag{2.42}$$

$$\Delta[\Phi^*_i \Phi^*_j \tilde{\Phi}_k \tilde{\Phi}_l] = \Delta[\Phi_i \Phi_j \tilde{\Phi}^*_k \tilde{\Phi}^*_l] = 2 - \frac{64}{3\pi^2 N_f} + O(1/N_f^2) \ . \tag{2.43}$$

2.1.4 bQED$_-$

The bQED$_-$ is reached with quartic deformation $V \sim (\sum |\Phi_i|^2 - |\tilde{\Phi}_i|^2)^2$ and by tuning mass terms to zero. Large N_f effective action is described by complex scalar fields $(\Phi_i, \tilde{\Phi}_i)$ minimally coupled to the effective photon and interacting with single HS field via cubic interaction.

$$\mathcal{L}_{eff} = \sum_{i=1}^{N_f/2} (|D\Phi_i|^2 + |D\tilde{\Phi}_i|^2) + \sigma_- (\sum_{i=1}^{N_f/2} |\Phi_i|^2 - \sum_{i=1}^{N_f/2} |\tilde{\Phi}_i|^2) \, . \tag{2.44}$$

Effective propagator for the photon is the same as in (2.8), and the effective propagators for the HS field σ_- is as follows

$$\langle \sigma_-(x) \sigma_-(0) \rangle = \frac{8}{\pi^2 N_f |x|^4} \ . \tag{2.45}$$

In the Feynman graphs we will use red dashed line for the effective propagator of σ_-. The global symmetry of the bQED$_-$ action is the same as for ep-bQED (2.30).

Scaling dimension of low-lying scalar operators

The N_f^2 quadratic gauge invariant operators are decomposed into irreducible representations of $SU(N_f/2)^2$ as in (2.31). Feynman graphs that contribute to the scaling dimensions of the operators $\{|\Phi|^2_{adj}, |\tilde{\Phi}|^2_{adj}\}$ are those in the left column of Tab. 2.4. The same graphs can be used to calculate scaling dimension of the bifundamental operators $\{\Phi_i\tilde{\Phi}^*_j, \Phi^*_i\tilde{\Phi}_j\}$, however the graph with HS field σ_- joining propagators Φ and $\tilde{\Phi}$ contributes with the opposite sign compared to the similar graph in the bQED$_+$. This is because the cubic vertices with HS field coupled to the scalar flavors $(\Phi, \tilde{\Phi})$ have different signs as it follows from the effective action (2.44). Notice that EOM of the HS field σ_- sets to zero the operator $(\sum|\Phi_i|^2 - \sum|\tilde{\Phi}_i|^2)$. Therefore that operator is out of the spectrum, while the plus combination is in the spectrum and has a dimension 1 at leading order.

The N_f^4 quartic gauge invariant operators are decomposed into irreducible representations of $SU(N_f/2)^2$ as in (2.34). Notice that in the last line of (2.34) not all the operators are excluded from the spectrum: the quartic operators which are a product of a quadratic operator $(\sum|\Phi_i|^2+\sum|\tilde{\Phi}_i|^2)$ and a quadratic adjoint or bifundamental operator, as well as the quartic operator $(\sum|\Phi_i|^2 + \sum|\tilde{\Phi}_i|^2)^2$ are in the spectrum and have scaling dimension equal to 2 in the leading order. In the table Tab. 2.7 we collected all the graphs that contribute to the anomalous scaling dimension of the quartic bifundamental operator $\frac{\left(\sum|\Phi_k|^2+\sum|\tilde{\Phi}_k|^2\right)\Phi_i\tilde{\Phi}^*_j}{\sqrt{N_f}}$. Similar computations can be done for the other operators. Below we give the list of operators and their scaling dimensions.

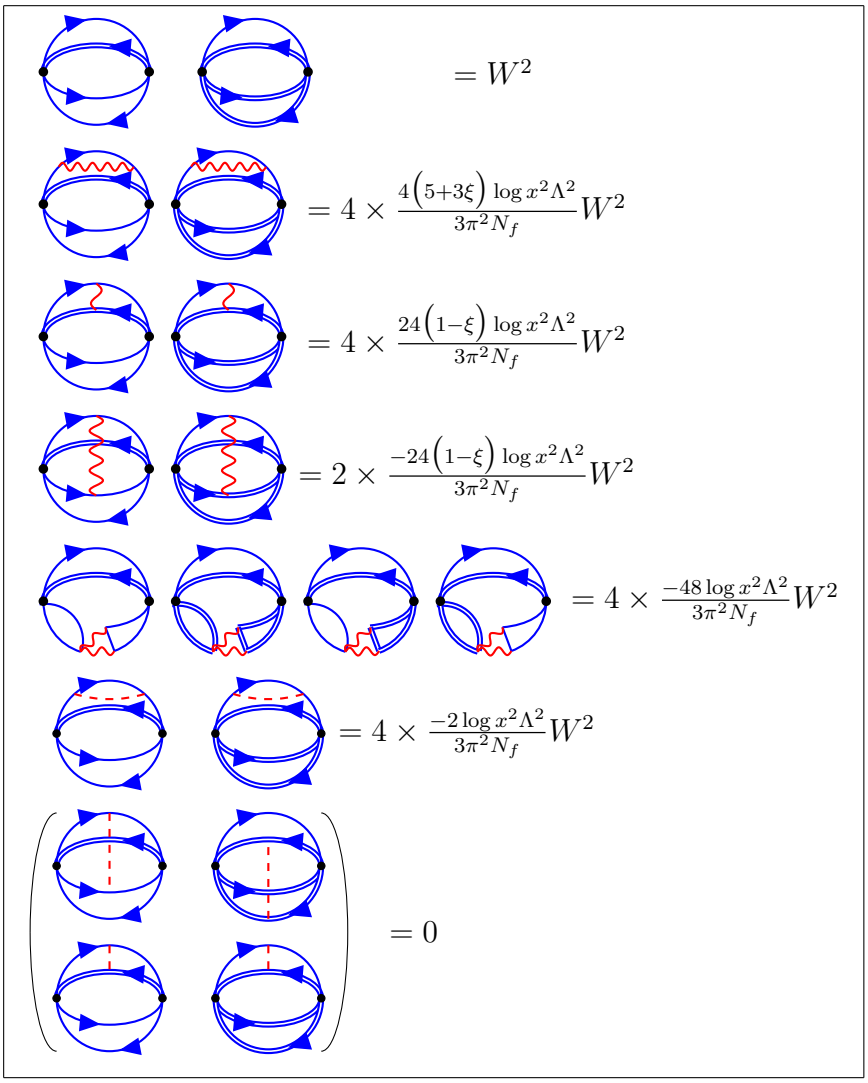

Table 2.7: (bQED$_-$) quartic bifundamental operator renormalization. Each graph has the flavor index $k = 1, ..., N_f$ running in its bottom loop.

$$\Delta[|\Phi|^2_{adj}] = \Delta[|\tilde{\Phi}|^2_{adj}] = 1 - \frac{48}{3\pi^2 N_f} + O(1/N_f^2) \ , \tag{2.46}$$

$$\Delta[\Phi_i \tilde{\Phi}^*_j] = \Delta[\Phi^*_i \tilde{\Phi}_j] = 1 - \frac{72}{3\pi^2 N_f} + O(1/N_f^2) \ , \tag{2.47}$$

$$\Delta\big[\big(\sum |\Phi_i|^2 + \sum |\tilde{\Phi}_i|^2\big)\big] = 1 + \frac{144}{3\pi^2 N_f} + O(1/N_f^2) \ , \tag{2.48}$$

$$\Delta[|\Phi|^4_{adj-2}] = \Delta[|\tilde{\Phi}|^4_{adj-2}] = 2 - \frac{48}{3\pi^2 N_f} + O(1/N_f^2) \ , \tag{2.49}$$

$$\Delta[\tilde{\Phi}^*_l (\Phi_i \Phi_j \Phi^*_k)_{[2,0,\ldots,0,1]}] = \Delta[\tilde{\Phi}_l (\Phi_k \Phi^*_i \Phi^*_j)_{[1,0,\ldots,0,2]}] = 2 - \frac{120}{3\pi^2 N_f} + O(1/N_f^2) \ , \tag{2.50}$$

$$\Delta[\Phi^*_l (\tilde{\Phi}_i \tilde{\Phi}_j \tilde{\Phi}^*_k)_{[2,0,\ldots,0,1]}] = \Delta[\Phi_l (\tilde{\Phi}_k \tilde{\Phi}^*_i \tilde{\Phi}^*_j)_{[1,0,\ldots,0,2]}] = 2 - \frac{120}{3\pi^2 N_f} + O(1/N_f^2) \ , \tag{2.51}$$

$$\Delta[|\Phi|^2_{adj} |\tilde{\Phi}|^2_{adj}] = 2 - \frac{144}{3\pi^2 N_f} + O(1/N_f^2) \ , \tag{2.52}$$

$$\Delta[\Phi^*_i \Phi^*_j \tilde{\Phi}_k \tilde{\Phi}_l] = \Delta[\Phi_i \Phi_j \tilde{\Phi}^*_k \tilde{\Phi}^*_l] = 2 - \frac{144}{3\pi^2 N_f} + O(1/N_f^2) \ , \tag{2.53}$$

$$\Delta\big[|\Phi|^2_{adj} \sum \big(|\Phi_i|^2 + |\tilde{\Phi}_i|^2\big)\big] = \Delta\big[|\tilde{\Phi}|^2_{adj} \sum \big(|\Phi_i|^2 + |\tilde{\Phi}_i|^2\big)\big] = 2 + \frac{96}{3\pi^2 N_f} + O(1/N_f^2) \ , \tag{2.54}$$

$$\Delta\big[\Phi_i \tilde{\Phi}^*_j \sum \big(|\Phi_i|^2 + |\tilde{\Phi}_i|^2\big)\big] = \Delta\big[\Phi^*_i \tilde{\Phi}_j \sum \big(|\Phi_i|^2 + |\tilde{\Phi}_i|^2\big)\big] = 2 + \frac{72}{3\pi^2 N_f} + O(1/N_f^2) \ , \tag{2.55}$$

$$\Delta[\sigma_-] = 2 + \frac{48}{3\pi^2 N_f} + O(1/N_f^2) \ , \tag{2.56}$$

$$\Delta\big[\big(\sum |\Phi_i|^2 + \sum |\tilde{\Phi}_i|^2\big)^2\big] = 2 + \frac{288}{3\pi^2 N_f} + O(1/N_f^2) \ . \tag{2.57}$$

2.2 Four fermionic QED fixed points in the large N_f limit

In this section we study fermionic QED, with large N_f complex fermionic flavors, imposing at least $U(N_f/2)^2$ global symmetry. There are four different fixed points, two fixed points have $U(N_f)$ global symmetry, two fixed points have $U(N_f/2)^2$ global symmetry.

Let us consider the following UV (Euclidean) lagrangian

$$\begin{aligned}\mathcal{L} =& \frac{1}{4e^2} F_{\mu\nu} F^{\mu\nu} + \sum_{i=1}^{N_f/2} (\bar{\Psi}_i \not{D} \Psi^i + \bar{\tilde{\Psi}}_i \not{D} \tilde{\Psi}^i) + \rho_+ \sum_{i=1}^{N_f/2} (\bar{\Psi}_i \Psi^i + \bar{\tilde{\Psi}}_i \tilde{\Psi}^i) \\ &+ \rho_- \sum_{i=1}^{N_f/2} (\bar{\Psi}_i \Psi^i - \bar{\tilde{\Psi}}_i \tilde{\Psi}^i) + m_+^2 \rho_+^2 + m_-^2 \rho_-^2 + \ldots \ ,\end{aligned} \tag{2.58}$$

where the dots stand for kinetic terms and quartic interactions of the Hubbard-Stratonovich fields ρ_+ and ρ_- [8]. We choose the gamma matrices to be equal to the Pauli matrices: $\gamma^0 = \sigma_2,\ \gamma^1 = \sigma_1,\ \gamma^2 = \sigma_3$, and $\not{D} = \gamma^\mu D_\mu$. The two-component Dirac fermions $(\Psi_i, \tilde{\Psi}_i)$ $(i = 1, ..., N_f/2)$ carry charge $+1$ under the gauge group. We also implicitly assume a conformal gauge fixing term. These type of theories (2.58) have been studied using various techniques, e.g. solving Schwinger-Dyson gap equations, epsilon expansion, functional RG flow [21, 22, 23, 26, 27, 28, 29, 32, 33, 76, 77, 78, 79].

Depending on the form of the Yukawa interactions, there are four different fixed points:

- fQED, both HS fields are massive and the Yukawa interactions are absent,
- QED-GN$_+$, the Yukawa interaction involving HS field ρ_+ is turned on and the HS field ρ_- is massive,
- QED-NJL (gauged Nambu-Jona-Lasinio), both HS fields $\rho_\pm$ are massless, and both Yukawa interactions are turned on,
- QED-GN$_-$, the Yukawa interaction involving HS field ρ_- is turned on and the HS field ρ_+ is massive.

2.2.1 fQED

In fQED both HS fields are massive and therefore decoupled from the IR spectrum. The large N_f effective action for the fQED fixed point is described by N_f copies of Dirac fermions Ψ_i (we collected all the fermions $(\Psi, \tilde{\Psi})$ into a single field and denoted it by Ψ) minimally coupled to the effective photon

$$\mathcal{L}_{eff} = \sum_{i=1}^{N_f} \bar{\Psi}^i \not{D} \Psi_i \ . \tag{2.59}$$

The effective photon propagator is obtained summing geometric series of bubble diagrams (2.1), where all the scalar (blue) loops are exchanged with fermion (green) loops.

$$\langle A_\mu(x) A_\nu(0) \rangle_{\text{eff}} = \frac{8}{\pi^2 N_f |x|^2} \Big((1-\xi)\delta_{\mu\nu} + 2\xi \frac{x_\mu x_\nu}{x^2} \Big) \ . \tag{2.60}$$

[8] The IR fixed points of the model (2.58) correspond to the UV fixed points of the gauged four-fermion model with interactions $g_1 \big[\sum_{i=1}^{N_f/2} (\bar{\Psi}_i \Psi^i + \bar{\tilde{\Psi}}_i \tilde{\Psi}^i) \big]^2 + g_2 \big[\sum_{i=1}^{N_f/2} (\bar{\Psi}_i \Psi^i - \bar{\tilde{\Psi}}_i \tilde{\Psi}^i) \big]^2$, where the couplings g_1 and g_2 have mass dimension -1. Introducing two HS fields ρ recasts the quartic interactions in the form of Yukawa couplings and "mass" terms like in (2.58). In this language the "mass" terms are schematically $\sim \frac{\rho^2}{g}$. Giving mass to ρ is equivalent to turning off the four-fermion couplings $g_{1,2}$.

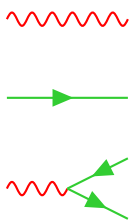

$= \langle A_\mu(x) A_\nu(0) \rangle_{\text{eff}}$

$= \frac{\not{x}}{4\pi |x|^3}$

$= -i\gamma_\mu$

Table 2.8: (fQED) Feynman rules for propagators and vertices.

We notice that the effective photon propagator in the fQED coincides with the effective photon propagator in the bosonic QED's. This is because the fermion and boson loops that appear in the geometric sums are equal to each other. Feynman rules for the vertices and for the propagators are given in Tab. 2.8.

The faithful global symmetry is

$$\frac{SU(N_f) \times U(1)_{\text{top}}}{\mathbb{Z}_{N_f}} \rtimes \mathbb{Z}_2^{\mathcal{C}} \ , \tag{2.61}$$

where $\mathbb{Z}_{N_f}$ is generated by $\left(e^{2\pi i/N_f}\mathbb{I}, -1\right) \in SU(N_f) \times U(1)_{\text{top}}$ (this fact comes from a careful treatment of the monopoles operators, which are dressed with fermionic zero-modes). $\mathbb{Z}_2^{\mathcal{C}}$ is the charge-conjugation symmetry. There is also symmetry under parity[9].

Scaling dimension of low-lying scalar operators [10]

The N_f^2 gauge invariant operators $\bar{\Psi}_i \Psi^j$ transform in the adjoint plus singlet of $SU(N_f)$. Their scaling dimensions at large N_f can be extracted from Feynman graphs in Tab. 2.9 and have already been discussed in [82, 83, 84]

$$\Delta[|\Psi|^2_{adj}] = 2 - \frac{64}{3\pi^2 N_f} + O(1/N_f^2) \ , \tag{2.62}$$

$$\Delta[|\Psi|^2_{sing}] = 2 + \frac{128}{3\pi^2 N_f} + O(1/N_f^2) \ . \tag{2.63}$$

2.2.2 QED-GN$_+$

In the QED-GN$_+$ fixed point the action is (2.58), with Yukawa interaction involving HS field ρ_+, while the HS field ρ_- is massive and is decoupled from the IR spectrum. The large N_f

[9] It is crucial to have even number of Dirac fermions, otherwise the theory suffers from parity anomaly.

[10] Check [80, 81] for scaling dimensions of quartic operators, which at infinite N_f have $\Delta = 4$.

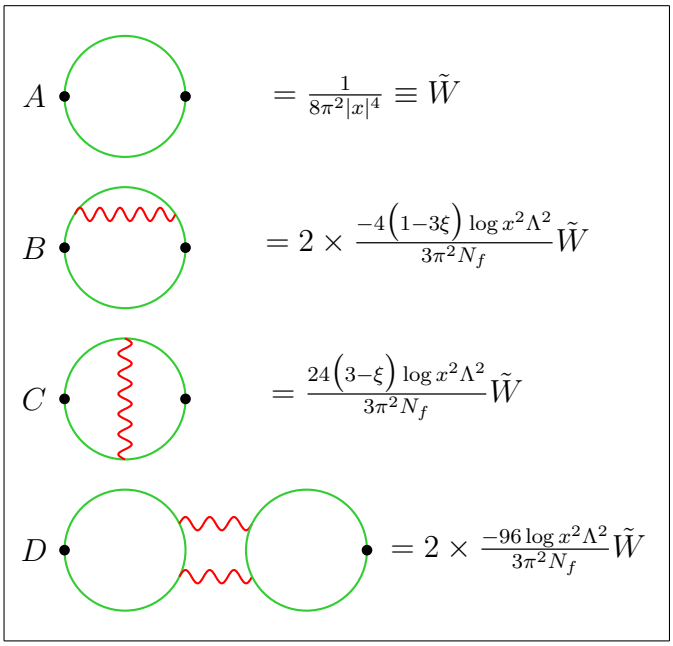

Table 2.9: (fQED) Results for individual Feynman graphs appearing in the 2-point correlation function for the fermion-bilinear operators.

effective action is described by N_f copies of Dirac fermions Ψ_i (we collected all the fermions $(\Psi, \tilde{\Psi})$ into a single field and denoted it by Ψ) minimally coupled to the effective photon and interacting with HS field ρ_+ via Yukawa interaction

$$\mathcal{L}_{eff} = \sum_{i=1}^{N_f} \bar{\Psi}_i \not{D} \Psi^i + \rho_+ \sum_{i=1}^{N_f} \bar{\Psi}_i \Psi^i \ . \tag{2.64}$$

The effective propagator for the photon is the same as in the fQED (2.60). The effective propagator for the HS field ρ_+ follows from summing geometric series of bubble diagrams as in Fig. 2.2 with all the scalar (blue) loops exchanged with fermion (green) loops

$$\langle \rho_+(x)\rho_+(0)\rangle_{eff} = \frac{4}{\pi^2 N_f |x|^2} \ . \tag{2.65}$$

In the Feynman graphs we use a red dashed line in order to represent the ρ_+ propagator. The global symmetry is the same as in fQED (2.61). There is also parity symmetry (ρ_+ is parity-odd).

Scaling dimension of low-lying scalar operators

As in fQED, the N_f^2 gauge invariant operators $\bar{\Psi}_i \Psi^j$ transform in the adjoint plus singlet representation of $SU(N_f)$. However, the singlet operator is set to zero by the equation of

motion of the HS field ρ_+. Order $O(1/N_f)$ scaling dimensions for the adjoint operator and for ρ_+ can be read using Tab. 2.10, for ρ_+^2 using Tab. 2.11 [11]

$$\Delta[|\Psi|^2_{adj}] = 2 - \frac{48}{3\pi^2 N_f} + O\left(1/N_f^2\right) \ , \tag{2.66}$$

$$\Delta[\rho_+] = 1 - \frac{144}{3\pi^2 N_f} + O\left(1/N_f^2\right) \ , \tag{2.67}$$

$$\Delta[\rho_+^2] = 2 - \frac{240}{3\pi^2 N_f} + O\left(1/N_f^2\right) \ . \tag{2.68}$$

We stress that in QED-GN$_+$ the Aslamazov-Larkin graph, which is the 6th graph in Tab. 2.10, gives a big contribution to the 2-point function of the HS field ρ_+. Instead in QED-GN$_-$ (see section 2.2.4) in the 2-point function of HS field ρ_- such AL graphs cancel each other. In the literature (see for instance [77, 89]) the QED-GN$_-$ is referred as QED-GN. The scaling dimension of the order parameter ρ_+^2 is related to the critical exponent ν:

$$\nu^{-1} = 3 - \Delta[\rho_+^2] = 1 + \frac{240}{3\pi^2 N_f} + O\left(1/N_f^2\right) \ . \tag{2.69}$$

[11] Soon after we presented these results in [6], also [85] computed the scaling dimensions (2.66, 2.67, 2.68). Their results agree with ours.

$= \langle \rho_+(x)\rho_+(0)\rangle_{eff} \equiv \tilde{U}$	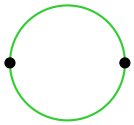 $= \tilde{W}$
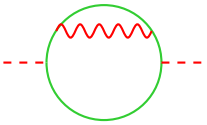 $= 2 \times \frac{4\left(1-3\xi\right)\log x^2\Lambda^2}{3\pi^2 N_f}\tilde{U}$	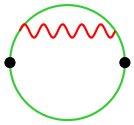 $= 2 \times \frac{-4\left(1-3\xi\right)\log x^2\Lambda^2}{3\pi^2 N_f}\tilde{W}$
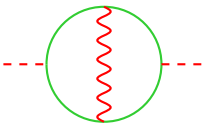 $= -\frac{24\left(3-\xi\right)\log x^2\Lambda^2}{3\pi^2 N_f}\tilde{U}$	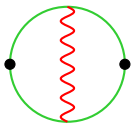 $= \frac{24\left(3-\xi\right)\log x^2\Lambda^2}{3\pi^2 N_f}\tilde{W}$
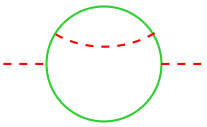 $= 2 \times \frac{2\log x^2\Lambda^2}{3\pi^2 N_f}\tilde{U}$	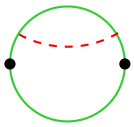 $= 2 \times \frac{-2\log x^2\Lambda^2}{3\pi^2 N_f}\tilde{W}$
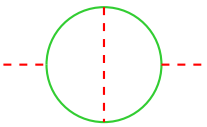 $= \frac{12\log x^2\Lambda^2}{3\pi^2 N_f}\tilde{U}$	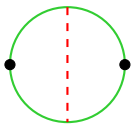 $= -\frac{12\log x^2\Lambda^2}{3\pi^2 N_f}\tilde{W}$
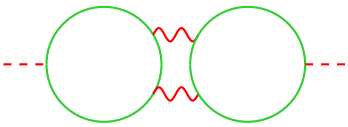 $= 2 \times \frac{96\log x^2\Lambda^2}{3\pi^2 N_f}\tilde{U}$	
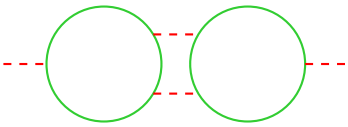 $= 0$	

Table 2.10: (QED-GN$_+$) Results for individual Feynman graphs appearing in the 2-point correlation functions $\langle \rho_+(x)\rho_+(0)\rangle$(left column)[12] and $\langle |\Psi|^2_{adj}(x)|\Psi|^2_{adj}(0)\rangle$ (right column).

[12]The last graph is vanishing (both the divergent and finite parts are zero). This is because parity invariance forbids single parity odd HS field to decay into 2 HS fields.

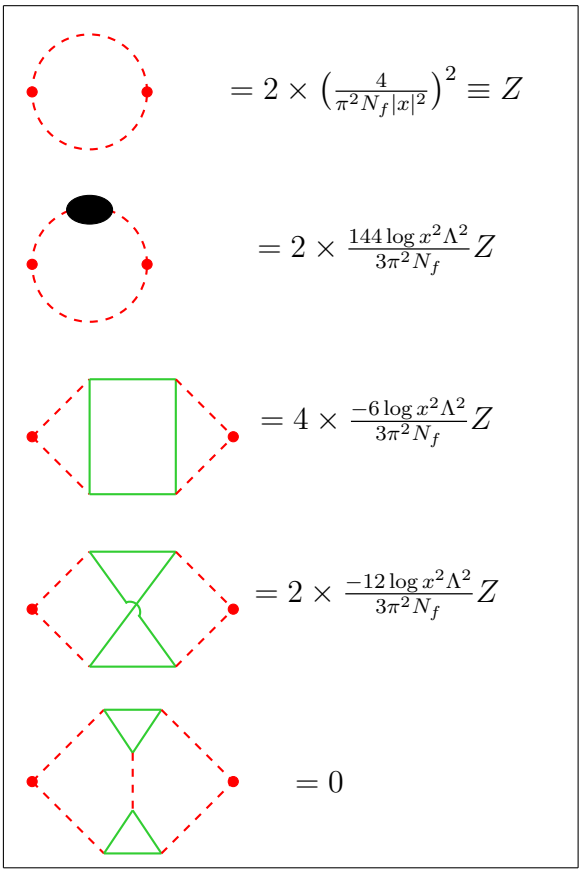

Table 2.11: (QED-GN$_+$) Feynman graphs appearing in the 2-point correlation function of the composite operator ρ_+^2 [13]. The black ellipse in the second diagram means dressing HS field propagator with graphs in the left column of Tab. 2.10.

2.2.3 QED-NJL

In the QED-NJL fixed point, the action is (2.58). It involves Yukawa interactions and the masses of the HS fields are tuned to zero. The large N_f effective action is described by N_f Dirac fermions $(\Psi_i, \tilde{\Psi}_i)$ minimally coupled to the effective photon and interacting with the HS fields $(\rho, \tilde{\rho})$ via Yukawa interactions

$$\mathcal{L}_{eff} = \sum_{i=1}^{N_f/2} \bar{\Psi}_i \not{D} \Psi^i + \sum_{i=1}^{N_f/2} \bar{\tilde{\Psi}}_i \not{D} \tilde{\Psi}^i + \rho \sum_{i=1}^{N_f/2} \bar{\Psi}_i \Psi^i + \tilde{\rho} \sum_{i=1}^{N_f/2} \bar{\tilde{\Psi}}_i \tilde{\Psi}^i \ , \tag{2.70}$$

[13] The last Feynman graph is vanishing because the triangle subgraphs made by fermion propagators are identically zero.

where

$$\rho = \rho_+ + \rho_- \ , \tag{2.71}$$

$$\tilde{\rho} = \rho_+ - \rho_- \ . \tag{2.72}$$

The photon "sees" all the flavors, therefore effective photon propagator is the same as in fQED (2.60). The effective propagators for the HS fields are

$$\langle \rho(x)\rho(0)\rangle = \langle \tilde{\rho}(x)\tilde{\rho}(0)\rangle = \frac{4}{\pi^2(N_f/2)|x|^2} \ . \tag{2.73}$$

The continuous global symmetry is:

$$\frac{(SU(N_f/2) \times SU(N_f/2) \times U(1)_b \times U(1)_{\text{top}}) \rtimes \mathbb{Z}_2^e}{\mathbb{Z}_{N_f}} \rtimes \mathbb{Z}_2^C \ . \tag{2.74}$$

Parity is preserved, provided $(\rho, \tilde{\rho})$ and $\rho_\pm$ are odd under parity transformation. The other global symmetries act as follows. $U(1)_b$: $\{\Psi \to e^{i\alpha}\Psi,\ \tilde{\Psi} \to e^{-i\alpha}\tilde{\Psi}\}$, $\mathbb{Z}_2^e$: $\{\Psi \leftrightarrow \tilde{\Psi}, \rho \leftrightarrow \tilde{\rho}\}$.

Scaling dimension of low-lying scalar operators

The gauge invariant fermion bilinear operators are classified as irreducible representations (2.31) under $SU(N_f/2)^2$ symmetry group. The calculation of the scaling dimensions for the adjoint and the bifundamental operators is parallel to the calculation of the scaling dimensions of the similar operators in the ep-bQED and can be done using the graphs in Tab. 2.10.

The quadratic singlet operators are out of the spectrum, they are set to zero by the EOM of the HS fields $(\rho, \tilde{\rho})$. The two-point correlation function for the ρ field can be calculated using the left column diagrams of Tab. 2.10. Taking into account the necessary changes we get

$$\langle \rho(x)\rho(0)\rangle = \Big(1 + \frac{64 \log x^2\Lambda^2}{3\pi^2 N_f}\Big)\Big(\frac{4}{\pi^2(N_f/2)|x|^2}\Big) \ . \tag{2.75}$$

Notice that at order $O(1/N_f)$ there is a mixing between ρ and $\tilde{\rho}$, Fig. 2.4.

$$\langle \rho(x)\tilde{\rho}(0)\rangle = \frac{96 \log x^2\Lambda^2}{3\pi^2 N_f}\Big(\frac{4}{\pi^2(N_f/2)|x|^2}\Big) \ . \tag{2.76}$$

Instead, the fields (ρ_+, ρ_-) do not mix, they are the eigenvectors of the mixing matrix. Using (2.75, 2.76) one can calculate anomalous dimensions of these fields.

In Tab. 2.12 we collected all the graphs that contribute to the mixing of operators quadratic in HS fields: $\{\rho^2(x), \tilde{\rho}^2(x), \sqrt{2}\rho\tilde{\rho}(x)\}$. We get the following mixing matrix

$$\begin{pmatrix} 1+\frac{32\log x^2\Lambda^2}{3\pi^2 N_f} & 0 & \frac{96\sqrt{2}\log x^2\Lambda^2}{\pi^2 N_f} \\ 0 & 1+\frac{32\log x^2\Lambda^2}{3\pi^2 N_f} & \frac{96\sqrt{2}\log x^2\Lambda^2}{\pi^2 N_f} \\ \frac{96\sqrt{2}\log x^2\Lambda^2}{\pi^2 N_f} & \frac{96\sqrt{2}\log x^2\Lambda^2}{\pi^2 N_f} & 1+\frac{128\log x^2\Lambda^2}{3\pi^2 N_f} \end{pmatrix} \times \tilde{Z} \ , \tag{2.77}$$

where $\tilde{Z}$ is defined in Tab. 2.12. Using (2.77) it is straightforward to pass to the eigenbasis and find the scaling dimension for each of the eigenbasis operators. Below we give the list of operators and their scaling dimensions

$$\Delta[|\Psi|^2_{adj}] = \Delta[|\tilde{\Psi}|^2_{adj}] = 2 - \frac{32}{3\pi^2 N_f} + O(1/N_f^2) \ , \tag{2.78}$$

$$\Delta[\bar{\tilde{\Psi}}_i \Psi_j] = \Delta[\bar{\Psi}_j \tilde{\Psi}_i] = 2 - \frac{56}{3\pi^2 N_f} + O(1/N_f^2) \ , \tag{2.79}$$

$$\Delta[\rho_+] = 1 - \frac{160}{3\pi^2 N_f} + O(1/N_f^2) \ , \tag{2.80}$$

$$\Delta[\rho_-] = 1 + \frac{32}{3\pi^2 N_f} + O(1/N_f^2) \ , \tag{2.81}$$

$$\Delta[\rho_+\rho_-] = 2 - \frac{32}{3\pi^2 N_f} + O(1/N_f^2) \ , \tag{2.82}$$

$$\Delta[\rho_+^2 + (4+\sqrt{17})\rho_-^2] = 2 - \frac{16(5-3\sqrt{17})}{3\pi^2 N_f} + O(1/N_f^2) \ , \tag{2.83}$$

$$\Delta[\rho_+^2 + (4-\sqrt{17})\rho_-^2] = 2 - \frac{16(5+3\sqrt{17})}{3\pi^2 N_f} + O(1/N_f^2) \ . \tag{2.84}$$

A similar model with two HS scalars was studied in [86]. Their model seems to be different from QED-NJL we discuss, in particular the anomalous dimensions of HS fields are different from ours.

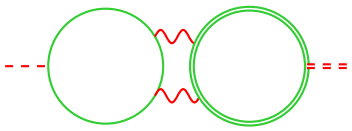

$$= 2 \times \frac{48\log x^2\Lambda^2}{3\pi^2 N_f} \frac{4}{\pi^2 (N_f/2)|x|^2}$$

Figure 2.4: Diagram responsible for mixing $\langle \rho(x)\tilde{\rho}(0)\rangle$.

$\langle\rho^2(x)\rho^2(0)\rangle$:	$= 2\times\left(\frac{4}{\pi^2(N_f/2)\lvert x\rvert^2}\right)^2 \equiv \tilde{Z}$ $= 2\times\frac{64\log x^2\Lambda^2}{3\pi^2 N_f}\tilde{Z}$ 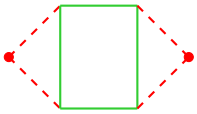 $= 4\times\frac{-12\log x^2\Lambda^2}{3\pi^2 N_f}\tilde{Z}$ 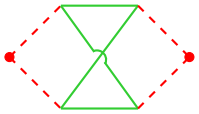 $= 2\times\frac{-24\log x^2\Lambda^2}{3\pi^2 N_f}\tilde{Z}$
$\langle\sqrt{2}\rho\tilde{\rho}(x)\sqrt{2}\rho\tilde{\rho}(0)\rangle$:	$= \tilde{Z}$ $= 2\times\frac{64\log x^2\Lambda^2}{3\pi^2 N_f}\tilde{Z}$
$\langle\rho^2(0)\sqrt{2}\rho\tilde{\rho}(0)$:	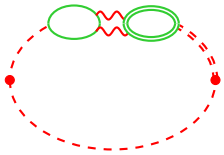 $= \frac{96\sqrt{2}\log x^2\Lambda^2}{3\pi^2 N_f}\tilde{Z}$

Table 2.12: (QED-NJL) mixing of quadratic in HS field operators.

2.2.4 QED-GN$_-$

In the QED-GN$_-$ fixed point the action is (2.58), with Yukawa interaction involving the HS field ρ_-, while the HS field ρ_+ is massive and is decoupled from the IR spectrum. The large N_f effective action is described by Dirac fermions $(\Psi_i, \tilde{\Psi}_i)$ minimally coupled to the effective photon and interacting with the HS field ρ_- via Yukawa interaction

$$\mathcal{L}_{eff} = \sum_{i=1}^{N_f/2}(\bar{\Psi}_i \not{D}\Psi^i + \bar{\tilde{\Psi}}_i \not{D}\tilde{\Psi}^i) + \rho_-(\sum_{i=1}^{N_f/2}\bar{\Psi}_i\Psi^i - \sum_{i=1}^{N_f/2}\bar{\tilde{\Psi}}_i\tilde{\Psi}^i)\,. \tag{2.85}$$

The effective photon propagator is as in (2.60) because the photon "sees" all the flavors. The effective propagator for the HS field ρ_- is

$$\langle\rho_-(x)\rho_-(0)\rangle = \frac{4}{\pi^2 N_f|x|^2}\ . \tag{2.86}$$

The continuous global symmetry is the same as that of QED-NJL (2.74). Parity is preserved provided HS field ρ_- is odd under parity transformation. The discrete symmetry $\mathbb{Z}_2^e$ acts: $\{\Psi \leftrightarrow \tilde{\Psi}, \rho_- \leftrightarrow -\rho_-\}$.

Scaling dimension of low-lying scalar operators

The fermion bilinear operators are classified according to the irreducible representations of $SU(N_f/2)^2$, like in (2.31). Notice that ρ_- takes the operator $\sum_{i=1}^{N_f/2}(\bar{\Psi}_i\Psi^i - \bar{\tilde{\Psi}}_i\tilde{\Psi}^i)$ out from the spectrum, while the plus combination remains in the spectrum and has dimension 2 at the leading order.

The scaling dimension of the HS field ρ_- is calculated using the graphs in the left column of Tab. 2.10. The contributions of the first 5 graphs remain unchanged, while there are 4 AL graphs (each with two photons) and they are canceling each other. This is due to the fact that ρ_- field couples to the fermion flavors $(\Psi, \tilde{\Psi})$ with different signs and therefore the three loop graph which has fermions Ψ running in one of its loops and fermions $\tilde{\Psi}$ running in the other loop comes with an opposite sign with respect to the three loop graph made solely by fermions Ψ (or $\tilde{\Psi}$). The scaling dimensions for the other operators can be calculated easily.

$$\Delta[|\Psi|^2_{adj}] = \Delta[|\tilde{\Psi}|^2_{adj}] = 2 - \frac{48}{3\pi^2 N_f} + O(1/N_f^2) \ , \tag{2.87}$$

$$\Delta[\bar{\tilde{\Psi}}_i\Psi_j] = \Delta[\bar{\Psi}_j\tilde{\Psi}_i] = 2 - \frac{72}{3\pi^2 N_f} + O(1/N_f^2) \ , \tag{2.88}$$

$$\Delta\big[\frac{1}{\sqrt{N_f}}\big(\sum|\Psi_i|^2 + \sum|\tilde{\Psi}_i|^2\big)\big] = 2 + \frac{144}{3\pi^2 N_f} + O(1/N_f^2) \ , \tag{2.89}$$

$$\Delta[\rho_-] = 1 + \frac{48}{3\pi^2 N_f} + O(1/N_f^2) \ , \tag{2.90}$$

$$\Delta[\rho_-^2] = 2 + \frac{144}{3\pi^2 N_f} + O(1/N_f^2) \ . \tag{2.91}$$

Some of these results have been obtained in [87, 88, 89], which also include some scaling dimensions at order $O(1/N_f^2)$.

2.3 Super-QED in the large N_f limit

In this section we compute the large N_f scaling dimension of mesonic operators in QED with minimal supersymmetry, and then compare the results, at $N_f = 2$, with a dual Gross-Neveu-Yukawa model. At the end we also consider an $\mathcal{N} = 2$ super-QED.

The UV action of $2+1d$ QED with minimal supersymmetry, $\mathcal{N} = 1$ (i.e. 2 supercharges), N_f flavors and zero superpotential

$$\mathcal{W}_{\mathcal{N}=1} = 0 \, , \tag{2.92}$$

has the form

$$S_{UV} = \int d^3x \Big(-\frac{1}{4e^2} F_{\mu\nu}F^{\mu\nu} + \frac{1}{2e^2}\bar{\lambda} i\partial\!\!\!/ \lambda + \bar{\Psi}_j i\gamma^\mu D_\mu \Psi^j + \overline{D_\mu \Phi_j} D^\mu \Phi^j$$
$$+ i\bar{\Psi}_j \lambda \Phi^j - i\bar{\lambda}\Psi^j \Phi_j^* - \frac{N_f}{32i(1-\xi)} \int d^3y \frac{\partial_\mu A^\mu(x)\partial_\nu A^\nu(y)}{2\pi^2|x-y|^2} \Big) \ . \tag{2.93}$$

The action (2.93) is written in the Minkowski metric. Our convention for the Minkowski metric is $(+,-,-)$. The kinetic terms for the photon and for the gaugino are non canonically normalised, the covariant derivative is $D_\mu = \partial_\mu + iA_\mu$. We have N_f flavors of Dirac fermions and complex scalars: $\Psi^j,\ \Phi^j,\ j = 1, ..., N_f$. Our conventions for the gamma matrices are: $\gamma^0 = \sigma_2,\ \gamma^1 = i\sigma_1,\ \gamma^2 = i\sigma_3$, where σ_i are the Pauli matrices. We define $\bar{\Psi} = \Psi^\dagger \gamma^0$. Notice that gaugino is a Majorana fermion, with our conventions for the gamma matrices it has two real components.

The action (2.93) is written in the Wess-Zumino gauge, which explicitly breaks supersymmetry, the remaining gauge symmetry is fixed by adding the conformal gauge fixing term in the action. The $\mathcal{N} = 1$ supersymmetry of the action (2.93) becomes obvious when one constructs it using superspace integrals and superfields, for more details check [91]. The fields are organized in $\mathcal{N} = 1$ super-multiplets: a vector multiplet $\{\lambda, A_\mu\}$ and N_f scalar matter multiplets $\{\Phi^i, \Psi^i, F^i\}$. Going on-shell one sets $F^i = 0$. The global symmetry of the action is

$$\frac{SU(N_f) \times U(1)_{\text{top}}}{\mathbb{Z}_{N_f}} \rtimes \mathbb{Z}_2^{\mathcal{C}} \ . \tag{2.94}$$

Additionally there is parity invariance. These symmetries prevent the generation of additional interactions (quadratic or quartic superpotential interactions would break parity invariance), therefore there is no need of tuning interactions to zero.

The large N_f effective action of the $\mathcal{N} = 1$ SQED is described by N_f scalar and N_f fermion flavors minimally coupled to the effective photon and interacting with the effective gaugino via a Yukawa interaction

$$S_{IR} = \int d^3x \big(\bar{\Psi}_j i\gamma^\mu D_\mu \Psi^j + \overline{D_\mu \Phi_j} D^\mu \Phi^j + i\bar{\Psi}_j \lambda \Phi^j - i\bar{\lambda}\Psi^j \Phi_j^\dagger \big) \ . \tag{2.95}$$

The effective photon propagator is obtained by summing a geometric series of bubble diagrams with fermion and scalar loops. We give the effective photon propagator after Wick rotation from Minkowski to Euclidean space

$$\langle A_\mu(x) A_\nu(0) \rangle_{\text{eff}} = -\frac{4i}{\pi^2 N_f |x|^2} \big((1-\xi)\delta_{\mu\nu} + 2\xi \frac{x_\mu x_\nu}{|x|^2} \big) \ . \tag{2.96}$$

The effective gaugino propagator is obtained by summing a geometric series of bubble diagrams with each bubble made by one fermion and one boson propagators, after Wick rotation we have following expression

$$\left\langle \lambda(x)\lambda^T(0)\right\rangle_{\text{eff}} = \frac{8i(\not{x}\gamma^0)}{\pi^2 N_f |x|^4} \ . \tag{2.97}$$

We use red dotted line to represent effective gaugino propagator in the Feynman graphs.

2.3.1 Scaling dimension of low-lying mesonic operators

The following three quadratic operators sit inside the same $\mathcal{N}=1$ supermultiplet

$$\begin{pmatrix} \Phi^*\Phi \\ \Phi^*\Psi_\alpha + \Phi\Psi^*_\alpha \\ \bar{\Psi}\Psi \end{pmatrix} \ . \tag{2.98}$$

where α is a spinor index. Depending how the flavor indices are contracted we can construct a singlet and an adjoint representation of the global symmetry $SU(N_f)$.

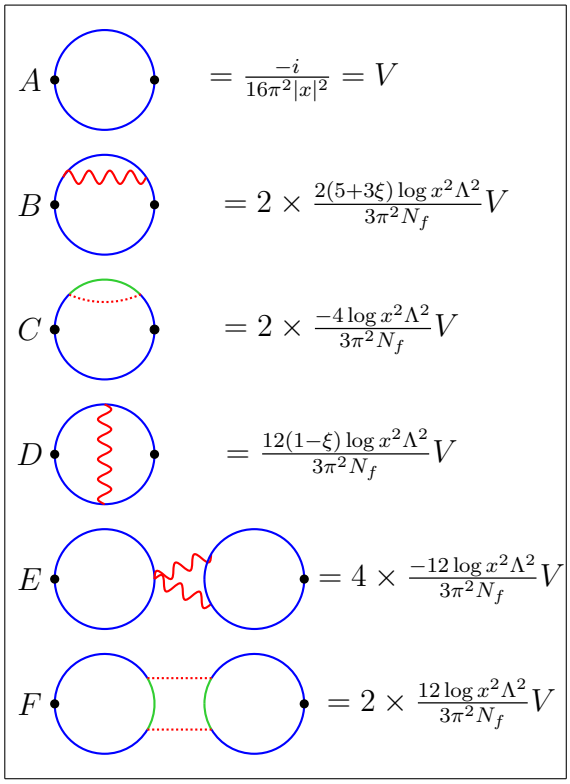

Table 2.13: ($\mathcal{N}=1$ SQED) Results for individual Feynman graphs appearing in the 2-point correlation function for the scalar-bilinear operators.

Let us first discuss the adjoint supermultiplet. Using the graphs A,B,C,D from Tab. 2.13 we can extract the scaling dimension of the adjoint scalar-bilinear operator

$$\begin{aligned}\langle|\Phi|^2_{adj}(x)|\Phi|^2_{adj}(0)\rangle &= \frac{-i}{16\pi^2|x|^2} + \frac{-i}{16\pi^2|x|^2}\Big(\frac{4(5+3\xi)}{3\pi^2 N_f} - \frac{8}{3\pi^2 N_f} + \frac{12(1-\xi)}{3\pi^2 N_f}\Big)\log x^2\Lambda^2 \\ &= \frac{-i}{16\pi^2|x|^2}\Big[1 - \Big(-\frac{24}{3\pi^2 N_f}\Big)\log x^2\Lambda^2\Big] \\ &= \frac{-i}{16\pi^2|x|^2}\Big(\frac{1}{x^2\Lambda^2}\Big)^{\Delta^{(1)}_{adj}} \ . \end{aligned} \tag{2.99}$$

The anomalous dimension of the adjoint operator is $\Delta^{(1)}_{adj} = -\frac{24}{3\pi^2 N_f}$. Due to supersymmetry the scaling dimensions of the components in (2.98) are related to each other.

$$\Delta[(\Phi^*\Phi)_{adj}] = 1 - \frac{24}{3\pi^2 N_f} + O(1/N_f^2) \ , \tag{2.100}$$

$$\Delta[(\Phi^*\Psi_\alpha + \Phi\Psi^*_\alpha)_{adj}] = \frac{3}{2} - \frac{24}{3\pi^2 N_f} + O(1/N_f^2) \ , \tag{2.101}$$

$$\Delta[(\bar\Psi\Psi)_{adj}] = 2 - \frac{24}{3\pi^2 N_f} + O(1/N_f^2) \ . \tag{2.102}$$

It is also possible to construct another scalar-fermion bilinear

$$(\Phi^*\Psi_\alpha - \Phi\Psi^*_\alpha)_{adj} \ . \tag{2.103}$$

We checked that anomalous dimension of (2.103) is vanishing at order $O(1/N_f)$. This is not surprising since operator (2.103) sits in the same supermultiplet with the gauge invariant flavor current operator $\big(\bar\Psi\gamma^\mu\Psi + i(\Phi^* D^\mu\Phi - \overline{D^\mu\Phi}\cdot\Phi)\big)_{adj}$, which is conserved and has a scaling dimension exactly equal to 2 for any N_f.

In order to compute the anomalous dimension of the singlet scalar-bilinear operator, we use all the graphs in the Tab. 2.13, since for this operator all of them contribute. It turns out that the anomalous scaling dimension vanishes at that order (there seems to be no reason to think that at higher orders in the $1/N_f$ expansion the anomalous corrections are going to be absent). Also the singlet supermultiplet (2.98) has the dimensions of its components related to each other:

$$\Delta[(\Phi^*\Phi)_{sing}] = 1 + O(1/N_f^2) \ , \tag{2.104}$$

$$\Delta[(\Phi^*\Psi_\alpha + \Phi\Psi^*_\alpha)_{sing}] = \frac{3}{2} + O(1/N_f^2) \ , \tag{2.105}$$

$$\Delta[(\bar\Psi\Psi)_{sing}] = 2 + O(1/N_f^2) \ . \tag{2.106}$$

Notice that the singlet counterpart of (2.103) is out of spectrum. This is precisely the operator that couples to gaugino in the effective action (2.95) and it is set to zero by the EOM of the gaugino field.

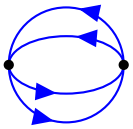	$= -\frac{i}{(4\pi\lvert x\rvert)^4} = H$
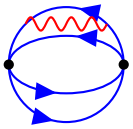	$= 4 \times \frac{2\left(5+3\xi\right)\log x^2\Lambda^2}{3\pi^2 N_f} H$
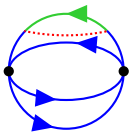	$= 4 \times \frac{-4\log x^2\Lambda^2}{3\pi^2 N_f} H$
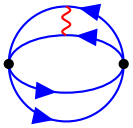	$= 2 \times \frac{-12\left(1-\xi\right)\log x^2\Lambda^2}{3\pi^2 N_f} H$
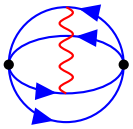	$= 4 \times \frac{12\left(1-\xi\right)\log x^2\Lambda^2}{3\pi^2 N_f} H$

Table 2.14: ($\mathcal{N} = 1$ SQED) quartic adjoint-2 operator renormalization.

Next we consider scalar quartic operators (2.15). In the equation (2.16) we decomposed this operator into irreducible representations of $SU(N_f)$ group: singlet, adjoint, adjoint-2. In order to extract the scaling dimension of the quartic adjoint-2 operator we need the Feynman graphs of Tab. 2.14. Similar calculations can be done for the other two operators. We skip the details and give the final result below

$$\Delta[|\Phi|^4_{adj-2}] = 2\Delta[|\Phi|^2_{adj}] + O(1/N_f^2) = 2 - \frac{48}{3\pi^2 N_f} + O(1/N_f^2) \ , \tag{2.107}$$

$$\Delta[|\Phi|^4_{adj}] = \Delta[|\Phi|^2_{adj}] + \Delta[|\Phi|^2_{sing}] + O(1/N_f^2) = 2 - \frac{24}{3\pi^2 N_f} + O(1/N_f^2) \ , \tag{2.108}$$

$$\Delta[|\Phi|^4_{sing}] = 2\Delta[|\Phi|^2_{sing}] + O(1/N_f^2) = 2 + O(1/N_f^2) \ . \tag{2.109}$$

2.3.2 The duality $\mathcal{N}$=1 SQED with N_f=2 $\leftrightarrow$ 7-field Wess-Zumino model: a quantitative check

The $\mathcal{N} = 1$ super-QED with two flavors ($N_f = 2$) has been argued to be dual to a cubic $\mathcal{N} = 1$ supersymmetric Wess-Zumino model with $SU(2) \times U(1)$ global symmetry [17, 18]. The field content of the WZ model is given by 7 real $\mathcal{N} = 1$ supermultiplets: a real triplet μ_I and a complex doublet M_α. The superpotential of the WZ model is dictated by the

$SU(2) \times U(1)$ global symmetry and by parity invariance:

$$\mathcal{W}_{\mathcal{N}=1} = \mu_I M_\alpha (\sigma_I)_{\alpha\beta} M^\dagger_\beta \ . \tag{2.110}$$

The real fields μ_I map to the quadratic mesons on the gauge theory side. The complex fields M_α map to the monopoles with minimal topological charge. This duality can be obtained starting from the $\mathcal{N} = 4$ mirror symmetry [92, 93], which in the IR relates abelian gauge theory with one hypermultiplet flavor to a free massless hypermultiplet. The $\mathcal{N} = 1$ duality also has a description in terms of S-duality of Type IIB brane setups [94].

In Tab. 2.15 we collect the basic gauge invariant operators. On the left side we list the operators which belong to the spectrum of $\mathcal{N} = 1$ SQED, their approximate scaling dimensions are calculated using the large N_f formulas obtained in the previous two sections. We also include the scaling dimension of the monopole operators $\mathfrak{M}^{\pm 1}$ in the large N_f limit ($\Delta[\mathfrak{M}^{\pm 1}] = 0.3619 N_f + O(1)$), which we extract from the results of [14] in appendix D. On the right side we list the operators of the dual WZ model, their scaling dimensions are calculated using $4-\epsilon$ expansion in [18]. Using the map discussed in detail in [18], on each row the two operators map into each other under the duality. We notice a quite good agreement between the dimensions of the corresponding operators, providing a nice quantitative check of the $\mathcal{N} = 1$ duality.

$\Delta[\mathfrak{M}^{\pm 1}] \sim 0.724$	$\Delta[M_\alpha] \sim 0.76$
$\Delta[(\Phi^*\Phi)_{spin-1}] \sim \left(1 - \frac{24}{3\pi^2 2}\right) = 0.595$	$\Delta[\mu_I] \sim 0.66$
$\Delta[(\Phi^*\Phi)_{sing}] \sim 1$	$\Delta[-2\sum \mu_I^2 + \sum \lvert M_\alpha \rvert^2] \sim 1$
$\Delta[\lvert\Phi\rvert^4_{spin-2}] \sim \left(2 - \frac{48}{3\pi^2 2}\right) = 1.19$	$\Delta[\mu_I \mu_J - \frac{\delta_{IJ}}{3} \sum \mu_K^2] \sim 1.33$
$\Delta[\lvert\Phi\rvert^4_{sing}] \sim 2$	$\Delta[2\sum \mu_I^2 + 3\sum \lvert M_\alpha \rvert^2] \sim 2.33$

Table 2.15: Operator mapping across the duality and the scaling dimensions of the operators .

2.3.3 The $\mathcal{N} = 1$ supersymmetric $O(N)$ sigma model and $\mathcal{N} = 2$ SQED

For completeness, we also discuss the large N_f limit of the "chiral" $\mathcal{N} = 2$ QED, with N_f flavors and 0 anti-flavors (also denoted as $(N_f, 0)$ flavors).

In $2+1$ dimensions, the $\mathcal{N}=2$ chiral multiplet has the field content

$$\Phi \quad \Psi \quad F \ , \tag{2.111}$$

where the Φ is a complex scalar, and Ψ is a two-component Dirac fermion and F is an auxiliary complex field. The vector multiplet has the field content

$$A_\mu \quad \sigma \quad \lambda_1 \quad \lambda_2 \quad D \ . \tag{2.112}$$

Where σ and D are real scalars, the $\lambda_{1,2}$ are real two-component Majorana fermions, which usually are combined into a single two-component Dirac fermion $(\lambda_1 + i\lambda_2)$. $(N_f, 0)$ flavored $\mathcal{N}=2$ SQED has N_f chiral multiplets (2.111) with charge $+1$ minimally coupled to a vector multiplet (2.112). One can write the action of this theory in $\mathcal{N}=1$ language. For this purpose we regroup the fields (2.111, 2.112) into the following $\mathcal{N}=1$ multiplets

$$\begin{aligned} V: &\quad A_\mu \quad \lambda_1 \ , \\ H: &\quad \sigma \quad \lambda_2 \quad D \ , \\ Q_i: &\quad \Phi^i \quad \Psi^i \quad F^i \ . \end{aligned} \tag{2.113}$$

The $\mathcal{N}=2$ SQED action can be written as a $\mathcal{N}=1$ SQED action (2.93), plus a kinetic term for H and interaction from the superpotential

$$\mathcal{W}_{\mathcal{N}=1} = H\bar{Q}_i Q^i \ . \tag{2.114}$$

Written in Lorentzian metric, the full action in components becomes

$$\begin{aligned} S^{\mathcal{N}=2} = S^{\mathcal{N}=1} &+ \frac{1}{2e^2}\int d^3x\big(\partial^\mu\sigma\partial_\mu\sigma + \bar{\lambda}_2 i\gamma^\mu\partial_\mu\lambda_2 + D^2\big) \\ &+ \int d^3x\big(-\sigma^2\Phi^*_j\Phi^j + \sigma\bar{\Psi}_j\Psi^j + (\bar{\Psi}_j\lambda_2\Phi^j + \bar{\lambda}_2\Psi^j\Phi^*_j) + D\Phi^*_j\Phi^j\big) \ . \end{aligned} \tag{2.115}$$

where the first term in the right hand side of (2.115) is defined in (2.93). The gaugino λ in (2.93) is replaced by λ_1. We have a quartic term in the second line because we have integrated out the auxiliary fields F^j:

$$F^*_j F^j - \sigma(\Phi^*_j F^j + \Phi^j F^*_j) \ \rightarrow \ -\sigma^2\Phi^*_j\Phi^j \ . \tag{2.116}$$

Performing a $1/N_f$ expansion with quartic vertix is usually more involved task than working with the cubic vertex, therefore one usually doesn't integrate out F^j (2.116). However at order $O(1/N_f)$ this is not a problem, and we work with the action (2.115), in order to have less fields. The scaling dimensions of the fields sitting in the chiral multiplet H at the IR fixed point are

$$\Delta[\sigma] = 1, \quad \Delta[\lambda_2] = 3/2, \quad \Delta[D] = 2 \ . \tag{2.117}$$

Due to supersymmetry, these dimensions are exact in $1/N_f$ expansion. This follows from the fact that the dimension of the gauge field A_μ is exactly 1 and the fields $(A_\mu, \sigma, \lambda_1, \lambda_2, D)$ sit in the same vector multiplet. The operator $(\Phi^*\Phi_{adj})$ has a scaling dimension exactly equal to 1, since it sits in the same $\mathcal{N}=2$ supermultiplet of the flavor $SU(N_f)$ currents.

These observations allow us to check our results for the singlet and adjoint operator dimensions obtained in $\mathcal{N}=1$ SQED. For this purpose first we notice that the action (2.115) without the first term is the $\mathcal{N}=1$ supersymmetric $O(N)$ sigma model [95]. The large N_f scaling dimensions of the field σ and of the bilinear adjoint operator for this model have been computed in [95] (see [96] for a finite-N_f study in the $4-\epsilon$ expansion):

$$\Delta[|\Phi|^2_{adj}]_{\mathcal{N}=1\,O(N)} = 1 + \frac{24}{3\pi^2 N_f} + O(1/N_f^2) \ , \tag{2.118}$$

$$\Delta[\sigma]_{\mathcal{N}=1\,O(N)} = 1 + O(1/N_f^2) \ . \tag{2.119}$$

For both of these operators the list of possible diagrams contributing to the 2-point correlation functions in $\mathcal{N}=2$ SQED are exhausted by the lists given in the context of $\mathcal{N}=1$ SQED and $\mathcal{N}=1$ supersymmetric sigma model (if one goes to the order $O(1/N_f^2)$ there might be graphs with propagators present from both multiplets V and H). Therefore the sum of this contributions should be such that anomalous scaling dimensions for $|\Phi|^2_{adj}$ and σ are exactly zero. As one can see from (2.118, 2.119) and (2.100, 2.106) this is true.

Finally, for completeness, we compute scaling dimensions of the scalar mesonic operators in $\mathcal{N}=2$ SQED, which at leading order have dimension 2, but are not protected. One such operator is the quartic adjoint-2: $|\Phi|^4_{adj-2}$, to calculate its scaling dimension one uses graphs in the Tab. 2.14, 2.16. The operator σ^2 has its scaling dimension twice the scaling dimension of σ field (which is exactly equal to 1) plus the contributions of the last three graphs in Tab. 2.11. The dimension of $\sigma|\Phi|^2_{adj}$ equals to the sum of: $\Delta[|\Phi|^2_{adj}] = 1$, $\Delta[\sigma] = 1$, plus the contribution of the graph (2.5). The final results are

$$\Delta[|\Phi|^4_{adj-2}] = 2 + \frac{48}{3\pi^2 N_f} + O(1/N_f^2) \ , \tag{2.120}$$

$$\Delta[\sigma^2] = 2 + \frac{48}{3\pi^2 N_f} + O(1/N_f^2) \ , \tag{2.121}$$

$$\Delta[\sigma|\Phi|^2_{adj}] = 2 + \frac{48}{\pi^2 N_f} + O(1/N_f^2) \ . \tag{2.122}$$

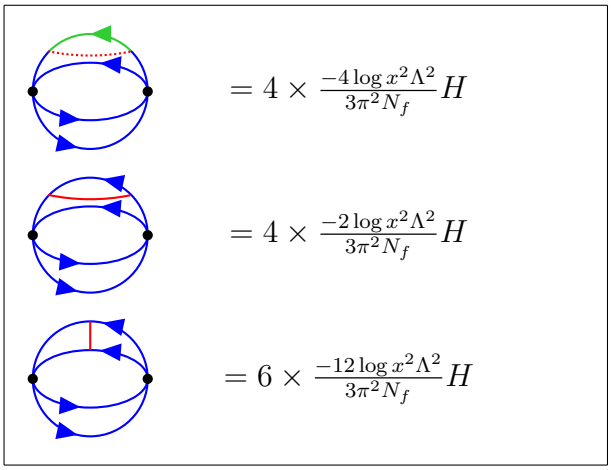

Table 2.16: ($\mathcal{N} = 2$ SQED) quartic adjoint-2 operator renormalization. Dotted red line stands for the effective gaugino λ_2 propagator. Thick red line stands for effective D-field propagator.

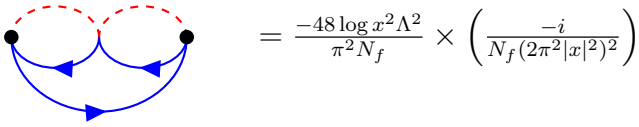

Figure 2.5: ($\mathcal{N} = 2$ SQED) $\sigma|\Phi|^2_{adj}$ operator renormalization. Dashed line stands for effective σ field propagator.

Chapter 3

QED's in $2+1$ dimensions and Complex CFT's

In this chapter we examine our interacting bosonic (2.1) and fermionic (2.58) QED's with $U(N_f/2)^2$-invariant quartic couplings with lower values of N_f. The theories live in 2+1 dimensions and all the flavors are massless. We first discuss the RG fixed points in the ungauged models, where the existence of four unitary fixed points can be established rigorously for any $N_f > 1$.

Upon gauging the $U(1)$ symmetry, the RG flow structure is the same for large enough N_f, but for small N_f the fate of the gauged fixed points can be different. We estimate in each case the N_f^* where the real fixed points collide. The collision is driven by mesonic operators becoming relevant and entering the action[1].

In the case of bosonic QED's we will interpret the collisions of fixed points as merging and annihilation into the complex plane of couplings. When $N_f < N_f^*$, the RG flow slows down passing close to the pair of complex conjugate CFT's, the runaway RG flow eventually experiences a first order phase transition. In the case of fermionic QED's, two fixed points with different symmetries collide. If we interpret these collisions as merging and annihilation, then again the RG flow will slow down passing close to the complex CFT's and eventually (parity invariant) mass for the fermions will be generated leading to DχSB. The RG flows

[1]It is conceivable that a similar mechanism is at play with monopole operators (this would break the $U(1)_{top}$ topological symmetry). In this thesis we disregard the possibility that monopoles enter the action. This is certainly the correct thing to do if the gauge group is non-compact ($\mathbb{R}$ instead of $U(1)$), since in this case monopoles do not exist. Studying possible mergings driven by monopoles is an interesting project that goes beyond the scope of this thesis.

eventually reach the Non-Linear-Sigma-Model with target space the complex Grassmannian

$$\frac{U(N_f)}{U(N_f/2) \times U(N_f/2)} \quad . \tag{3.1}$$

However, as we already stated in the introduction, it is not clear whether the fixed points with different symmetries can merge and become a complex CFT's. Another option is that fixed points after collision do not merge but pass through each other and continue to exist as real CFT's, exchanging their stability properties.

3.1 Bosonic QED

Let us first consider the ungauged model (1.33), with $2N_f$ real scalars and global symmetry is $(O(N_f) \times O(N_f)) \rtimes \mathbb{Z}_2^e$, becoming $O(2N_f)$ on the locus $\lambda = 2\lambda_{ep}$. In the ungauged model the N_f can be any integer. There are four fixed points:

1. Free fixed point, with $\lambda = \lambda_{ep} = 0$. Both quartic couplings are relevant, obviously.

2. Decoupled fixed point, with $\lambda_{ep} > 0, \lambda = 0$. It describes two decoupled $O(N_f)$ models. We know from the numerical bootstrap [97] that $\Delta[|\phi|^2_{singlet}]_{O(N_f)} > \frac{3}{2}$ (if $N_f > 1$)[2], so $\Delta[\sum |\phi_i|^2 \sum |\tilde{\phi}_j|^2]_{decoupled} = 2\Delta[|\phi|^2_{singlet}]_{O(N_f)} > 3$. This proves rigorously that, for any $N_f > 1$, this fixed point is attractive.

3. $O(2N_f)$ model, with $\lambda = 2\lambda_{ep} > 0$. $O(2N_f)$ global symmetry. A relevant symmetry breaking quartic deformation, $(\sum |\phi_i|^2 - |\tilde{\phi}_i|^2)^2$, drives the theory to the decoupled fixed point.

4. "Model-3" with $\lambda_{ep} > 0, \lambda < 0$. Global symmetry is $(O(N_f) \times O(N_f)) \rtimes \mathbb{Z}_2^e$. A relevant quartic deformation triggers an RG flow to the decoupled fixed point.

[2] In the $O(n)$ vector model, the rigorous scaling dimensions of the quadratic singlet operator is 1.412625(10) if $n = 1$ (Ising model), 1.5117(25) for the $O(2)$-model, 1.5957(55) for the $O(3)$-model, [97] and goes up to $\sim 2 - \frac{32}{3\pi^2 n}$ at large n. Notice the different qualitative structure at $n = 1$.

The RG flows looks as follows

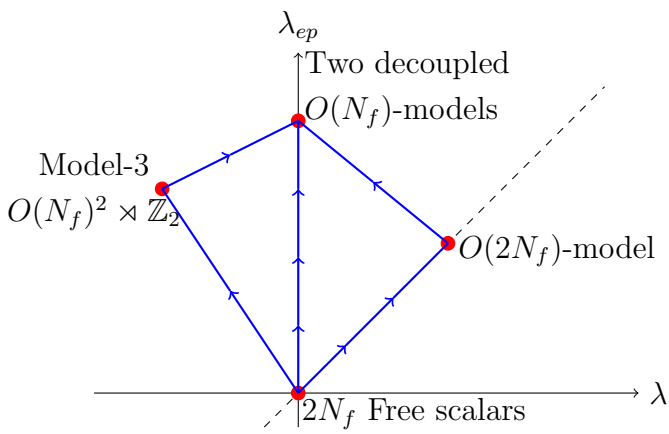

(3.2)

Let us emphasize that this is an exact result valid for any $N_f > 1$. Higher order calculations show that for $N_f = 1$ the Decoupled fixed point is unstable and the $O(2N_f)$ is the fully stable fixed point. The pattern agrees with the findings of [98].

Gauging the $U(1)$ symmetry at even N_f. When we gauge the global symmetry the four fixed points flow to four interacting QED fixed points[3].

If N_f is large enough, the qualitative features of the RG flows are not changing when turning on the U(1) gauge coupling, which triggers an RG flow from (3.2) to four interacting bosonic QED's:

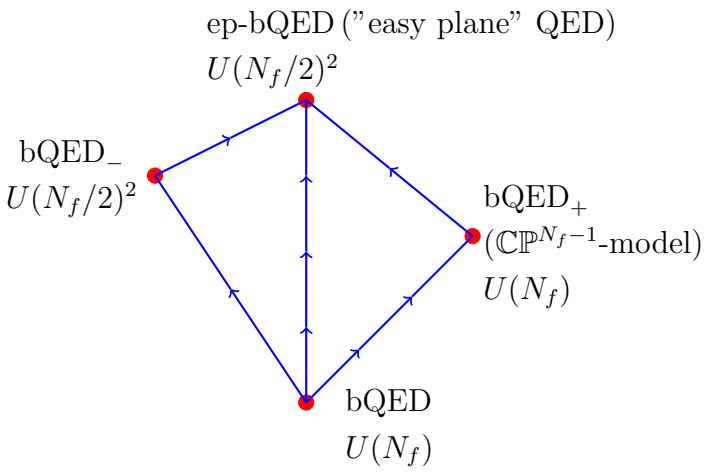

(3.3)

Assuming that below a certain N_f^* two or four fixed points become complex, the picture of the RG flows below N_f^* is different for the RG flows between complex conjugates CFT's, but

[3]In the $4-2\epsilon$ expansion, tricritical QED is described by a small $\lambda = 2\lambda_{ep} \sim 1/N_f^2$ fixed point, the ep-bQED has $\lambda_{ep} \sim 1/N_f$, $\lambda \sim 1/N_f^2$, while the other two fixed points have $\lambda_{ep} \sim 1/N_f$, $\lambda \sim 1/N_f$, see Appendix A.

still there are RG flows from the complex conjugated pair coming from bQED — bQED$_+$ to the complex conjugated pair coming from bQED$_-$ — ep-bQED.

At the fixed points bQED and bQED$_+$ the global symmetry is enhanced to

$$\left(\frac{SU(N_f)}{\mathbb{Z}_{N_f}} \times U(1)_{top}\right) \rtimes \mathbb{Z}_2^{\mathcal{C}} \ , \tag{3.4}$$

where $\mathbb{Z}_{N_f}$ is the center of $SU(N_f)$. All gauge invariant local operators, including the monopoles, transform in $SU(N_f)$ representations with zero N_f-ality. Notice that along the symmetry enhanced direction $\lambda = 2\lambda_{ep}$, the N_f can be considered to be any integer.

The two fixed points with $U(N_f)$ symmetry

The scaling dimensions of simple scalar operators in the large-N_f limit, at the fixed points with $U(N_f)$ symmetry, are studied in the chapter 2 and [73]:

bQED (tricritical) $U(N_f)$-symmetry	$\Delta[\Phi^*\Phi_{SU(N_f)-adjoint}] = 1 - \frac{64}{3\pi^2 N_f}$ $\Delta[\lvert\Phi\rvert^2_{SU(N_f)-singlet}] = 1 + \frac{128}{3\pi^2 N_f}$ $\Delta[\Phi_i^*\Phi_j^*\Phi^k\Phi^l - \text{traces}] = 2 - \frac{128}{3\pi^2 N_f}$ $\Delta[\lvert\Phi\rvert^4_{SU(N_f)-singlet}] = 2 + \frac{256}{3\pi^2 N_f}$
bQED$_+$($\mathbb{CP}^{N_f-1}$model) $U(N_f)$-symmetry	$\Delta[\Phi^*\Phi_{SU(N_f)-adjoint}] = 1 - \frac{48}{3\pi^2 N_f}$ $\Delta[\Phi_i^*\Phi_j^*\Phi^k\Phi^l - \text{traces}] = 2 - \frac{48}{3\pi^2 N_f}$ $\Delta[\sigma_+] = 2 - \frac{144}{3\pi^2 N_f}$ $\Delta[\frac{-5\mp\sqrt{37}}{12}\sigma_+^2 + F^{\mu\nu}F_{\mu\nu}] = 4 - \frac{32(4\pm\sqrt{37})}{3\pi^2 N_f}$

(3.5)

The quartic operators $[\Phi_i^*\Phi_j^*\Phi^k\Phi^l - \text{traces}]$ transform in the adjoint-2 representation of $SU(N_f)$, with Dynkin labels $[2, 0, \ldots, 0, 2]$.

We are not aware of any order $O(1/N_f^2)$ computation in bosonic QED's. Extrapolating finite-N_f numerical simulations, [35] estimated the order $O(1/N_f^2)$ correction to the adjoint in bQED$_+$ to be[4]

$$\Delta[\Phi^*\Phi_{SU(N_f)-adj}] = 1 - \frac{48}{3\pi^2 N_f} + \frac{1.8(2)}{N_f^2} \ . \tag{3.6}$$

The merging of these two fixed points happens when the $|\Phi|^4_{SU(N_f)-singlet}$ operator (that at $N_f = \infty$ has $\Delta = 2$) in bQED, decreasing N_f, hits $\Delta = 3$ from below, and the σ_+^2 operator (that at $N_f = \infty$ has $\Delta = 4$) in bQED$_+$ hits $\Delta = 3$ from above. Actually, the operator σ_+^2

[4]This is taken from η_N in the caption of figure 5 of [35], where there seems to be a sign typo.

mixes strongly with $F^{\mu\nu}F_{\mu\nu}$, that also has $\Delta = 4$ at $N_f = \infty$. The mixing was studied in [73], from which we take the results in the last line of Tab. 3.5.

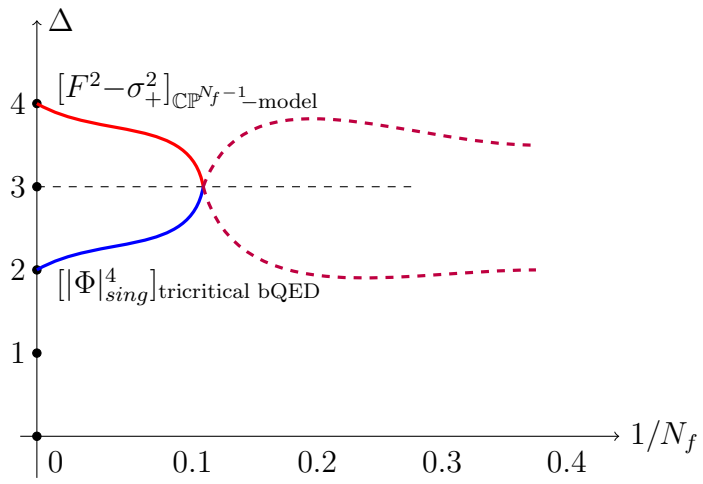

(3.7)

Imposing that the interactions reach marginality we can estimate N_f^*:

$$\Delta[|\Phi|^4_{SU(N_f)-singlet}]_{bQED} = 3 \quad \rightarrow \quad N_f^* \sim \frac{256}{3\pi^2} \simeq 8.6 \ , \tag{3.8}$$

$$\Delta[-0.924\sigma_+^2 + F^{\mu\nu}F_{\mu\nu}]_{bQED_+} = 3 \quad \rightarrow \quad N_f^* \sim \frac{32(4+\sqrt{37})}{3\pi^2} \simeq 10.9 \ . \tag{3.9}$$

Another way to estimate the merging point is to impose that the scaling dimension of the singlet bilinear in bQED is equal to the scaling dimension of the Hubbard-Stratonovich field σ_+ in bQED$_+$:

$$\Delta[|\Phi|^2_{SU(N_f)-singlet}]_{bQED} = 1 + \frac{128}{3\pi^2 N_f} = \Delta[\sigma_+]_{bQED_+} = 2 - \frac{144}{3\pi^2 N_f} \quad \rightarrow \quad N_f^* \sim 9.2 \ . \tag{3.10}$$

Even if these three arguments are not completely independent, it is encouraging to get somewhat consistent results. Obviously, the N_f^* should be unique (for two given fixed points colliding) and the somewhat different values for N_f^* (3.8, 3.9, 3.10) is probably related to the fact that we are truncating the series at order $O(1/N_f)$. It might happen that this truncation is good for the scaling dimensions of some observables but not so good for others. For instance it might happen that the order $O(1/N_f^2)$ correction to the $|\Phi|^4_{SU(N_f)-singlet}$ in bQED is small, instead the same order for the σ_+^2 in bQED$_+$ might be big. Then, in one case it will not affect the N_f^*, while in the other case it will. This can be verified only if one manages to find the scaling dimensions at all orders in $1/N_f$ (also including possible

non-perturbative effects), which seems to be out of the scope of the currently available techniques.

We mention that numerical lattice simulations [35] show a second order phase transitions for bQED$_+$ for all $N_f \geq 2$ (for N_f=2, [99] claims first order phase transition). However, if the phase transition is weakly first order (large correlation length as compared to the lattice spacing), it might be difficult in the lattice simulations to differentiate it from the continuous transition. On the other hand, in [60] authors claim $N_f^* \sim 12$, which is close to our prediction $N_f^* \sim 10$.

The two fixed points with $U(N_f/2)^2$ symmetry

Let us now move to the fixed points with $U(N_f/2)^2$ symmetry, the scaling dimensions of the mesonic gauge invariant operators are studied in the chapter 2 and [100]:

bQED$_-$ $U(N_f/2)^2$-symmetry	$\Delta[\Phi^*\Phi_{SU(N_f/2)-adj}, \tilde{\Phi}^*\tilde{\Phi}_{SU(N_f/2)-adj}] = 1 - \frac{48}{3\pi^2 N_f}$ $\Delta[\Phi_i^*\tilde{\Phi}_j, \Phi_i\tilde{\Phi}_j^*] = 1 - \frac{72}{3\pi^2 N_f}$ $\Delta[\Phi_i^*\Phi_j^*\tilde{\Phi}_k\tilde{\Phi}_l, \Phi_i\Phi_j\tilde{\Phi}_k^*\tilde{\Phi}_l^*] = 2 - \frac{144}{3\pi^2 N_f}$ $\Delta[\sum_{i=1}^{N_f/2} \lvert\Phi_i\rvert^2 + \lvert\tilde{\Phi}_i\rvert^2] = 1 + \frac{144}{3\pi^2 N_f}$ $\Delta[(\sum_{i=1}^{N_f/2} \lvert\Phi_i\rvert^2 + \lvert\tilde{\Phi}_i\rvert^2)^2] = 2 + \frac{288}{3\pi^2 N_f}$ $\Delta[\sigma_-] = 2 + \frac{48}{3\pi^2 N_f}$
easy plane bQED $U(N_f/2)^2$-symmetry	$\Delta[\Phi^*\Phi_{SU(N_f/2)-adj}, \tilde{\Phi}^*\tilde{\Phi}_{SU(N_f/2)-adj}] = 1 - \frac{32}{3\pi^2 N_f}$ $\Delta[\Phi_i^*\tilde{\Phi}_j, \Phi_i\tilde{\Phi}_j^*] = 1 - \frac{56}{3\pi^2 N_f}$ $\Delta[\Phi_i^*\Phi_j^*\tilde{\Phi}_k\tilde{\Phi}_l, \Phi_i\Phi_j\tilde{\Phi}_k^*\tilde{\Phi}_l^*] = 2 - \frac{64}{3\pi^2 N_f}$ $\Delta[\sigma_-] = 2 + \frac{32}{3\pi^2 N_f}$ $\Delta[\sigma_+] = 2 - \frac{160}{3\pi^2 N_f}$

(3.11)

Imposing that the singlet bilinear in bQED$_-$ meets the Hubbard-Stratonovich field σ_+ in ep-bQED:

$$\Delta[\sum_{i=1}^{N_f/2} |\Phi_i|^2 + |\tilde{\Phi}_i|^2]_{bQED_-} = \Delta[\sigma_+]_{ep-bQED} \quad \rightarrow \quad N_f^* \sim 10.3 \ . \tag{3.12}$$

Unfortunately in this case we do not have scaling dimensions of the pair of operators $\{\sigma_-^2, F^{\mu\nu}F_{\mu\nu}\}$. From the quartic operator in bQED$_-$ hitting $\Delta = 3$ from below we get

$$\Delta[(\sum_{i=1}^{N_f/2} |\Phi_i|^2 + |\tilde{\Phi}_i|^2)^2]_{bQED_-} = 3 \quad \rightarrow \quad N_f^* \sim 9.7 \ . \tag{3.13}$$

Let us also consider the possibility of a different collision pattern, for instance that bQED$_+$ collides with ep-bQED. It is easy to see that the scaling dimensions disfavour this scenario: in bQED$_+$, the anomalous dimension of $[\Phi_i^*\Phi_j^*\Phi^k\Phi^l - \text{traces}]$ is negative, so decreasing N_f such operators do not hit $\Delta = 3$, which would be required in order for bQED$_+$ to collide with ep-bQED.

Finally we want to mention that the merging and annihilation scenario between the bosonic fixed points with the same pattern is also confirmed in $d = 4-2\epsilon$ using the one-loop epsilon expansion (see Introduction and the appendix A for more details).

Improved estimate of N_f^*? A square-root ansatz

If the annihilation-of-fixed-points scenario is correct, it must be that the scaling dimensions of the various operators $\Delta[\mathcal{O}](N_f)$ present a square root behaviour when $N_f \searrow N_f^*$, and the anomalous dimensions becomes complex when $N_f < N_f^*$. For instance for the quartic singlet operator in tricritical bQED, we might use a simple ansatz of the form

$$\Delta[|\Phi|^4_{singlet}]_{bQED} = 3 - \sqrt{1 - N_f^*/N_f} \sim 2 + \frac{N_f^*}{2N_f} + \frac{(N_f^*)^2}{8N_f^2} + \frac{(N_f^*)^3}{16N_f^3} + O(1/N_f^4)\ . \tag{3.14}$$

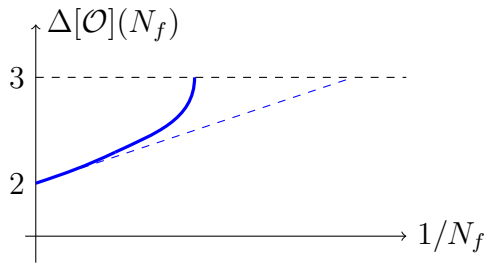

(3.15)

Notice that this ansatz predicts that all the higher order corrections have the same sign of the order $O(1/N_f)$ correction.

Using the order $O(1/N_f)$ result $\Delta[|\Phi|^4_{singlet}] = 2 + \frac{256}{3\pi^2 N_f}$, in the square-root ansatz (3.14) provides the estimate $N_f^* = 2 \cdot \frac{256}{3\pi^2} \sim 17.3$. This is a factor of 2 larger than the estimate in (3.8), which used a linear extrapolation. For all the operators in all the models considered in this section, the square-root ansatz (3.14) provides estimates of N_f^* which are a factor of 2 larger than the estimates using the linear extrapolation.

Let us emphasize that including the square root behavior at $N_f \to N_f^*$ is equivalent to imposing information about strongly coupled phenomena. It would be desirable to have

scaling dimensions at higher order in $1/N_f$: this would allow to test if ansatze that include the square root behavior (3.14) is better than the naive extrapolations.

In the case of the Abelian Higgs model, in the $4-2\epsilon$ expansion we already know (1.22) that the zeroes of the one loop beta function of the quartic coupling $\lambda|\Phi|^4$ are given by

$$\lambda_* = \frac{N_f + 18 \pm \sqrt{N_f^2 - 180N_f - 540}}{16N_f(N_f+4)}\epsilon\,. \tag{3.16}$$

The "+" solution is the bQED$_+$, the "−" solution is the tricritical bQED. From the previous equation it follows that in the limit $\epsilon \to 0^+$, the exact result for the fixed point merging is $N_f^* = 6(15+4\sqrt{15}) \sim 183$. On the other hand, we can perform a computation analogous to eqs. (3.8, 3.9, 3.10), in $d \to 4^-$, using the generic-d scaling dimensions computed in [73]. The result is $N_f^*(d \to 4^-) \sim 90$, which is indeed a factor of ~ 2 smaller than the exact result. This computation tells us that, in dimension $d \to 4^-$, the square-root ansatz (3.14) is better than the linear extrapolation, suggesting that the same might be true in dimension 3, and the linear extrapolation underestimates N_f^* also in $d = 3$.

Singlet sextic interactions of bosonic tricritical points

At the tricritical fixed point the sextic $SU(N_f)$-singlet operator at infinite N_f has $\Delta = 3$. The 1st order correction is

$$\Delta[(\sum_{i=1}^{N_f/2}(\Phi^i\Phi_i^* + \tilde{\Phi}^i\tilde{\Phi}_i^*))^3] = 3 + 3\frac{128}{3\pi^2 N_f} + O(1/N_f^2)\ . \tag{3.17}$$

So the sextic $SU(N_f)$ invariant deformation is irrelevant. Modulo tuning mass and quartic term to zero, tricritical bQED is a *stable fixed point*. At the merging of the tricritical fixed point with the critical fixed point sextic singlet interactions do not play a role. $3d$ bosonic gauge theories at the tricritical point (with quartic interactions tuned to zero) were studied in a completely different regime in [101, 102], where they named the model *regular boson theory*. [101, 102] found that for $U(N_c)_k$ Chern-Simons with 1 bosonic flavor, at large N_c and large k with N_c/k fixed, there is a stable fixed point and possibly (depending on the value of N_c/k) an unstable fixed point. Combining these two results, it is natural to suggest that at finite N_c, N_f, k, bosonic QCD always has a stable *tricritical*, or *regular*, fixed point.

3.2 Fermionic QED

We consider fermionic QED with $N_f/2$ flavors Ψ_i plus $N_f/2$ flavors $\tilde{\Psi}_i$ (each $\Psi, \tilde{\Psi}$ is a complex two-component $3d$ fermion). The quartic Gross-Neveu interactions are modeled by

Yukawa cubic couplings with two real Hubbard-Stratonovich scalar fields, ρ_+ and ρ_-.[5] ρ_+ and ρ_- are parity-odd, and all our theories are parity invariant. The Lagrangian reads

$$\mathcal{L} = \frac{1}{4e^2} F_{\mu\nu}F^{\mu\nu} + \sum_{i=1}^{N_f/2} (\bar{\Psi}^i \not{D} \Psi_i + \bar{\tilde{\Psi}}^i \not{D} \tilde{\Psi}_i) + \sum_{\pm} \rho_\pm \sum_{i=1}^{N_f/2} (\bar{\Psi}^i \Psi_i \pm \bar{\tilde{\Psi}}^i \tilde{\Psi}_i) + \dots \quad . \tag{3.18}$$

The $\dots$ stand for quartic interactions and kinetic terms for the $\rho_\pm$ fields. The mass terms for $\rho_\pm$ are relevant at large enough N_f.

We start discussing the ungauged model, with $O(N_f)^2 \rtimes \mathbb{Z}_2^e$ global symmetry, the RG flows between the 4 fixed points are triggered by mass terms for the scalars $\rho_\pm$. In the ungauged model N_f can be any integer.

There are 4 fixed points, similar to the bosonic case: a free theory, a decoupled fixed point with both ρ_+ and ρ_- (renaming $\rho_\pm = \rho \pm \tilde{\rho}$, it splits into two decoupled $O(N_f)$-invariant Gross-Neveu models), a Gross-Neveu fixed point with only ρ_- and $O(N_f)^2 \rtimes \mathbb{Z}_2^e$-symmetry, and a Gross-Neveu fixed point with only ρ_+ and $O(2N_f)$-symmetry.

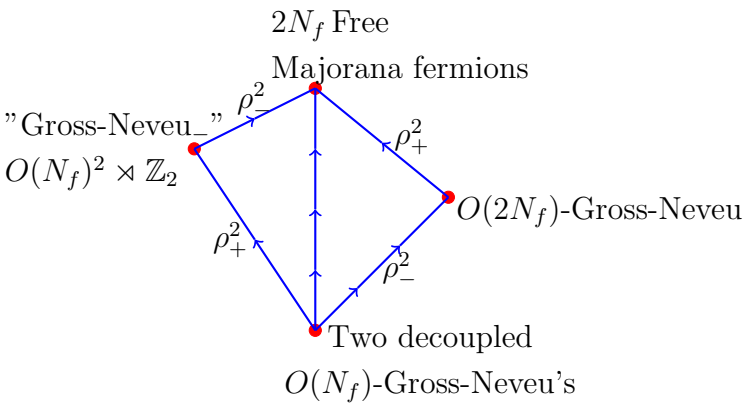

(3.19)

For any $N \geq 1$, it is known with good accuracy that in the $O(N)$ Gross-Neveu model, $\Delta[\rho^2] < 3$ (at large N $\Delta[\rho^2] \sim 2 + \frac{32}{3\pi^2 N}$, at $N = 1$ $\Delta[\rho^2] \sim 1.59$), so in particular the deformations ρ_+^2 and ρ_-^2 are relevant.

[5] Much of the existing literature considers QED's with N four-component Dirac fermions χ_i, $i = 1, \dots, N$, in generic dimension d. In $d = 3$, the global symmetry can be $U(2N)$ or $U(N)^2$, depending on the precise form of the Yukawa (or Gross-Neveu-Yukawa) couplings.

In terms of two-component $3d$ fermions $\chi_i = (\Psi_i, \tilde{\Psi}_i)$ and $(\bar{\chi}_i = \bar{\Psi}_i, -\bar{\tilde{\Psi}}_i)$. So $\sum_{i=1}^N \bar{\chi}_i \chi_i = \sum_{i=1}^N (\bar{\Psi}^i \Psi_i - \bar{\tilde{\Psi}}^i \tilde{\Psi}_i)$ is a $U(N)$-singlet in $d \neq 3$, but it is part of the $SU(2N)$-adjoint in $d = 3$. On the other hand $\sum_{i=1}^N \bar{\chi}_i \gamma_{35} \chi_i = \sum_{i=1}^N (\bar{\Psi}^i \Psi_i + \bar{\tilde{\Psi}}^i \tilde{\Psi}_i)$ is a $SU(2N)$-singlet in $d = 3$. See [77], for definition of γ_{35} and gamma matrices, which are 4-dimensional reducible representation of the Clifford algebra.

Often, what is called QED-Gross-Neveu has $\mathcal{L}_{int} = \sigma \sum_{i=1}^N \bar{\chi}_i \chi_i$, with $U(N)^2$ global symmetry in $d = 3$. We instead named this model QED-GN$_-$. On the other hand [8] calls QED-Gross-Neveu the model that we named QED-GN$_+$, with $d = 3$ global symmetry $U(2N)$.

Gauging the $U(1)$ symmetry at even N_f. As in the bosonic case, if N_f is large enough, gauging the $U(1)$ symmetry triggers an RG flow from (3.19) to the following 4 interacting fermionic fixed points:

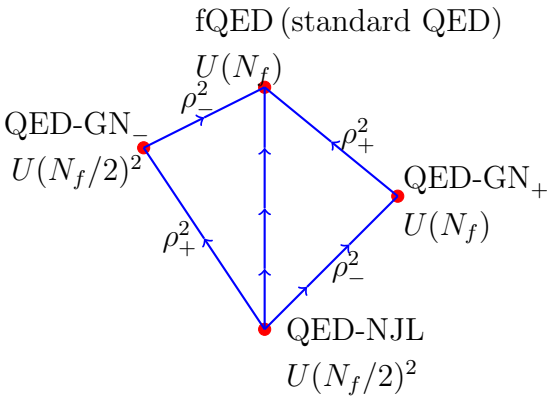

(3.20)

The global symmetry at the fixed points fQED and QED-GN$_+$ is enhanced to

$$\frac{SU(N_f)\times U(1)_{\text{top}}}{\mathbb{Z}_{N_f}} \rtimes \mathbb{Z}_2^{\mathcal{C}}\,. \tag{3.21}$$

Fermionic QED and its partner

The scaling dimensions of mesonic scalar gauge invariant operators to leading order in the large-N_f limit are studied in the chapter 2 and in [80, 81, 89, 90][6]:

fQED $U(N_f)$	$\Delta[\bar\Psi\Psi_{SU(N_f)-adj}] = 2 - \frac{64}{3\pi^2 N_f} + \frac{256(28-3\pi^2)}{9\pi^4 N_f^2} \sim 2 - \frac{2.16}{N_f} - \frac{0.47}{N_f^2}$ $\Delta[\bar\Psi\Psi_{SU(N_f)-singlet}] = 2 + \frac{128}{3\pi^2 N_f}$ $\Delta[\lvert\Psi\rvert^4_{[0,1,0\ldots,0,1,0]}] = 4 - \frac{192}{3\pi^2 N_f}$ $\Delta[\lvert\Psi\rvert^4_{[2,0,\ldots,0,2]}] = 4 + \frac{64}{3\pi^2 N_f}$ $\Delta[\{(\lvert\Psi\rvert^2_{singlet})^2, F^{\mu\nu}F_{\mu\nu}\}] = 4 + \frac{64(2\pm\sqrt{7})}{3\pi^2 N_f}$
QED-GN$_-$ $U(N_f/2)^2$	$\Delta[\bar\Psi\Psi_{SU(N_f/2)-adj}] = 2 - \frac{48}{3\pi^2 N_f} + \frac{64(100-9\pi^2)}{9\pi^4 N_f^2} \sim 2 - \frac{1.62}{N_f} + \frac{0.82}{N_f^2}$ $\Delta[\bar\Psi^i\tilde\Psi_j, \bar{\tilde\Psi}^i\Psi_j] = 2 - \frac{72}{3\pi^2 N_f}$ $\Delta[\sum_{i=1}^{N_f/2}(\bar\Psi^i\Psi_i + \bar{\tilde\Psi}^i\tilde\Psi_i)] = 2 + \frac{144}{3\pi^2 N_f}$ $\Delta[\rho_-] = 1 + \frac{48}{3\pi^2 N_f} - \frac{8(1232-243\pi^2)}{9\pi^4 N_f^2} \sim 1 + \frac{1.62}{N_f} + \frac{10.64}{N_f^2}$ $\Delta[\rho_-^2] = 2 + \frac{144}{3\pi^2 N_f}$

(3.22)

[6]Let us observe that, at order $O(1/N_f)$, the anomalous (not the total) dimensions of the fermionic fixed points (3.22, 3.26) are equal to the anomalous dimensions of the bosonic fixed points (3.5, 3.11). This is true for the Hubbard-Stratonovich fields and for quadratic operators in the charged fields.

The quartic fermionic operators in fQED were computed in [80, 81], we indicated the Dynkin labels of the $SU(N_f)$ representation under which they transform. The mixing between the quartic singlet and $F^{\mu\nu}F_{\mu\nu}$ is strong also here, and was solved in [81], the lowest eigenvalue of the singlets does not seem to run fast enough to hit $\Delta = 3$ (which would suggest the symmetry-preserving merging fQED$-$QED-GN$_+$). We also included the order $O(1/N_f^2)$ contributions, when known [89, 90][7]. The order $O(1/N_f^2)$ corrections to the adjoint are quite small, while ρ_- receives a big contribution at order $O(1/N_f^2)$, from which [26, 29] estimated chiral symmetry breaking below $N_f^c \sim 2.8469 \cdot 2 = 5.69$ in fQED[8].

The conjectural collision of the two fixed points fQED and QED-GN$_-$ happens when, decreasing N_f, the lowest quartic fermion operator ($|\Psi|^4_{[0,1,0,\ldots,0,1,0]}$) hits $\Delta = 3$ from above and the mass term of the Hubbard-Stratonovich field ρ_-^2 hits $\Delta = 3$ from below:

$$\Delta[|\Psi|^4_{[0,1,0\ldots,0,1,0]}]_{fQED} = 3 \quad \rightarrow \quad N_f^* \sim \frac{192}{3\pi^2} \simeq 6.5 \ , \tag{3.23}$$

$$\Delta[\rho_-^2]_{QED-GN_-} = 3 \quad \rightarrow \quad N_f^* \sim \frac{144}{3\pi^2} \simeq 4.9 \ . \tag{3.24}$$

Another estimate comes equating the adjoint in fQED with ρ_- in QED-GN$_-$, using the order $O(1/N_f^2)$ anomalous dimensions we get

$$\Delta[\bar{\Psi}\Psi_{SU(N_f)-adj}]_{fQED} = \Delta[\rho_-]_{QED-GN_-} \quad \rightarrow \quad N_f^* = \frac{56 + 2\sqrt{678\pi^2 - 3472}}{3\pi^2} \sim 5.72 \ . \tag{3.25}$$

Had we used the order $O(1/N_f)$ anomalous dimensions, we would have got $N_f^* \sim 3.8$. Hence, the 2nd order in $1/N_f$ corrections in fermionic QED's increase the value of the collision point. This is because the 2nd order corrections have the same sign of the 1st order corrections, both in $\Delta[\bar{\Psi}\Psi_{SU(N_f)-adj}]_{fQED}$ and in $\Delta[\rho_-]_{QED-GN_-}$ (if this collision is interpreted as merging and annihilation, then the fact that second order corrections increased the value of N_f^* gives more evidence to the square root behaviour which must be present if the merging scenario is correct, as discussed in section 3.1).

[7] [90] studies pure QED and eq. 27 gives the scaling dimension of $\sum_{i=1}^N \bar{\chi}_i\chi_i = \sum_{i=1}^N(\bar{\Psi}^i\Psi_i - \bar{\tilde{\Psi}}^i\tilde{\Psi}_i)$ which is part of the $SU(N_f{=}2N)$-adjoint in $d = 3$. See footnote 5.

The QED-GN$_-$ results are given eqs. 4.4 and 4.6 of [89], which studies a model (referred to as QED-Gross-Neveu in [89]) with $\mathcal{L}_{int} = \sigma \sum_{i=1}^N \bar{\chi}_i\chi_i$. When $d = 3$ this model is what we call QED-GN$_-$, with $U(N)^2$ $3d$ global symmetry. So the results of [89] are valid for our QED-GN$_-$ with $N_f{=}2N$ flavors. Moreover, [89] reports the dimension of $\sum_{i=1}^N \bar{\chi}_i\chi_i$, an operator which vanishes on-shell because of the equation of motion of σ. We report the scaling dimension of σ, using the relation $\Delta[\sigma] = 3 - \Delta[\sum_{i=1}^N \bar{\chi}_i\chi_i]$.

[8] We denoted by N_f^c the number of flavors for which chiral symmetry breaking takes place. We want to emphasise that N_f^* is the critical number of flavors for which the collisions happen, and only if these collisions are interpreted as merger and annihilation one can associate N_f^* to N_f^c.

Studying fermionic QED at finite N_f but continuous dimension d, [30] estimated $N_f^c \sim 2.89 \cdot 2 = 5.8$, while [31] found an upper bound for the merging: $N_f^c < 4.4 \cdot 2 = 8.8$.

QED-GN$_+$ and its partner

We now move to the last fixed points. The scaling dimensions for QED-GN$_+$ and QED-NJL are studied in the chapter 2:

QED-GN$_+$ $U(N_f)$	$\Delta[\bar{\Psi}\Psi_{SU(N_f)-adj}] = 2 - \frac{48}{3\pi^2 N_f}$ $\Delta[\rho_+] = 1 - \frac{144}{3\pi^2 N_f}$ $\Delta[\rho_+^2] = 2 - \frac{240}{3\pi^2 N_f}$
QED-NJL $U(N_f/2)^2$	$\Delta[\bar{\Psi}\Psi_{SU(N_f/2)-adj}] = 2 - \frac{32}{3\pi^2 N_f}$ $\Delta[\bar{\Psi}^i\tilde{\Psi}_j, \bar{\tilde{\Psi}}^i\Psi_j] = 2 - \frac{56}{3\pi^2 N_f}$ $\Delta[\rho_-] = 1 + \frac{32}{3\pi^2 N_f}$ $\Delta[\rho_+] = 1 - \frac{160}{3\pi^2 N_f}$ $\Delta[\rho_+\rho_-] = 2 - \frac{32}{3\pi^2 N_f}$ $\Delta[\rho_+^2 + (4 \mp \sqrt{17})\rho_-^2] = 2 - \frac{16(5\pm 3\sqrt{17})}{3\pi^2 N_f}$

(3.26)

We can estimate N_f^* in two ways. First, imposing that the adjoint in QED-GN$_+$ meets the singlet in QED-NJL:

$$\Delta[\bar{\Psi}\Psi_{SU(N_f)-adj}] = 2 - \frac{48}{3\pi^2 N_f} = \Delta[\rho_-] = 1 + \frac{32}{3\pi^2 N_f} \quad \rightarrow \quad N_f^* \sim 2.7 \ . \tag{3.27}$$

It is conceivable that, as in (3.25), including 2nd order anomalous dimensions moves this estimate up significantly. Second, looking at when ρ_-^2 (after having solved the mixing with ρ_+^2) hits $\Delta = 3$ from below:

$$\Delta[\rho_-^2 + 0.123\rho_+^2]_{QED-NJL} = 2 + \frac{16(3\sqrt{17}-5)}{3\pi^2 N_f} = 3 \quad \rightarrow \quad N_f^* \sim \frac{16(3\sqrt{17}-5)}{3\pi^2} \simeq 4 \ . \tag{3.28}$$

Notice that a collision between QED-NJL and QED-GN$_-$ is not favorable, since the operator ρ_+^2 at QED-NJL[9] has a negative anomalous scaling dimension and therefore lowering N_f it doesn't hit the marginal value.

[9] To be precise we should talk about the mixed state $(\rho_+^2 - 0.123\rho_-^2)$.

Chapter 4

Higher Derivative Gauge theory in $d = 6$ and the $\mathbb{CP}^{(N_f-1)}$ NLSM

4.1 Large N_f expansion of the critical $\mathbb{CP}^{(N_f-1)}$ NLSM

The $\mathbb{CP}^{(N_f-1)}$ Non-Linear-Sigma-Model is described by N_f complex scalar fields subject to the condition $\sum_{i=1}^{N_f} |\Phi_i|^2 = N_f$, with the following action

$$S_{\mathbb{CP}(N_f-1)} = \int d^d x \Big[\sum_{i=1}^{N_f} |\partial_\mu \Phi_i|^2 + \frac{1}{4N_f} \big(\sum_{i=1}^{N_f} (\Phi_i^* \partial_\mu \Phi_i - \partial_\mu \Phi_i^* \cdot \Phi_i) \big)^2 \Big] \ . \tag{4.1}$$

The action is easily proved to be gauge invariant under the local $U(1)$ transformations $\Phi_i(x) \to e^{i\alpha(x)} \Phi_i(x)$. Due to the constraint $\sum_{i=1}^{N_f} |\Phi_i|^2 = N_f$, the vector Φ_i lies on a sphere S^{2N_f-1}. Additionally the gauge invariance implies that the field configurations related by the gauge transformations are physically equivalent and inside the path integral one shouldn't integrate over these equivalent configurations. Geometrically this means that the target space becomes $\mathbb{CP}^{(N_f-1)} \sim S^{2N_f-1}/U(1)$.

As it is usually the case, for building the $1/N_f$ expansion it is comfortable to introduce master (HS) fields: a scalar field σ as a Lagrange multiplier for the constraint and a vector field A_μ to engineer the complicated quartic interaction with derivatives of (4.1) as a sum of quadratic and cubic terms (Hubbard-Stratonovich transformation). This allows to rewrite

the action (4.1) as follows

$$S = \int d^d x \big[\sum_{i=1}^{N_f} |\partial_\mu \Phi_i|^2 + i A_\mu \sum_{i=1}^{N_f} (\Phi_i^* \partial_\mu \Phi_i - \partial_\mu \Phi_i^* \cdot \Phi_i) + N_f A_\mu^2 + \sigma \big(\sum_{i=1}^{N_f} |\Phi_i|^2 - N_f \big) \big] \ . \tag{4.2}$$

After shifting $\sigma \to \sigma + A_\mu^2$ the action (4.2) takes the following simple form

$$S = \int d^d x \big[\sum_{i=1}^{N_f} |D_\mu \Phi_i|^2 + \sigma \big(\sum_{i=1}^{N_f} |\Phi_i|^2 - N_f \big) \big] \ . \tag{4.3}$$

The $U(1)$ gauge invariance of (4.3) is obvious with the vector field A_μ playing the role of a gauge field. The gauge fixing term is required to fix the redundancies, following [73] the standard $\mathbb{R}_\xi$ gauge is employed ($\xi = 0$ is the Landau gauge). From now on we are interested in the large N_f limit of the (4.3).

In [73] Vasil'ev and Nalimov studied (4.3) in the dimension $2 < d < 4$. They calculated, at the critical point, the leading order scaling dimensions of the master fields in the large N_f limit: $\Delta[\sigma] = 2$, $\Delta[A_\mu] = 1$. They also observed that the scalar QED in $2 < d < 4$ (applying HS transformation on the Φ^4 interaction), is in the same universality class with the $\mathbb{CP}^{(N_f-1)}$ NLSM. The NLO corrections to the scaling dimensions of various observables were also calculated in [73]. We will summarize their results at the end of this section. Before proceeding, we briefly remind why in the scalar QED ($2 < d < 4$) in the large N_f limit $\Delta[A_\mu] = 1$. The scalar QED action (after applying the HS transformation on Φ^4 interaction) is defined by (4.3), adding to it a kinetic term for the photon $F_{\mu\nu}^2/4e^2$. In the large N_f limit, only the following bubble graphs contribute to the 2-point function of the photon.

$\langle A_\mu(p) A_\nu(-p) \rangle =$ 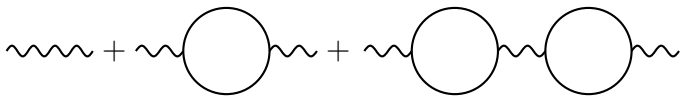 $+ \ \ldots \ ,$ (4.4)

The wavy line in the graphs (4.4) represents the tree level photon propagator in the Landau gauge $D_{\alpha\beta}(p) = \frac{e^2}{p^2}\big(\delta_{\alpha\beta} - \frac{p_\alpha p_\beta}{p^2}\big)$. For a single bubble graph we have

$$\begin{aligned} \Pi_{\alpha\beta}(p) &= N_f \int \frac{d^d q}{(2\pi)^d} \frac{(2q+p)_\alpha (2q+p)_\beta}{q^2 (p+q)^2} \\ &= N_f \frac{2^{2-d}\sqrt{\pi}\Gamma(1-d/2)\Gamma(d/2)}{(4\pi)^{d/2}\Gamma(d/2+1/2)} \big(\delta_{\alpha\beta} - \frac{p_\alpha p_\beta}{p^2}\big) p^{d-2} = N_f B(d) \big(\delta_{\alpha\beta} - \frac{p_\alpha p_\beta}{p^2}\big) p^{d-2} \ , \end{aligned} \tag{4.5}$$

where the factor N_f is due to N_f complex scalar flavors circulating inside the closed loop (4.4). The fraction in (4.5) is denoted by $B(d)$. Summing geometric series of the bubble

graphs in (4.4) gives

$$\langle A_\mu(p)A_\nu(-p)\rangle = D_{\mu\rho}(1-\Pi D)^{-1}_{\rho\nu} = \frac{e^2}{p^2}\big(\delta_{\mu\nu} - \frac{p_\mu p_\nu}{p^2}\big)\frac{1}{1-N_f B(d)e^2 p^{d-4}} \ . \tag{4.6}$$

Therefore we conclude that in $2 < d < 4$, the scaling dimension of the photon in the IR limit is $\Delta[A_\mu] = 1$

$$\langle A_\mu(p)A_\nu(-p)\rangle|_{p\to 0} = -\frac{\big(\delta_{\mu\nu} - \frac{p_\mu p_\nu}{p^2}\big)p^{2-d}}{N_f B(d)} \ . \tag{4.7}$$

We are interested to examine (4.3) in the dimension $4 < d < 6$. The analysis made in [73] still holds, in particular we can use their results by simply analytically continuing the dimension d. However there is a one crucial difference: in $d < 4$ the critical $\mathbb{CP}^{(N_f-1)}$ is realized as an IR fixed point of the scalar QED with Φ^4 interaction, while in $d > 4$ it is an UV interacting fixed point of that theory. Indeed, it follows from (4.6) that for $d > 4$, one recovers the scaling behaviour (4.7) when $p \to \infty$ (UV limit).

We propose a Higher Derivative Gauge (HDG) theory as a UV completion of the action (4.3): including in it the kinetic terms $(\partial_\mu\sigma)^2, (\partial_\mu F_{\alpha\beta})^2$ and the interaction terms $\sigma^3, \sigma F^2_{\alpha\beta}$. In the next section we will see that the HDG is asymptotically free. Apart from the above mentioned terms, in the HDG action one can include also "mass" terms $(\sigma^2, F^2_{\alpha\beta})$, which are relevant deformations. Tuning to zero these terms (also the Φ^2 term), the HDG flows to the IR critical point $\mathbb{CP}^{(N_f-1)}$. Indeed, below we will show that in the large N_f limit the IR scaling dimensions are $\Delta[\sigma] = 2,\ \Delta[A_\mu] = 1$. Therefore the operators $(\partial_\mu\sigma)^2, (\partial_\mu F_{\alpha\beta})^2, \sigma^3, \sigma F^2_{\alpha\beta}$ are irrelevant at the critical point and the HDG in the IR limit is effectively described by (4.3). In the case, when the term $F^2_{\alpha\beta}$ is turned on, in the IR limit we end up on the critical $U(N_f)$-Yukawa. Instead, when the σ^2 is turned on, in the IR limit we end up on the critical scalar-QED (one may call it a pure scalar QED, since the Yukawa $(\sigma\Phi^2)$ interactions are absent). Notice that in the dimension $4 < d < 6$ the Φ^4 operator is irrelevant as opposed to the $d < 4$ case.

Let us check the statement $\Delta[A_\mu] = 1$ (similarly one can check that tuning σ^2 to zero, in large N_f limit $\Delta[\sigma] = 2$). Since we tuned the "mass" term $F^2_{\alpha\beta}$ to zero, the tree level propagator for the photon is solely determined by the higher-derivative kinetic term, which gives $D(p) \sim \frac{1}{p^4}$ (see more details in the next section). Repeating the steps of (4.5), with that tree level propagator one obtains

$$\langle A_\mu(p)A_\nu(-p)\rangle = \frac{e^2}{p^4}\big(\delta_{\mu\nu} - \frac{p_\mu p_\nu}{p^2}\big)\frac{1}{1-N_f B(d)e^2 p^{d-6}} \ . \tag{4.8}$$

From (4.8) it follows that in the IR limit $p \to 0$, one recovers the behaviour (4.7), which proves $\Delta[A_\mu] = 1$.

We pass the following parallels between the many-flavor bosonic ($4 < d < 6$) and many-flavor fermionic ($2 < d < 4$) QED's. The $U(N_f)$-Gross-Neveu-Yukawa model with N_f four component fermions is the analog of $U(N_f)$-Yukawa model. The $SU(N_f)$ pure fermionic QED (no $\rho\Psi^2$ interaction) is the analog of the $SU(N_f)$ scalar QED. The QED-GNY is the analog of the $\mathbb{CP}^{(N_f-1)}$. This analogy lies on the following observation: the quartic interaction Φ^4 is irrelevant in $4 < d < 6$, while four fermion interaction Ψ^4 is irrelevant in $2 < d < 4$. The IR fixed points of the $U(N_f)$-Gross-Neveu-Yukawa and of the $SU(N_f)$ pure fermionic QED in $2 < d < 4$ are respectively related to the UV fixed points of the Gross-Neveu and of the Thirring models.

Let us review the findings of [73] about the critical $\mathbb{CP}^{(N_f-1)}$ model in d-dimensions. The scaling dimension of the fundamental scalar field in the Landau gauge is

$$\Delta[\Phi_i] = \frac{d-2}{2} + \frac{1}{4}\Big(1 + \frac{4(d-1)^2}{d-4}\Big)\frac{\eta_1}{N_f} + O\Big(\frac{1}{N_f^2}\Big) \ , \tag{4.9}$$

where the η_1 is defined in (1.8). At the critical point, due to gauge invariance it is expected that the scaling dimension of the gauge field is exactly equal to $\Delta[A_\mu] = 1$. The absence of the anomalous dimension was confirmed in [73] at the order $O(1/N_f)$. The scaling dimension of the HS field σ is

$$\Delta[\sigma] = 2 + \frac{4d^2(d-1)(2-d)}{4-d}\frac{\eta_1}{N_f} + O\Big(\frac{1}{N_f^2}\Big) \ . \tag{4.10}$$

In [103] it was observed, that at the critical point the condition $\Phi^2 = 0$ (which is equivalent to saying that the singlet quadratic operator is out of spectrum) doesn't hold, after one introduces the analytic regularization. This regularization was employed in [73]. However in [103] using the Schwinger equations, it was proved that the Φ^2 doesn't give any new scaling dimension, instead

$$\Delta[\Phi^2] = d - \Delta[\sigma] = \nu^{-1} \ . \tag{4.11}$$

This relation is known as a "shadow relation". The anomalous scaling dimensions of the operators $O_1 = \frac{\sigma^2}{2}$ and $O_2 = \frac{F_{\mu\nu}^2}{4}$ was also studied. These operators have a scaling dimension 4 at leading order, and at the order $O(1/N_f)$ they mix. The mixing matrix in d-dimensions has the following form

$$\frac{\gamma}{N_f} = -\frac{4a\big(2-\frac{d}{2}\big)a\big(\frac{d}{2}-1\big)}{N_f a(2)\Gamma\big(\frac{d}{2}+1\big)}\begin{bmatrix}\gamma_{11} & \gamma_{12}\\ \gamma_{21} & \gamma_{22}\end{bmatrix} \ , \tag{4.12}$$

where

$$\gamma_{11} = \frac{d(d-1)^2(3-2d)}{4-d} \ , \tag{4.13}$$

$$\gamma_{12} = \frac{(4-d)(d+1)}{2} \ , \tag{4.14}$$

$$\gamma_{21} = \frac{d(d-1)^3(d+1)}{4-d} \ , \tag{4.15}$$

$$\gamma_{22} = \frac{(d^2-d-4)(d-1)}{2} \ . \tag{4.16}$$

The eigenvalues of the matrix γ/N_f are the anomalous dimensions which we denote by $\gamma_{1,2}/N_f$. The eigenstates are mixtures of the operators O_1 and O_2. The full scaling dimensions are

$$\Delta_1 = 4 + \frac{\gamma_1(d)}{N_f} + O\Big(\frac{1}{N_f^2}\Big) \ , \tag{4.17}$$

$$\Delta_2 = 4 + \frac{\gamma_2(d)}{N_f} + O\Big(\frac{1}{N_f^2}\Big) \ . \tag{4.18}$$

The analytic expression for $\gamma_{1,2}$ as a function of d are very cumbersome. In the Fig. 4.1 we plot them in the region $2 < d < 6$ (and a separate small plot shows the same functions in the region $2 < d < 4$).

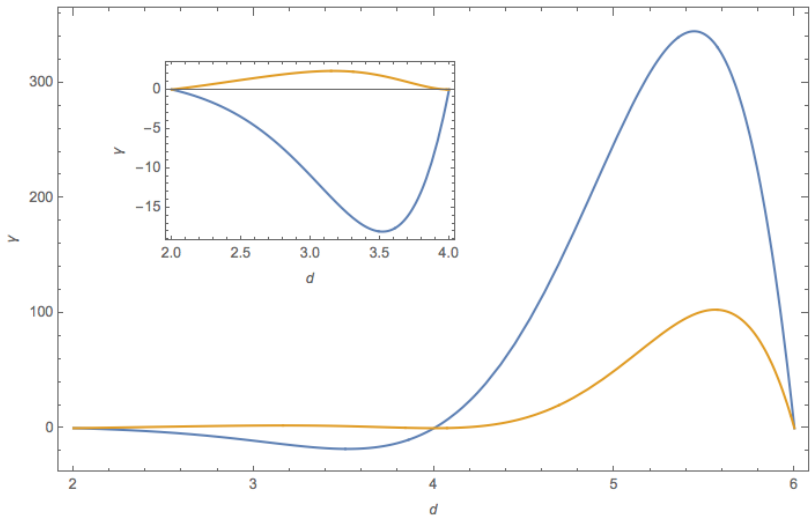

Figure 4.1: $\gamma_1(d)$ (blue) and $\gamma_2(d)$ (orange)

For our future purpose we will need the scaling dimensions (4.9, 4.10, 4.11, 4.17, 4.18)

at $d = 6 - 2\epsilon$ expanded for small ϵ

$$\Delta[\Phi_i] = 2 - \epsilon + \frac{51}{N_f}\epsilon - \frac{167}{2N_f}\epsilon^2 + O(\epsilon^3) \ , \tag{4.19}$$

$$\Delta[\sigma] = 2 + \frac{1440}{N_f}\epsilon - \frac{3456}{N_f}\epsilon^2 + O(\epsilon^3) \ , \tag{4.20}$$

$$\Delta[A_\mu] = 1 \tag{4.21}$$

$$\Delta[\Phi^2] = 4 - 2\epsilon - \frac{1440}{N_f}\epsilon + \frac{3456}{N_f}\epsilon^2 + O(\epsilon^3) \ , \tag{4.22}$$

$$\Delta_1 = 4 + \frac{40(50 + 7\sqrt{10})}{N_f}\epsilon - \frac{2(8275 + 827\sqrt{10})}{3N_f}\epsilon^2 + O(\epsilon^3) \ , \tag{4.23}$$

$$\Delta_2 = 4 + \frac{40(50 - 7\sqrt{10})}{N_f}\epsilon - \frac{2(8275 - 827\sqrt{10})}{3N_f}\epsilon^2 + O(\epsilon^3) \ . \tag{4.24}$$

To our knowledge the critical pure scalar-QED in $4 < d < 6$ has not been studied yet. We calculated scaling dimensions at order $O(1/N_f)$ for few operators. Below we give the results without providing details on calculations

$$\Delta[\Phi_i] = \frac{d-2}{2} + \frac{(d-1)^2}{(d-4)}\frac{\eta_1}{N_f} + O\Big(\frac{1}{N_f^2}\Big) \ , \tag{4.25}$$

$$\Delta[A_\mu] = 1 \ , \tag{4.26}$$

$$\Delta[\Phi^2] = d - 2 + \frac{(d-1)^2(d(d-1)-2)}{4-d}\frac{\eta_1}{N_f} + O\Big(\frac{1}{N_f^2}\Big) \ . \tag{4.27}$$

The dimension of Φ_i (4.25) is given in the Landau gauge. Expanding (4.25, 4.27) at $d = 6-2\epsilon$ for small ϵ gives

$$\Delta[\Phi_i] = 2 - \epsilon + \frac{50}{N_f}\epsilon - \frac{245}{3N_f}\epsilon^2 + O(\epsilon^3) \ , \tag{4.28}$$

$$\Delta[\Phi^2] = 4 - 2\epsilon - \frac{1400}{N_f}\epsilon + \frac{10160}{3N_f}\epsilon^2 + O(\epsilon^3) \ . \tag{4.29}$$

4.2 Higher Derivative Gauge theory in $d = 6$

The HDG is defined with the following Euclidean (bare) action

$$S = \int d^dx \Big[\overline{D_\mu\Phi_i}D^\mu\Phi^i + \frac{1}{2}\partial_\mu\sigma\partial^\mu\sigma + \frac{1}{4}\partial_\mu F_{\alpha\beta}\partial^\mu F^{\alpha\beta} + \tau_1^{(0)}\Phi_i^*\Phi^i + \frac{\tau_2^{(0)}\sigma^2}{2} + \frac{\tau_3^{(0)}F_{\alpha\beta}F^{\alpha\beta}}{4}$$
$$+ g_1^{(0)}\sigma\Phi_i^*\Phi^i + \frac{g_2^{(0)}\sigma^3}{6} + \frac{\lambda^{(0)}\sigma F_{\alpha\beta}F^{\alpha\beta}}{2} + \frac{1}{2\xi}\big(\partial_\mu\partial_\alpha A^\alpha\big)\big(\partial^\mu\partial_\beta A^\beta\big)\Big] \tag{4.30}$$

where $D_\mu = \partial_\mu + ie_0A_\mu$. The action (4.30) has a $SU(N_f)$ global symmetry, the complex scalar fields $\Phi_i,\ i = 1, ..., N_f$ transform in the fundamental representation of $SU(N_f)$. The

real scalar field σ is a $SU(N_f)$ singlet. The kinetic term for the gauge field A_μ contains 4-derivatives as opposed to the standard two-derivative kinetic terms, hence the name "higher derivative gauge theory". The last term in the action (4.30) is the gauge fixing. We call it a $\mathbb{R}_\xi$ gauge borrowing the name of the standard gauge fixing: $\frac{(\partial A)^2}{2\xi}$, commonly used in the 4-dimensional gauge theories. The propagator of the gauge field A_μ in the $\mathbb{R}_\xi$ gauge has the following form.

$$D_{\alpha\beta}(p) = \langle A_\alpha(p) A_\beta(-p)\rangle = \frac{1}{p^2(p^2+\tau_3)}\Big[\delta_{\alpha\beta} + \frac{(\xi-1)p^2 + \xi\tau_3}{p^2}\frac{p_\alpha p_\beta}{p^2}\Big] \ . \tag{4.31}$$

We will work in the Landau gauge $\xi = 0$. In the Landau gauge the propagator is transverse: $D_{\alpha\beta}(p)p^\beta = 0$.

The canonical dimensions of the scalar and gauge fields in $d = 6$ are: $d[\Phi] = d[\sigma] = 2$, $d[A] = 1$. Following the general rules, in the action (4.30) we included all the possible terms (scalar gauge invariant operators preserving the $SU(N_f)$ symmetry) that have dimensions less or equal 6. There are 3 mass terms: $\Phi^2, \sigma^2, F^2_{\alpha\beta}$ with dimensions equal to 4 (relevant operators) and there are 3 cubic interactions: $\sigma\Phi^2, \sigma^3, \sigma F^2_{\alpha\beta}$ with dimensions equal to 6 (marginal operators). The scalars Φ_i are minimally coupled to the gauge field which introduces the standard cubic and quartic interactions between these fields. To distinguish the bare parameters from the physical ones, we denoted the former with a superscript (4.30).

The marginal operator $F_{\alpha\beta}F_{\beta\gamma}F_{\gamma\alpha}$ is identically vanishing, since under the exchange $\alpha \leftrightarrow \beta$ the $F_{\alpha\beta}$ is antisymmetric and the $F_{\beta\gamma}F_{\gamma\alpha}$ is symmetric. Notice that besides the kinetic term for the gauge field that appears in (4.30), there is another dimension 6, 4-derivative operator: $\sim \partial_\mu F_{\alpha\beta}\partial_\alpha F_{\mu\beta}$. However we can prove that it is not an independent operator, indeed

$$\partial_\mu F_{\alpha\beta}\partial_\alpha F_{\mu\beta} = \partial_\mu F_{\alpha\beta}\big(\partial_\alpha F_{\mu\beta} - \partial_\beta F_{\mu\alpha}\big) = \partial_\mu F_{\alpha\beta}\partial_\mu F_{\alpha\beta} \ , \tag{4.32}$$

where in the last step we used the Bianchi identity: $\partial_\mu F_{\alpha\beta} + \partial_\alpha F_{\beta\mu} + \partial_\beta F_{\mu\alpha} = 0$. Therefore we conclude that in the action (4.30) we should include only one of these 4-derivative operators, which is what we did.

In order to cure the divergencies appearing in the Green functions we need to renormalize the action (4.30). We perform the renormalization in the Minimal Subtraction (MS) scheme. First we introduce dimensional regularization, i.e. we define the theory (4.30) in the dimension $d = 6 - 2\epsilon$. The canonical dimensions of the fields in $d = 6 - 2\epsilon$ are: $d[\Phi] = d[\sigma] = 2 - \epsilon$, $d[A] = 1 - \epsilon$. The bare action (4.30) is related to the renormalized

action by field renormalizations:

$$S_R(\Phi,\sigma,A) = S(Z_\Phi\Phi, Z_\sigma\sigma, Z_A A) \tag{4.33}$$

$$Z_\Phi = Z_\Phi(g_1,g_2,e,\lambda,\epsilon) \tag{4.34}$$

$$Z_\sigma = Z_\sigma(g_1,g_2,e,\lambda,\epsilon) \tag{4.35}$$

$$Z_A = Z_A(g_1,g_2,e,\lambda,\epsilon) \tag{4.36}$$

The bare masses $\tau_a^{(0)}$ are related to the renormalized masses τ_a

$$\tau_a^{(0)} = \sum_b Z^\tau_{ab}(g_1,g_2,e,\lambda,\epsilon)\tau_b \ , \quad a,b = 1,2,3 \ , \tag{4.37}$$

The canonical dimensions of the mass parameters are $d[\tau_a^{(0)}] = d[\tau_a] = 2$. The canonical dimensions of the bare couplings are $d[g_1^{(0)}] = d[g_2^{(0)}] = d[e^{(0)}] = d[\lambda^{(0)}] = \epsilon$. The renormalized couplings in (4.38) are dimensionless, this is achieved by introducing the MS scheme parameter μ, which has a mass dimension equal to one. For convenience let us denote $(e = g_3, \lambda = g_4)$, then the relation between the bare and renormalized couplings can be written in the compact form

$$g_u^{(0)} = \sum_v Z_{uv}(g_1,g_2,e,\lambda,\epsilon)\mu^\epsilon g_v \ , \quad u,v = 1,2,3,4 \ , \tag{4.38}$$

The gauge coupling is actually renormalized multiplicatively

$$e^{(0)} = Z_e(g_1,g_2,e,\lambda,\epsilon)\mu^\epsilon e \ , \tag{4.39}$$

In other words $Z_{31} = Z_{32} = Z_{34} = 0$ and $Z_{33} \equiv Z_e$ in (4.38). It follows from the gauge invariance of the action (4.30) that $Z_e Z_A = 1$. Therefore we do not need to separately renormalize the gauge interaction vertices $(A_\alpha^2|\Phi|^2, A_\alpha\Phi^*\overleftrightarrow{\partial}_\alpha\Phi)$, instead we determine $Z_A = 1/Z_e$ by studing the renormalization of the gauge field propagator.

We remind that the renormalized action is a function either of bare parameters or of renormalized parameters, since only one set can be considered to be independent. We choose S_R to be a function of renormalized masses and couplings.

$$\begin{aligned}
S_R = \int d^dx \Big[& \overline{D_\mu\Phi_i}D^\mu\Phi^i + \frac{1}{2}\partial_\mu\sigma\partial^\mu\sigma + \frac{1}{4}\partial_\mu F_{\alpha\beta}\partial^\mu F^{\alpha\beta} + \tau_1\Phi_i^*\Phi^i + \frac{\tau_2\sigma^2}{2} + \frac{\tau_3 F_{\alpha\beta}F^{\alpha\beta}}{4} \\
& + g_1\mu^\epsilon\sigma\Phi_i^*\Phi^i + \frac{g_2\mu^\epsilon\sigma^3}{6} + \frac{\lambda\mu^\epsilon\sigma F_{\alpha\beta}F^{\alpha\beta}}{2} + \frac{1}{2\xi}\big(\partial_\mu\partial_\alpha A^\alpha\big)\big(\partial^\mu\partial_\beta A^\beta\big) \\
& + (Z_\Phi^2 - 1)\overline{D_\mu\Phi_i}D^\mu\Phi^i + \frac{Z_\sigma^2 - 1}{2}\partial_\mu\sigma\partial^\mu\sigma + \frac{Z_A^2 - 1}{4}\partial_\mu F_{\alpha\beta}\partial^\mu F^{\alpha\beta} \\
& + \big(Z_\Phi^2\sum Z^\tau_{1a}\tau_a - \tau_1\big)\Phi_i^*\Phi^i + \frac{\big(Z_\sigma^2\sum Z^\tau_{2a}\tau_a - \tau_2\big)\sigma^2}{2} + \frac{\big(Z_A^2\sum Z^\tau_{3a}\tau_a - \tau_3\big)F_{\alpha\beta}F^{\alpha\beta}}{4} \\
& + \big(Z_\Phi^2 Z_\sigma\sum Z_{1u}g_u - g_1\big)\mu^\epsilon\sigma\Phi_i^*\Phi^i + \frac{\big(Z_\sigma^3\sum Z_{2u}g_u - g_2\big)\mu^\epsilon\sigma^3}{6} + \frac{\big(Z_\sigma Z_A^2\sum Z_{4u}g_u - \lambda\big)\mu^\epsilon\sigma F_{\alpha\beta}F^{\alpha\beta}}{2}\Big] \ .
\end{aligned} \tag{4.40}$$

Using (4.40) we define the Feynman rules for the vertices (see Tab. 4.1) and for the counter-vertices (CV). The graphical representation for the propagators and vertices are collected in Tab. 4.1.

$$CV^{(\sigma\Phi\Phi^*)} = -(Z_\Phi^2 Z_\sigma Z_{11} - 1)g_1\mu^\epsilon - Z_\Phi^2 Z_\sigma Z_{12} g_2\mu^\epsilon - Z_\Phi^2 Z_\sigma Z_{13} e\mu^\epsilon - Z_\Phi^2 Z_\sigma Z_{14}\lambda\mu^\epsilon \ , \tag{4.41}$$

$$CV^{(\sigma\sigma\sigma)} = -Z_\sigma^3 Z_{21} g_1\mu^\epsilon - (Z_\sigma^3 Z_{22} - 1)g_2\mu^\epsilon - Z_\sigma^3 Z_{23} e\mu^\epsilon - Z_\sigma^3 Z_{24}\lambda\mu^\epsilon \ , \tag{4.42}$$

$$CV^{\left(\sigma A_\alpha(p) A_\beta(q)\right)} = 2\left[Z_A^2 Z_\sigma Z_{41} g_1\mu^\epsilon + Z_A^2 Z_\sigma Z_{42} g_2\mu^\epsilon + Z_A^2 Z_\sigma Z_{43} e\mu^\epsilon + (Z_A^2 Z_\sigma Z_{44} - 1)\lambda\mu^\epsilon\right] L_{\alpha\beta}(p,q) \ . \tag{4.43}$$

where we defined $L_{\alpha\beta}(p,q) \equiv \delta_{\alpha\beta} p\cdot q - p_\beta q_\alpha$. The counter-terms for the kinetic and for the mass terms are given in the first lines of the Tab. 4.3, 4.4, 4.5, 4.6.

The 1-PI Green-functions of the renormalized theory are constructed in the form of perturbative expansion in the renormalized couplings. All the terms of this expansion can be represented graphically: connected Feynman graphs with amputated external legs and such that cutting any single internal leg doesn't split the graph into disconnected components. The Feynman graphs already at one-loop typically are divergent integrals (when we put $\epsilon = 0$). Demanding that the Green functions are free of divergencies one determines order-by-order the renormalization constants (Z's) defined in (4.34, 4.35, 4.36, 4.37, 4.38, 4.39) and the counter-vertices. In the next section we determine Z_Φ, Z_σ, Z_A and the the matrix Z_{uv} (4.38). To determine these constants it is sufficient to renormalize the 2-point and the 3-point Green functions in the massless limit: $\tau_a = 0,\ a = 1,2,3$.

4.3 Renormalization of fields and cubic vertices: anomalous dimensions of fields and beta functions

We study the 1-PI two-point Green-functions for the scalar and gauge fields at the one-loop order. The Tab. 4.2 contain all the one-loop graphs that appear in those Green-functions. For our purposes, it is sufficient to calculate the divergent parts of the one-loop integrals, which are (simple) poles in $\epsilon \to 0$. Some of the graphs (G_1, G_4, G_5) in the Tab. 4.2 have already been evaluated in the context of the $O(N)$-Yukawa theory [65], which is the ungauged version of our theory[1].

[1] More precisely one should take $N = 2N_f$ in the $O(N)$-Yukawa theory, then to gauge the $U(1)$ factor in the $U(1)\times SU(N_f) \subset O(2N_f)$. As a result one will obtain the $SU(N_f)$ symmetric higher derivative gauge theory (4.30).

	$= \langle \Phi_i(p)\Phi_j^*(-p)\rangle = \frac{\delta_{ij}}{p^2+\tau_1}$
	$= \langle \sigma(p)\sigma(-p)\rangle = \frac{1}{p^2+\tau_2}$
	$= \langle A_\alpha(p)A_\beta(-p)\rangle = (4.31)$
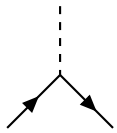	$= -\mu^\epsilon g_1$
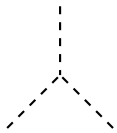	$= -\mu^\epsilon g_2$
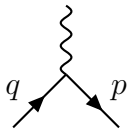	$= \mu^\epsilon e(p+q)_\alpha$
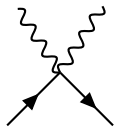	$= -2\mu^{2\epsilon}\delta_{\alpha\beta}e^2$
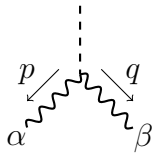	$= 2\mu^\epsilon\lambda(\delta_{\alpha\beta}p\cdot q - p_\beta q_\alpha) = 2\mu^\epsilon\lambda L_{\alpha\beta}(p,q)$

Table 4.1: Feynman rules for tree-level propagators and vertices.

Using (B.8), we obtain for the graph G_1

$$G_1 = (-g_1)^2\mu^{2\epsilon}\int\frac{d^dq}{(2\pi)^d}\frac{1}{q^2(q+p)^2} = (-g_1)^2\mu^{2\epsilon}\frac{\Gamma(2-\epsilon)^2\Gamma(-1+\epsilon)}{(4\pi)^{3-\epsilon}\Gamma(1)^2\Gamma(4-2\epsilon)}p^{2-2\epsilon}$$
$$\overset{\epsilon\to 0}{=} -\frac{g_1^2}{6(4\pi)^3\epsilon}p^2 \ . \tag{4.44}$$

The graph G_2 gives

$$\begin{aligned} G_2 &= e^2\mu^{2\epsilon}\int\frac{d^dq}{(2\pi)^d}\frac{(2p+q)_\alpha(2p+q)_\beta}{(p+q)^2}\frac{\delta_{\alpha\beta}-\frac{q_\alpha q_\beta}{q^2}}{q^4} \\ &= 4e^2\mu^{2\epsilon}\Big(p^2\int\frac{d^dq}{(2\pi)^d}\frac{1}{(p+q)^2q^4} - p_\alpha p_\beta\int\frac{d^dq}{(2\pi)^d}\frac{q_\alpha q_\beta}{(p+q)^2q^6}\Big) \\ &\overset{\epsilon\to 0}{=} 4e^2\Big(\frac{p^2}{2(4\pi)^3\epsilon}-\frac{p^2}{12(4\pi)^3\epsilon}\Big) = \frac{5e^2}{3(4\pi)^3\epsilon}p^2 \ . \end{aligned} \tag{4.45}$$

To pass to the second line in (4.45), we used the transversality condition of the photon propagator. The first integral of the second line is evaluated using (B.8), the second integral is evaluated introducing Feynman parametrization (B.7) and then using formulas (B.9, B.10). The tadpole G_3 is vanishing in the dimensional regularization in the massless limit and therefore it does not contribute to the field renormalization. However we will see in the next section that the tadpoles are important for mass renormalizations. The counter-term $CV^{(\Phi\Phi^*)} = -(Z_\Phi^2-1)p^2$ must be such that the Green function $\Gamma^{(\Phi\Phi^*)}$, thus

$$Z_\Phi = 1 - \frac{g_1^2}{12(4\pi)^3\epsilon} + \frac{5e^2}{6(4\pi)^3\epsilon} \ . \tag{4.46}$$

The graphs G_4, G_5 have the same topology as the graph G_1, and can be evaluated similarly. Their values are given in the Tab. 4.2. The graph G_6 gives

$$G_6 = 2\lambda^2\mu^{2\epsilon}\int\frac{d^dq}{(2\pi)^d}L_{\alpha\mu}(q,p-q)D_{\alpha\beta}(q)L_{\beta\nu}(-q,q-p)D_{\mu\nu}(p-q) \overset{\epsilon\to 0}{=} -\frac{5\lambda^2}{(4\pi)^3\epsilon}p^2 \ . \tag{4.47}$$

The integral in (4.47) can be simplified using the transversality condition and the identity $q(q-p) = \frac{q^2+(q-p)^2-p^2}{2}$. The resulting integrals are evaluated introducing the Feynman parametrization and with the help of formulas (B.9, B.10, B.11). We omit the details of a long and tedious calculation.

The counter-term $CV^{(\sigma\sigma)} = -(Z_\sigma^2-1)p^2$ should cancel the divergencies in the Green function $\Gamma^{(\sigma\sigma)}$, thus

$$Z_\sigma = 1 - \frac{N_f g_1^2}{12(4\pi)^3\epsilon} - \frac{g_2^2}{24(4\pi)^3\epsilon} - \frac{5\lambda^2}{2(4\pi)^3\epsilon} \ . \tag{4.48}$$

The graph G_7 gives

$$G_7 = N_f e^2 \mu^{2\epsilon} \int \frac{d^d q}{(2\pi)^d} \frac{(p+2q)_\alpha (p+2q)_\beta}{q^2 (p+q)^2} \overset{\epsilon \to 0}{=} \frac{N_f e^2}{30(4\pi)^3 \epsilon} (\delta_{\alpha\beta} p^4 - p_\alpha p_\beta p^2) \ . \tag{4.49}$$

The factor N_f is due to the N_f scalar flavors circulating in the loop of the graph G_7. Notice that the G_7 (4.49) is transverse. This was expected since G_7 contributes to the self-energy of the photon, which in turn must be transverse due to the gauge invariance. The tadpole G_8 is vanishing in the dimensional regularization in the massless limit. The graph G_9 has no pole

$$G_9 = 4\lambda^2 \mu^{2\epsilon} \int \frac{d^d q}{(2\pi)^d} \frac{1}{(p-q)^2} L_{\alpha\mu}(-p,q) D_{\mu\nu}(q) L_{\nu\beta}(-q,p) \overset{\epsilon \to 0}{=} 0 \ . \tag{4.50}$$

The integral (4.50) is simplified noticing that $D_{\mu\nu}(q) L_{\nu\beta}(-q,p) = L_{\mu\beta}/q^4$, the resulting integral is simply calculated with the help of formulas of appendix B.

We choose the Z_A such that the counter-term $CV^{(AA)} = -(Z_A^2 - 1)(\delta_{\alpha\beta} p^4 - p_\alpha p_\beta p^2)$ cancels the divergencies in the Green function $\Gamma^{(AA)}$

$$Z_A = 1 + \frac{N_f e^2}{60(4\pi)^3 \epsilon} \ . \tag{4.51}$$

The anomalous dimensions of the fields are constructed using the field renormalization constants (4.46, 4.48, 4.51) as follows

$$\gamma_\Phi = \frac{d \ln Z_\Phi}{d \ln \mu} = \frac{g_1^2 - 10 e^2}{6(4\pi)^3} \ , \tag{4.52}$$

$$\gamma_\sigma = \frac{d \ln Z_\sigma}{d \ln \mu} = \frac{2 N_f g_1^2 + g_2^2 + 60\lambda^2}{12(4\pi)^3} \ , \tag{4.53}$$

$$\gamma_A = \frac{d \ln Z_A}{d \ln \mu} = -\frac{N_f e^2}{30(4\pi)^3} \ , \tag{4.54}$$

where we used the chain rule $\frac{d \ln Z}{d \ln \mu} = \sum_u \beta_{g_u} \frac{d \ln Z}{d g_u}$ and the beta functions in the trivial approximation $\beta_{g_u} = (-\epsilon g_u + ...)$.

Next we proceed with the renormalization of the 3-point 1-PI Green functions, i.e. the vertices. All the one-loop graphs appearing in those Green functions are collected in Tab. 4.3. In the first line of Tab. 4.3 we draw the counter-vertices. To calculate the graphs that appear in the Green functions $\Gamma^{(\sigma\Phi\Phi^*)}, \Gamma^{(\sigma\sigma\sigma)}$ we do not need to prescribe arbitrary momenta to the external legs (subject to the obvious condition that the total sum of the momenta is zero), it is sufficient to choose two of the external legs with opposite non-zero momenta and the remaining leg with zero momentum. Crucially the choice can vary from graph to graph, the only requirement is that the graph with a given choice of momenta "leak" should not

$\Gamma^{(\Phi\Phi^*)}$		$\Gamma^{(\sigma\sigma)}$	
	$= -(Z_\Phi^2 - 1)p^2$		$= -(Z_\sigma^2 - 1)p^2$
G_1 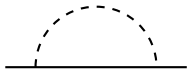	$= -\frac{g_1^2}{6(4\pi)^3\epsilon}p^2$	G_4 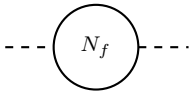	$= -\frac{N_f g_1^2}{6(4\pi)^3\epsilon}p^2$
G_2 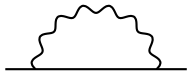	$= -\frac{5e^2}{3(4\pi)^3\epsilon}p^2$	G_5	$= -\frac{g_2^2}{12(4\pi)^3\epsilon}p^2$
G_3 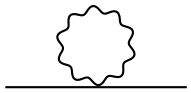	$= 0$	G_6 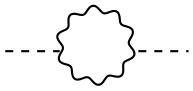	$= -\frac{5\lambda^2}{(4\pi)^3\epsilon}p^2$

$\Gamma^{(AA)}$	
	$= -(Z_A^2 - 1)(\delta_{\alpha\beta}p^4 - p_\alpha p_\beta p^2)$
G_7 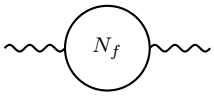	$= \frac{N_f e^2}{30(4\pi)^3\epsilon}(\delta_{\alpha\beta}p^4 - p_\alpha p_\beta p^2)$
G_8 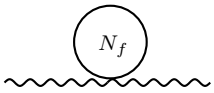	$= 0$
G_9	$= 0$

Table 4.2: 2-point Green functions in the one-loop approximation.

$\Gamma^{(\sigma\Phi\Phi^*)}$	$\Gamma^{(\sigma\sigma\sigma)}$	$\Gamma^{(\sigma AA)} = \langle A_\alpha(p)A_\beta(-p)\sigma(0)\rangle$
$= (4.41)$	$= (4.42)$	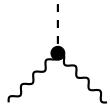 $= (4.43)$
G_{10} 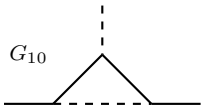 $= -\frac{g_1^3}{2(4\pi)^3\epsilon}$	G_{15} 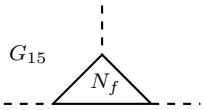 $= -\frac{N_f g_1^3}{(4\pi)^3\epsilon}$	G_{18} 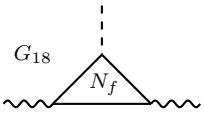 $= -\frac{N_f g_1 e^2}{3(4\pi)^3\epsilon}L_{\alpha\beta}$
G_{11} $= -\frac{g_1^2 g_2}{2(4\pi)^3\epsilon}$	G_{16} $= -\frac{g_2^3}{2(4\pi)^3\epsilon}$	G_{19} 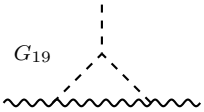 $= \frac{2g_2\lambda^2}{3(4\pi)^3\epsilon}L_{\alpha\beta}$
G_{12} 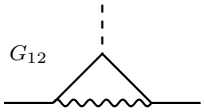 $= 0$	G_{17} 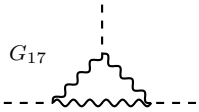 $= -\frac{20\lambda^3}{(4\pi)^3\epsilon}$	G_{20} 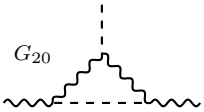 $= \frac{4\lambda^3}{3(4\pi)^3\epsilon}L_{\alpha\beta}$
G_{13} 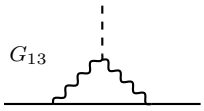 $= 0$		G_{21} 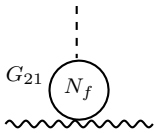 $= 0$
G_{14} 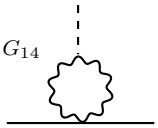 $= \frac{5e^2\lambda}{(4\pi)^3\epsilon}$		

Table 4.3: 3-point Green functions in the one-loop approximation. $L_{\alpha\beta} = p_\alpha p_\beta - \delta_{\alpha\beta}p^2$.

have infrared divergencies. This freedom, known as "Infrared rearrangement" [104, 105], is due to the graphs in the Green functions $\Gamma^{(\sigma\Phi\Phi^*)}, \Gamma^{(\sigma\sigma\sigma)}$ being only logarithmically divergent. With a good choice of momenta leak, the integrals can simplify a lot (this could be especially useful if one wants to do higher loop calculations). In the case of Green function $\Gamma^{(\sigma AA)}$, the graphs are quadratically divergent and so the momenta leak should be fixed and must be the same for all the graphs.

The graphs $G_{10}, G_{11}, G_{15}, G_{16}$ have already been evaluated in [65]. In all the one-loop graphs of $\Gamma^{(\sigma\Phi\Phi^*)}$, we choose the momenta leak in the external lines as follows: $\sigma(-p)\ \Phi(p)\ \Phi^*(0)$. The graph G_{10} gives

$$G_{10} = (-g_1)^3 \mu^{3\epsilon} \int \frac{d^d q}{(2\pi)^d} \frac{1}{(p+q)^2 q^4} \overset{\epsilon\to 0}{=} -\frac{g_1^3}{2(4\pi)^3\epsilon} \ . \tag{4.55}$$

The graph G_{11} has the same topology as the graph G_{10}, and it can be evaluated similarly. Its value is given in the Tab. 4.3. It is easy to see that G_{12}, G_{13} have no poles. This is because in each of these graphs, with the right external leg (with our choice) carries a zero momentum and therefore the internal propagators adjacent to it have the same momenta, then using the transversality condition the integral vanishes. The graph G_{14} gives

$$\begin{aligned} G_{14} &= -\,2e^2\lambda\mu^{3\epsilon} \int \frac{d^d q}{(2\pi)^d} \delta_{\alpha\beta} D_{\alpha\mu}(q) D_{\beta\nu}(p-q) L_{\mu\nu}(q, p-q) \\ &= 2e^2\lambda\mu^{3\epsilon} \int \frac{d^d q}{(2\pi)^d} \Big(\frac{d-2}{q^2(p-q)^4} + \frac{[q\cdot(p-q)]^2}{q^4(p-q)^6} \Big) \\ &\overset{\epsilon\to 0}{=} 2e^2\lambda \Big(\frac{2}{(4\pi)^3\epsilon} + \frac{1}{2(4\pi)^3\epsilon} \Big) = \frac{5e^2\lambda}{(4\pi)^3\epsilon} \ . \end{aligned} \tag{4.56}$$

To pass to the second line we replaced $L_{\mu\nu}(q, p-q) = \delta_{\mu\nu} q\cdot(p-q) - q_\nu (p-q)_\mu \to -\delta_{\mu\nu} q^2$, because the terms in $L_{\mu\nu}(q, p-q)$ that are linear in q will not give poles after integration and the term $q_\mu q_\nu$ gives zero contribution after tensor contraction with the photon propagators. In the counter-vertex $CV^{(\sigma\Phi\Phi^*)}$ (4.41) we choose the constants $(Z_\Phi^2 Z_\sigma Z_{1u},\ u = 1,2,3,4)$ as to cancel the divergencies coming from G_{10}, G_{11}, G_{14}. Then using values of Z_Φ and Z_σ from (4.46, 4.48) we find the $(Z_{1u},\ u = 1,2,3,4)$

$$Z_{11} = 1 + \frac{(N_f-4)g_1^2}{12(4\pi)^3\epsilon} - \frac{g_1 g_2}{2(4\pi)^3\epsilon} + \frac{g_2^2}{24(4\pi)^3\epsilon} - \frac{5e^2}{3(4\pi)^3\epsilon} + \frac{5\lambda^2}{2(4\pi)^3\epsilon} \ , \tag{4.57}$$

$$Z_{12} = Z_{13} = 0 \ , \tag{4.58}$$

$$Z_{14} = \frac{5e^2}{(4\pi)^3\epsilon} \ . \tag{4.59}$$

In all the one-loop graphs of $\Gamma^{(\sigma\sigma\sigma)}$ we choose the momenta leak as follows: $\sigma(-p)\ \sigma(p)\ \sigma(0)$. The graphs G_{15}, G_{16} have the same topology as G_{10}, and can be evaluated similarly. Their

values are reported in the Tab. 4.3. The graph G_{17} gives

$$G_{17} = 8\lambda^3\mu^{3\epsilon}\int\frac{d^dq}{(2\pi)^d}L_{\alpha\rho}(q,p-q)D_{\alpha\beta}(q)L_{\beta\mu}(-q,q)D_{\mu\nu}(q)L_{\nu\sigma}(-q,q-p)D_{\rho\sigma}(p-q)$$
$$\overset{\epsilon\to 0}{=} -\frac{20\lambda^3}{(4\pi)^3\epsilon}\ . \tag{4.60}$$

Demanding the counter-vertex $CV^{(\sigma\sigma\sigma)}$ (4.42) to cancel the divergencies coming from G_{15}, G_{16}, G_{17} (i.e. to render the Green function $\Gamma^{(\sigma\sigma\sigma)}$) and using the value of Z_σ from (4.48) we find the $(Z_{2u},\ u = 1,2,3,4)$

$$Z_{21} = -\frac{N_f g_1^2}{(4\pi)^3\epsilon}\ , \tag{4.61}$$
$$Z_{22} = 1 + \frac{N_f g_1^2}{4(4\pi)^3\epsilon} - \frac{3g_2^2}{8(4\pi)^3\epsilon} + \frac{15\lambda^2}{2(4\pi)^3\epsilon}\ , \tag{4.62}$$
$$Z_{23} = 0\ , \tag{4.63}$$
$$Z_{24} = -\frac{20\lambda^2}{(4\pi)^3\epsilon}\ . \tag{4.64}$$

In the Green function $\Gamma^{(\sigma AA)}$ we choose the momenta leak as follows: $A_\alpha(p)\ A_\beta(-p)\ \sigma(0)$. The graphs G_{18}, G_{19}, G_{20} give

$$G_{18} = -2N_f g_1 e^2\mu^{3\epsilon}\int\frac{d^dq}{(2\pi)^d}\frac{(p+2q)_\alpha(p+2q)_\beta}{q^4(q+p)^2} \overset{\epsilon\to 0}{=} -\frac{N_f g_1 e^2}{3(4\pi)^3\epsilon}L_{\alpha\beta}\ , \tag{4.65}$$

$$G_{19} = -4g_2\lambda^2\mu^{3\epsilon}\int\frac{d^dq}{(2\pi)^d}L_{\alpha\mu}(-p,q)D_{\mu\nu}(q)L_{\nu\beta}(-q,p)\frac{1}{(p-q)^4} \overset{\epsilon\to 0}{=} \frac{2g_2\lambda^2}{3(4\pi)^3\epsilon}L_{\alpha\beta}\ , \tag{4.66}$$

$$G_{20} = 8\lambda^3\mu^{3\epsilon}\int\frac{d^dq}{(2\pi)^d}L_{\alpha\mu}(-p,q)D_{\mu\nu}(q)L_{\nu\rho}(-q,q)D_{\rho\sigma}(q)L_{\sigma\beta}(-q,p)\frac{1}{(p-q)^2} \overset{\epsilon\to 0}{=} \frac{4\lambda^3}{3(4\pi)^3\epsilon}L_{\alpha\beta}\ , \tag{4.67}$$

where we introduced a shorthand notation $L_{\alpha\beta} \equiv L_{\alpha\beta}(p,-p)$. Notice that the graphs G_{18}, G_{19}, G_{20} are one-loop corrections to the tree-level vertex $(\sigma - A - A)$ Tab. 4.1 and hence they must be proportional to the same rank-2 tensor $(L_{\alpha\beta})$ as the tree-level vertex, which is confirmed by (4.65, 4.66, 4.67). The graph G_{21} is zero in dimensional regularization in the massless limit. Demanding the counter-vertex $CV^{(\sigma AA)}$ (4.43) to cancel the divergencies coming from G_{18}, G_{19}, G_{20} and using the values of Z_σ and Z_A from (4.48, 4.51) we find

the $(Z_{4u},\ u=1,2,3,4)$

$$Z_{41} = \frac{N_f e^2}{6(4\pi)^3\epsilon} \ , \tag{4.68}$$

$$Z_{42} = -\frac{\lambda^2}{3(4\pi)^3\epsilon} \ , \tag{4.69}$$

$$Z_{43} = 0 \ , \tag{4.70}$$

$$Z_{44} = 1 + \frac{N_f g_1^2}{12(4\pi)^3\epsilon} + \frac{g_2^2}{24(4\pi)^3\epsilon} - \frac{N_f e^2}{30(4\pi)^3\epsilon} + \frac{11\lambda^2}{6(4\pi)^3\epsilon} \ . \tag{4.71}$$

In principle we could have renormalized the vertex $A-\Phi-\Phi^*$ as well. However as we already remarked in the section (4.2), the gauge coupling is renormalized multiplicatively (4.39) and due to gauge invariance

$$Z_e = 1/Z_A = 1 - \frac{N_f e^2}{60(4\pi)^3\epsilon} \ . \tag{4.72}$$

The final step is the construction of the beta functions with the help of the following equations

$$\epsilon g_u + \beta_{g_u} + Z_{uw}^{-1}\frac{dZ_{wv}}{dg_h} g_v \cdot \beta_{g_h} = 0 \ , \ u=1,2,3,4 \ , \tag{4.73}$$

where summation over indices w, v, h is assumed. The equations (4.73) follow from the Callan-Symanzik equations. Plugging values of the mixing matrix Z_{uv} into (4.73) we find the beta functions

$$\beta_{g_1} = -\epsilon g_1 + \frac{(N_f-4)g_1^3}{6(4\pi)^3} - \frac{g_1^2 g_2}{(4\pi)^3} + \frac{g_1 g_2^2}{12(4\pi)^3} - \frac{10 g_1 e^2}{3(4\pi)^3} + \frac{5 g_1 \lambda^2}{(4\pi)^3} + \frac{10\lambda e^2}{(4\pi)^3} \ , \tag{4.74}$$

$$\beta_{g_2} = -\epsilon g_2 - \frac{2N_f g_1^3}{(4\pi)^3} + \frac{N_f g_1^2 g_2}{2(4\pi)^3} - \frac{3g_2^3}{4(4\pi)^3} + \frac{15 g_2 \lambda^2}{(4\pi)^3} - \frac{40\lambda^3}{(4\pi)^3} \ , \tag{4.75}$$

$$\beta_e = -\epsilon e - \frac{N_f e^3}{30(4\pi)^3} \ , \tag{4.76}$$

$$\beta_\lambda = -\epsilon\lambda + \frac{N_f g_1 e^2}{3(4\pi)^3} - \frac{2g_2\lambda^2}{3(4\pi)^3} + \frac{N_f g_1^2 \lambda}{6(4\pi)^3} + \frac{\lambda g_2^2}{12(4\pi)^3} - \frac{N_f \lambda e^2}{15(4\pi)^3} + \frac{11\lambda^3}{3(4\pi)^3} \ . \tag{4.77}$$

It is obvious that the HDG is asymptotically free in the UV limit in $d = 6 - 2\epsilon$.

Large N_f limit of the beta functions: We solve the beta functions (4.74, 4.75, 4.76, 4.77) in the large N_f limit. Besides the trivial fixed point where all the couplings vanish, we find three IR interacting fixed points. One of the fixed points has a vanishing gauge coupling. It is the fixed point of the $O(2N_f)$-Yukawa theory [65]. The other two fixed points have a

non-vanishing gauge coupling. We denote them as FP_1 and FP_2. The values of couplings at those fixed points are

$$\mathrm{FP}_1:$$

$$g_1 = \sqrt{\frac{6(4\pi)^3\epsilon}{N_f}}\Big(1+\frac{336}{N_f}+O\big(\frac{1}{N_f^2}\big)\Big)\ , \tag{4.78}$$

$$g_2 = 6\sqrt{\frac{6(4\pi)^3\epsilon}{N_f}}\Big(1+O\big(\frac{1}{N_f}\big)\Big)\ , \tag{4.79}$$

$$e^2 = -\frac{30(4\pi)^3\epsilon}{N_f}\ , \tag{4.80}$$

$$\lambda = 5\sqrt{\frac{6(4\pi)^3\epsilon}{N_f}}\Big(1+O\big(\frac{1}{N_f}\big)\Big)\ . \tag{4.81}$$

$$\mathrm{FP}_2:$$

$$g_1 = g_2 = \lambda = 0\ , \tag{4.82}$$

$$e^2 = -\frac{30(4\pi)^3\epsilon}{N_f}\ . \tag{4.83}$$

Since at the fixed point FP_2 the couplings g_1, g_2, λ vanish, the σ field does not interact with any other field (including itself) and propagates freely. At the FP_2 the scalar flavors Φ_i are minimally coupled to the gauge field, with non-zero gauge coupling (4.83). The irrelevant Φ^4 operator cannot be generated along the flow (at least if we are close to d=6). Therefore we can foresee that the FP_2 describes the critical scalar QED. Instead at the fixed point FP_1 neither of the couplings vanish (4.78, 4.79, 4.80, 4.82) and it describes the critical $\mathbb{CP}^{(N_f-1)}$.

In order to test these statements, below we evaluate the scaling dimensions of the fields (Φ, σ, A) at the fixed points $\mathrm{FP}_{1,2}$. Plugging in (4.52, 4.53, 4.54) the FP_1 values of the couplings we obtain

$$\Delta[\Phi_i] = 2-\epsilon+\frac{51\epsilon}{N_f}+O(\epsilon^2)\ , \tag{4.84}$$

$$\Delta[\sigma] = 2+\frac{1440\epsilon}{N_f}+O(\epsilon^2)\ , \tag{4.85}$$

$$\Delta[A_\mu] = 1\ . \tag{4.86}$$

The scaling dimension of the gauge field at the interacting fixed point is equal to 1 (actually this holds true at all orders in the perturbative expansion). We see a perfect match with the scaling dimensions of the fields (Φ, σ, A) calculated at the critical point $\mathbb{CP}^{(N_f-1)}$ (4.19, 4.20, 4.21) with the help of a large N_f expansion.

Similarly, plugging in (4.52, 4.53, 4.54) the FP_2 values of the couplings we obtain (as we have already mentioned the σ field is free, and its scaling dimension is that of a free scalar

field in $d = 6 - 2\epsilon$)

$$\Delta[\Phi_i] = 2 - \epsilon + \frac{50\epsilon}{N_f} + O(\epsilon^2) \ , \tag{4.87}$$

$$\Delta[A_\mu] = 1 \ . \tag{4.88}$$

Again, we find an agreement with the scaling dimensions of the fields (Φ, A) calculated at the critical pure scalar QED (4.25, 4.26).

4.4 Renormalization of the mass parameters and the anomalous dimensions of the quadratic operators

Until now we considered the theory (4.30) in the massless limit. When one turns on the masses, additional divergencies appear in the 2-point 1PI Green functions which must be cancelled with the appropriate mass counter-terms. The strategy for calculating these counter-terms is to first differentiate the 2-point Green functions with respect to the mass and then to put the mass equal to zero. In this way, quadratically divergent Green functions $\Gamma^{(\Phi\Phi^*)}$ and $\Gamma^{(\sigma\sigma)}$ become logarithmically divergent and the quarticly divergent Green function $\Gamma^{(AA)}$ becomes quadratically divergent. The graphs which appear in the differentiated Green functions are collected in the Tab. 4.4, 4.5, 4.6. We use the slash to mark the propagators which have been differentiated in a given graph. In the first lines of the Tab. 4.4, 4.5, 4.6 we provide the differentiated mass counter-terms, which are necessary for curing the divergencies.

Using (B.9) for the graph G_{22} we obtain

$$G_{22} = -g_1^2 \mu^{2\epsilon} \int \frac{d^d q}{(2\pi)^d} \frac{1}{q^4 (p-q)^2} \overset{\epsilon \to 0}{=} -\frac{g_1^2}{2(4\pi)^4 \epsilon} \ . \tag{4.89}$$

The minus sign in front of the integral (4.89) comes from the differentiation of the scalar propagator $\frac{\partial}{\partial \tau_1}\left(\frac{1}{q^2+\tau_1}\right)\Big|_{\tau_1=0} = -\frac{1}{q^4}$. The graph G_{23} gives

$$G_{23} = -e^2 \mu^{2\epsilon} \int \frac{d^d q}{(2\pi)^d} \frac{(2p-q)_\alpha (2p-q)_\beta}{(p-q)^4} D_{\alpha\beta}(q) = \text{finite} \ . \tag{4.90}$$

The absence of a pole in G_{23} can be proved using the transversality condition $D_{\alpha\beta} q_\alpha = 0$ in (4.90). Using (4.89) and the value of Z_ϕ from (4.46), we find

$$Z_{11}^\tau = 1 - \frac{g_1^2}{3(4\pi)^3 \epsilon} - \frac{5e^2}{3(4\pi)^3 \epsilon} \ . \tag{4.91}$$

The pole of the graph G_{24} is the same as that of the G_{22}. Using it we find

$$Z_{12}^\tau = -\frac{g_1^2}{2(4\pi)^3 \epsilon} \ . \tag{4.92}$$

The graph G_{25} is finite (using the transversality condition). The tadpole G_{26} gives

$$G_{26} = e^2\mu^{2\epsilon}\int \frac{d^dq}{(2\pi)^d}\delta_{\alpha\beta}\frac{\delta_{\alpha\beta}-\frac{q_\alpha q_\beta}{q^2}}{(q^2+\tau_3)^3} \overset{\epsilon\to 0}{=} \frac{5e^2}{2(4\pi)^3\epsilon} \ . \tag{4.93}$$

In the graph G_{26}, the gauge propagator is differentiated with respect to the gauge mass τ_3. In order to avoid the IR divergencies, in the integral (4.93) we kept a non-zero mass (which obviously doesn't effect the UV pole of the G_{26}). Using (4.93) we find

$$Z^\tau_{13} = \frac{5e^2}{2(4\pi)^3\epsilon} \ . \tag{4.94}$$

Notice that the loops in some of the graphs in Tab. 4.2 are made by the propagators of the same field. Therefore differentiation will give two equivalent graphs with one propagator differentiated and the other one not. Since they are equivalent we simply multiply those graphs by two in the Tab. 4.4, 4.5. The poles of the graphs G_{27} and G_{28} are extracted doing a calculation similar to the one in (4.89). Using their values, which are recorded in the Tab. 4.4 and the value of Z_σ we obtain

$$Z^\tau_{21} = -\frac{N_f g_1^2}{(4\pi)^3\epsilon} \ , \tag{4.95}$$

$$Z^\tau_{22} = 1 + \frac{N_f g_1^2}{6(4\pi)^3\epsilon} - \frac{5g_2^2}{12(4\pi)^3\epsilon} + \frac{5\lambda^2}{(4\pi)^3\epsilon} \ . \tag{4.96}$$

The graph G_{29} gives

$$G_{29} = -4\lambda^2\mu^{2\epsilon}\int \frac{d^dq}{(2\pi)^d}L_{\alpha\mu}(q,p-q)\frac{D_{\alpha\beta}(q)}{q^2}L_{\beta\nu}(q,p-q)D_{\mu\nu}(p-q) \overset{\epsilon\to 0}{=} -\frac{10\lambda^2}{(4\pi)^3\epsilon} \ . \tag{4.97}$$

The minus sign in front of the integral (4.97) comes from the differentiation of the photon propagator (4.31): $\left.\frac{\partial D_{\alpha\beta}(q)}{\partial\tau_3}\right|_{\tau_3=0} = -\frac{D_{\alpha\beta}(q)}{q^2}$. To extract the divergent part of the integral (4.97), it is sufficient to replace in it $L_{\alpha\mu}(q,p-q)\to -\delta_{\alpha\mu}q^2$ and $L_{\beta\nu}(q,p-q)\to -\delta_{\beta\nu}q^2$. This is because other terms inside these vertices either give finite contributions or vanish after multiplying them with photon propagators in (4.97). Using ((4.97)) we find

$$Z^\tau_{23} = -\frac{10\lambda^2}{(4\pi)^3\epsilon} \ . \tag{4.98}$$

The graph G_{30} gives

$$G_{30} = -2N_f e^2\mu^{2\epsilon}\int \frac{d^dq}{(2\pi)^d}\frac{(p+2q)_\alpha(p+2q)_\beta}{q^4(q+p)^2} \overset{\epsilon\to 0}{=} -\frac{N_f e^2}{3(4\pi)^3\epsilon}L_{\alpha\beta} \ . \tag{4.99}$$

The integral (4.99) is calculated introducing Feynman parametrization and using formulas (B.9, B.10). The tadpole G_{31} is vanishing in the dimensional regularization. Using the (4.99) we obtain

$$Z^\tau_{31} = \frac{N_f e^2}{3(4\pi)^3\epsilon} \ . \tag{4.100}$$

The graphs G_{32} and G_{33} are different but it turns out that their poles are equal

$$G_{32} = -4\lambda^2\mu^{2\epsilon}\int\frac{d^dq}{(2\pi)^d}\frac{1}{(p-q)^4}L_{\alpha\mu}(-p,q)D_{\mu\nu}(q)L_{\nu\beta}(-q,p) \overset{\epsilon\to 0}{=} \frac{2\lambda^2}{3(4\pi)^3\epsilon}L_{\alpha\beta}\ , \tag{4.101}$$

$$G_{33} = -4\lambda^2\mu^{2\epsilon}\int\frac{d^dq}{(2\pi)^d}\frac{1}{(p-q)^2}L_{\alpha\mu}(-p,q)\frac{D_{\mu\nu}(q)}{q^2}L_{\nu\beta}(-q,p) \overset{\epsilon\to 0}{=} \frac{2\lambda^2}{3(4\pi)^3\epsilon}L_{\alpha\beta}\ . \tag{4.102}$$

Using (4.101, 4.102) and the value of Z_A from (4.51) we find

$$Z^\tau_{32} = -\frac{2\lambda^2}{3(4\pi)^3\epsilon}\ , \tag{4.103}$$

$$Z^\tau_{33} = 1 - \frac{N_f e^2}{30(4\pi)^3\epsilon} - \frac{2\lambda^2}{3(4\pi)^3\epsilon}\ . \tag{4.104}$$

Having constructed the renormalization matrix Z^τ_{ab}, which is responsible for the mixing between the masses (4.37), we now proceed to find the mixing matrix of the mass parameters. Those are defined as follows

$$\gamma^\tau_{ab} = \frac{d\ln Z^\tau_{ab}}{d\ln\mu} = (Z^\tau)^{-1}_{ac}\frac{dZ^\tau_{cb}}{dg_v}\beta_{g_v}\ ; \qquad a,b = 1,2,3\ , \tag{4.105}$$

Where summation over the indices $c = 1,2,3$ and $v = 1,2,3,4$ is assumed. Plugging in (4.105) the values of Z^τ matrix, we find

$$\gamma^\tau_{ab} = \frac{1}{(4\pi)^3}\begin{bmatrix} \frac{2g_1^2}{3}+\frac{10e^2}{3} & g_1^2 & -5e^2 \\ 2N_f g_1^2 & -\frac{N_f g_1^2}{3}+\frac{5g_2^2}{6}-10\lambda^2 & 20\lambda^2 \\ -\frac{2N_f e^2}{3} & \frac{4\lambda^2}{3} & \frac{N_f e^2}{15}+\frac{4\lambda^2}{3} \end{bmatrix}\ , \tag{4.106}$$

where we factored out the common factor $1/(4\pi)^3$.

The scaling dimensions of the mass operators at the fixed points: We remind that the mixing matrix of the mass operators $(\Phi^2, \sigma^2, F^2_{\alpha\beta})$ is minus the (4.106). This is because the sum of the scaling dimensions of the mass and the mass operator should be equal to $d = 6-2\epsilon$ and we know that the classical dimensions of the mass and of mass operator are respectively 2 and $4-2\epsilon$.

First, let us construct the mixing matrix of the mass parameters at the fixed point FP_1. Plugging in (4.106) the FP_1 values of the couplings (4.78, 4.79, 4.80, 4.82) and keeping the entries of the matrix to the order $1/N_f$ we find

$$\gamma^\tau_{ab}\Big|_{\mathrm{FP}_1} = \epsilon\begin{bmatrix} \frac{-96}{N_f} & \frac{6}{N_f} & \frac{150}{N_f} \\ 12\big(1+\frac{672}{N_f}\big) & -2\big(1+\frac{1332}{N_f}\big) & \frac{3000}{N_f} \\ 20 & \frac{200}{N_f} & -2\big(1-\frac{100}{N_f}\big) \end{bmatrix}\ . \tag{4.107}$$

The eigenvalues of the matrix (4.107), taken with an opposite sign are the anomalous scaling dimensions of the mass operators [2]. The full scaling dimensions are as follows

$$\Delta_1^{(\mathrm{FP}_1)} = 4 - 2\epsilon - \Big(- 2\epsilon - \frac{2000 + 280\sqrt{10}}{N_f}\epsilon\Big) + O(\epsilon^2) = 4 + \frac{40(50 + 7\sqrt{10})}{N_f}\epsilon + O(\epsilon^2) \ , \quad (4.108)$$

$$\Delta_2^{(\mathrm{FP}_1)} = 4 - 2\epsilon - \Big(- 2\epsilon - \frac{2000 - 280\sqrt{10}}{N_f}\epsilon\Big) + O(\epsilon^2) = 4 + \frac{40(50 - 7\sqrt{10})}{N_f}\epsilon + O(\epsilon^2) \ , \quad (4.109)$$

$$\Delta_3^{(\mathrm{FP}_1)} = 4 - 2\epsilon - \frac{1440\epsilon}{N_f} + O(\epsilon^2) \ . \quad (4.110)$$

Again we find a perfect agreement with the scaling dimensions of these operators at the critical point $\mathbb{CP}^{(N_f-1)}$ (4.22, 4.23, 4.24).

Finally, let us plug in (4.106) the FP_2 values of the couplings to determine the anomalous mixing matrix of the mass parameters at that fixed point

$$\gamma^{\tau}_{ab}\Big|_{\mathrm{FP}_2} = \epsilon \begin{bmatrix} -\frac{100}{N_f} & \frac{150}{N_f} \\ 20 & -2 \end{bmatrix} \ . \quad (4.111)$$

The eigenvalues of the matrix (4.111), taken with an opposite sign are the anomalous scaling dimensions of the mass operators $(\Phi^2, F^2_{\alpha\beta})$. The full scaling dimensions are as follows

$$\Delta_1^{(\mathrm{FP}_2)} = 4 - 2\epsilon - \frac{1400}{N_f}\epsilon + O(\epsilon^2) \ , \quad (4.112)$$

$$\Delta_2^{(\mathrm{FP}_2)} = 4 + \frac{1500}{N_f}\epsilon + O(\epsilon^2) \ . \quad (4.113)$$

One of the eigenvalues, $\Delta_1^{(\mathrm{FP}_2)}$, matches with the scaling dimension of the Φ^2 operator calculated at the critical scalar QED (4.29). We do not have a formula for the scaling dimension (order $O(1/N_f)$) of the $F^2_{\alpha\beta}$ operator at the critical scalar QED, and so we cannot provide a check for (4.113). We remind that at the fixed point FP_2 the σ field doesn't interact, therefore the scaling dimension of the operator σ^2 is simply twice a scaling dimension of a free scalar field.

[2] To be more precise we should refer to the mass eigenstates rather than to the mass operators, since after diagonalization of the matrix (4.107) the operators $(\Phi^2, \sigma^2, F^2_{\alpha\beta})$ mix with each other.

$\partial_{\tau_1}\Gamma^{(\Phi\Phi^*)}\vert_{\tau_1=\tau_2=\tau_3=0}$	$\partial_{\tau_2}\Gamma^{(\Phi\Phi^*)}\vert_{\tau_1=\tau_2=\tau_3=0}$	$\partial_{\tau_3}\Gamma^{(\Phi\Phi^*)}\vert_{\tau_1=\tau_2=\tau_3=0}$
$\frac{\partial}{\partial\tau_1}$ 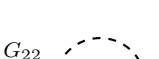 $= -(Z_\Phi^2 Z_{11}^\tau - 1)$	$\frac{\partial}{\partial\tau_2}$ $= -Z_\Phi^2 Z_{12}^\tau$	$\frac{\partial}{\partial\tau_3}$ $= -Z_\Phi^2 Z_{13}^\tau$
G_{22} $= -\frac{g_1^2}{2(4\pi)^3\epsilon}$	G_{24} 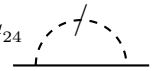 $= -\frac{g_1^2}{2(4\pi)^3\epsilon}$	G_{25} 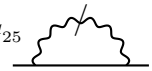 $= 0$
G_{23} $= 0$		G_{26} 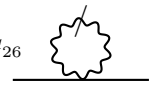 $= \frac{5e^2}{2(4\pi)^3\epsilon}$

Table 4.4: 2-point Green function $\Gamma^{(\Phi\Phi^*)}$ differentiated w.r.t masses

$\partial_{\tau_1}\Gamma^{(\sigma\sigma)}\vert_{\tau_1=\tau_2=\tau_3=0}$	$\partial_{\tau_2}\Gamma^{(\sigma\sigma)}\vert_{\tau_1=\tau_2=\tau_3=0}$	$\partial_{\tau_3}\Gamma^{(\sigma\sigma)}\vert_{\tau_1=\tau_2=\tau_3=0}$
$\frac{\partial}{\partial\tau_1}$ 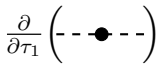 $= -Z_\sigma^2 Z_{21}^\tau$	$\frac{\partial}{\partial\tau_2}$ $= -(Z_\sigma^2 Z_{22}^\tau - 1)$	$\frac{\partial}{\partial\tau_3}$ $= -Z_\sigma^2 Z_{23}^\tau$
$2\times$ 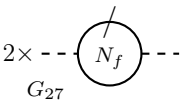 $= -\frac{N_f g_1^2}{(4\pi)^3\epsilon}$ G_{27}	$2\times$ 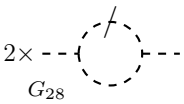 $= -\frac{g_2^2}{2(4\pi)^3\epsilon}$ G_{28}	$2\times$ 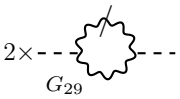 $= -\frac{10\lambda^2}{(4\pi)^3\epsilon}$ G_{29}

Table 4.5: 2-point Green function $\Gamma^{(\sigma\sigma)}$ differentiated w.r.t masses

$\partial_{\tau_1}\Gamma^{(AA)}\vert_{\tau_1=\tau_2=\tau_3=0}$	$\partial_{\tau_2}\Gamma^{(AA)}\vert_{\tau_1=\tau_2=\tau_3=0}$	$\partial_{\tau_3}\Gamma^{(AA)}\vert_{\tau_1=\tau_2=\tau_3=0}$
$\frac{\partial}{\partial\tau_1}$ 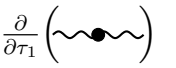 $= Z_A^2 Z_{31}^\tau L_{\alpha\beta}$	$\frac{\partial}{\partial\tau_2}$ $= Z_A^2 Z_{32}^\tau L_{\alpha\beta}$	$\frac{\partial}{\partial\tau_3}$ $= (Z_A^2 Z_{33}^\tau - 1) L_{\alpha\beta}$
$2\times$ 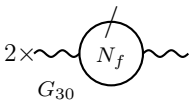 $= -\frac{N_f e^2}{3(4\pi)^3\epsilon} L_{\alpha\beta}$ G_{30}	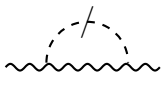 $= \frac{2\lambda^2}{3(4\pi)^3\epsilon} L_{\alpha\beta}$ G_{32}	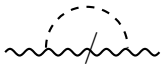 $= \frac{2\lambda^2}{3(4\pi)^3\epsilon} L_{\alpha\beta}$ G_{33}
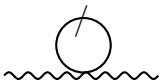 $= 0$ G_{31}		

Table 4.6: 2-point Green function $\Gamma^{(AA)}$ differentiated w.r.t masses

Appendix A

Bosonic QED's in the $4-2\epsilon$ expansion

We consider the bosonic QED's with global symmetry $SU(N_f/2)\times SU(N_f/2)\times U(1)$ in dimension $d=4-2\epsilon$

$$\begin{aligned}\mathcal{L} =&\frac{1}{4}F^{\mu\nu}F_{\mu\nu}+\sum_{i=1}^{N_f/2}\overline{D^\mu\Phi_i}D_\mu\Phi^i+\sum_{i=1}^{N_f/2}\overline{D^\mu\tilde{\Phi}_i}D_\mu\tilde{\Phi}^i+\lambda_{ep}\Big(\big(\sum_{i=1}^{N_f/2}|\Phi^i|^2\big)^2+\big(\sum_{i=1}^{N_f/2}|\tilde{\Phi}^i|^2\big)^2\Big)\\ &+\lambda\sum_{i=1}^{N_f/2}|\Phi^i|^2\sum_{j=1}^{N_f/2}|\tilde{\Phi}^j|^2+(\text{gauge fixing term})\ ,\end{aligned}\tag{A.1}$$

where the $D_\mu=\partial_\mu+ieA_\mu$, and the kinetic term for the photon is canonically normalized. Using [106, 107] the beta functions of the gauge and quartic couplings at one loop order are

$$\beta_e=\frac{de}{dl}=\epsilon e-\frac{1}{(4\pi)^2}\frac{2N_fe^3}{6}\ ,\tag{A.2}$$

$$\beta_{\lambda_{ep}}=\frac{d\lambda_{ep}}{dl}=2\epsilon\lambda_{ep}-\frac{1}{(4\pi)^2}\big[8(N_f+8)\lambda_{ep}^2+2N_f\lambda^2-12\lambda_{ep}e^2+\frac{3}{2}e^4\big]\ ,\tag{A.3}$$

$$\beta_\lambda=\frac{d\lambda}{dl}=2\epsilon\lambda-\frac{1}{(4\pi)^2}\big(16\lambda^2+16(N_f+2)\lambda\lambda_{ep}-12\lambda e^2+3e^4\big)\ .\tag{A.4}$$

The beta function of the gauge coupling has two zeroes. One trivial zero is when the gauge coupling vanishes, then we have the ungauged $O(N_f)\times O(N_f)$ vector model. See Introduction and chapter 3 for discussions about the ungauged fixed points and RG flow. The other zero is when

$$e^2=\frac{48\pi^2}{N_f}\epsilon\ .\tag{A.5}$$

Plugging this value into the beta functions (A.3, A.4) we generically expect to find four fixed points. There are two fixed points (which we identify with bQED and bQED$_+$ discussed in

the main text) for which $\lambda = 2\lambda_{ep}$ with a global symmetry group $SU(N_f)$. The values of the quartic couplings at those fixed points are

$$\lambda = 2\lambda_{ep} = \frac{N_f + 18 \pm \sqrt{N_f^2 - 180N_f - 540}}{N_f(N_f+4)}\pi^2 2\epsilon \ . \tag{A.6}$$

It follows from (A.6) that for $N_f < 182.95$ the quartic couplings become complex. Similarly one writes solutions for the remaining two fixed points (which we identify with ep-bQED and bQED$_-$ discussed in the main text), for which global symmetry is $SU(N_f/2) \times SU(N_f/2)$:

$$\lambda = \frac{-(N_f+18)(N_f-4) \mp \sqrt{\mathcal{D}}}{N_f(N_f^2+8)}\pi^2 2\epsilon \ , \tag{A.7}$$

$$\lambda_{ep} = \frac{288 + 160N_f + 62N_f^2 + 3N_f^3 \pm (4-N_f)\sqrt{\mathcal{D}}}{2N_f(N_f+8)(N_f^2+8)}\pi^2 2\epsilon \ , \tag{A.8}$$

where we defined the discriminant

$$\mathcal{D} = N_f^4 - 188N_f^3 - 1676N_f^2 - 3744N_f - 8640 \ . \tag{A.9}$$

It follows from (A.9) that at these two fixed points the quartic couplings become complex when $N_f < 196.22$.

We provide the expansions of solutions (A.6, A.7, A.8) in the large N$_f$ limit ($\epsilon = 1/2$)

$$\text{bQED (tricritical):} \quad \lambda_{ep} = \frac{54\pi^2}{N_f^2} + \frac{1944\pi^2}{N_f^3} + O\Big(\frac{1}{N_f^4}\Big), \ \lambda = 2\lambda_{ep} \ , \tag{A.10}$$

$$\text{bQED}_+\text{:} \quad \lambda_{ep} = \frac{\pi^2}{N_f} - \frac{40\pi^2}{N_f^2} - \frac{2000\pi^2}{N_f^3} + O\Big(\frac{1}{N_f^4}\Big), \ \lambda = 2\lambda_{ep} \ , \tag{A.11}$$

$$\text{bQED}_-\text{:} \ \lambda_{ep} = \frac{\pi^2}{N_f} + \frac{72\pi^2}{N_f^2} + \frac{1936\pi^2}{N_f^3} + O\Big(\frac{1}{N_f^4}\Big), \lambda = -\frac{2\pi^2}{N_f} + \frac{80\pi^2}{N_f^2} + \frac{5344\pi^2}{N_f^3} + O\Big(\frac{1}{N_f^4}\Big) \ , \tag{A.12}$$

$$\text{ep-bQED:} \ \lambda_{ep} = \frac{2\pi^2}{N_f} - \frac{34\pi^2}{N_f^2} - \frac{2104\pi^2}{N_f^3} + O\Big(\frac{1}{N_f^4}\Big), \ \lambda = -\frac{108\pi^2}{N_f^2} - \frac{5184\pi^2}{N_f^3} + O\Big(\frac{1}{N_f^4}\Big) \ . \tag{A.13}$$

Notice that at the tricritical point: $\lambda \sim 1/N_f^2$, while in bQED$_+$: $\lambda \sim 1/N_f$. Similarly, in bQED$_-$: $\lambda, \lambda_{ep} \sim 1/N_f$, while in ep-bQED: $\lambda_{ep} \sim 1/N_f$, $\lambda \sim 1/N_f^2$. This justifies our identification with the four fixed points discussed at large N_f in the main text.

The Fig. A.1 is an example of RG flow and fixed points in the space of quartic couplings.

Figure A.1: RG flow in scalar QED: $N_f = 250,\ e^2 = \frac{48\pi^2}{N_f}\ (\epsilon = 1/2)$.

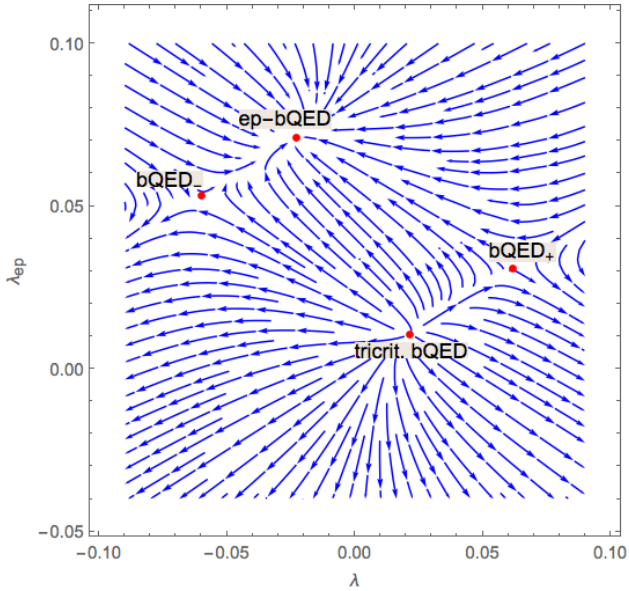

Appendix B

Useful formulae

$$G(x) = \int \frac{d^d p}{(2\pi)^d} e^{-ipx} G(p) \ , \tag{B.1}$$

$$G(p) = \int \frac{d^d x}{1} e^{ipx} G(x) \ , \tag{B.2}$$

$$\frac{1}{|x|^{2\alpha}} = \frac{\Gamma(\frac{d}{2} - \alpha)}{\pi^{\frac{d}{2}} 2^{2\alpha} \Gamma(\alpha)} \int d^d p \frac{e^{-ipx}}{|p|^{d-2\alpha}} \ , \tag{B.3}$$

$$\frac{x_\mu}{|x|^{2(\alpha+1)}} = \frac{\Gamma(\frac{d}{2} - \alpha)}{\pi^{\frac{d}{2}} 2^{2\alpha+1} \alpha \Gamma(\alpha)} \int d^d p \frac{e^{-ipx} i p_\mu}{|p|^{d-2\alpha}} \ , \tag{B.4}$$

$$\int \frac{d^3 q}{(2\pi)^3} \frac{1}{q^2 (q+p)^2} = \frac{1}{8|p|} \ , \tag{B.5}$$

$$\int \frac{d^3 q}{(2\pi)^3} \frac{q_\mu}{q^4 (q+p)^2} = -\frac{p_\mu}{16|p|^3} \ , \tag{B.6}$$

Feynman parametrization:

$$A_1^{\alpha_1}...A_n^{\alpha_n} = \frac{\Gamma\big(\sum\limits_{i=1}^{n}\alpha_i\big)}{\prod\limits_{i=1}^{n}\Gamma\big(\lambda_i\big)}\int_0^1 dx_1...\int_0^1 dx_n \frac{\delta\big(\sum\limits_{i=1}^{n}x_i-1\big)\prod\limits_{i=1}^{n}x_i^{\lambda_i-1}}{\Big[\sum\limits_{i=1}^{n}A_i x_i\Big]^{\sum\lambda_i}} \ , \tag{B.7}$$

$$\int \frac{d^dq}{(2\pi)^d}\frac{1}{(q-p)^{2\alpha}q^{2\beta}} = \frac{\Gamma(\frac{d}{2}-\alpha)\Gamma(\frac{d}{2}-\beta)\Gamma(\alpha+\beta-\frac{d}{2})}{(4\pi)^{d/2}\Gamma(\alpha)\Gamma(\beta)\Gamma(d-\alpha-\beta)}p^{d-2\alpha-2\beta} \ , \tag{B.8}$$

$$\int \frac{d^dq}{(2\pi)^d}\frac{1}{(q^2+\tau)^{\alpha}q^{2\beta}} = \frac{\Gamma(\alpha+\beta-\frac{d}{2})\Gamma(\frac{d}{2}-\beta)}{(4\pi)^{d/2}\Gamma(\alpha)\Gamma(\frac{d}{2})}\tau^{d/2-\alpha-\beta} \ , \tag{B.9}$$

$$\int \frac{d^dq}{(2\pi)^d}f(q^2)q_\mu q_\nu = \frac{\delta_{\mu\nu}}{d}\int \frac{d^dq}{(2\pi)^d}f(q^2)q^2 \ , \tag{B.10}$$

$$\int \frac{d^dq}{(2\pi)^d}f(q^2)q_\mu q_\nu q_\rho q_\sigma = \frac{\delta_{\mu\nu}\delta_{\rho\sigma}+\delta_{\mu\rho}\delta_{\nu\sigma}+\delta_{\mu\sigma}\delta_{\nu\rho}}{d(d+2)}\int \frac{d^dq}{(2\pi)^d}f(q^2)q^4 \ . \tag{B.11}$$

Appendix C

Feynman graphs

In this appendix we give some examples of computation of the Feynman diagrams, using an approach similar for instance to [81]. We read the graphs using position space Feynman rules, then we identify the region from where UV logarithmic divergences appear.

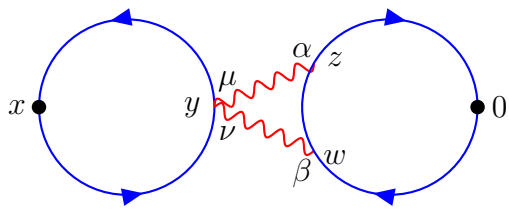

Figure C.1: Symmetry factor is 4 .

The Feynman graph (C.1) using the Feynman rules (2.1) can be read as follows

$$\text{Graph } (C.1) = 4N_f \int d^3y d^3z d^3w \Big(\frac{1}{4\pi|x-y|}\Big)^2 (-\delta_{\mu\nu}) \frac{8\delta_{\mu\alpha}}{N_f\pi^2|y-z|^2} \frac{8\delta_{\nu\beta}}{N_f\pi^2|y-w|^2} \times \Big[\frac{1}{4\pi|w|} i\overleftrightarrow{\partial}^w_\beta \frac{1}{4\pi|w-z|} i\overleftrightarrow{\partial}^z_\alpha \frac{1}{4\pi|z|}\Big] \,. \tag{C.1}$$

where the 4 is the symmetry factor of the graph (C.1). Each blue loop in the graph gives a factor N_f, and since we normalized singlet bilinear operator as follows $\frac{1}{\sqrt{N_f}}\sum_{i=1}^{N_f}|\Phi_i|^2$ we also get a factor $1/N_f$. After cancelation we obtain the factor N_f in (C.1). Also we choose to work in the $\xi = 0$ gauge since the graph (C.1) turns to be independent from the choice of the gauge parameter.

The logarithmic divergences come from the region where y, z, w are close to 0.

$$\text{Graph } (C.1) = \frac{4N_f}{(4\pi|x|)^2}\int d^3y d^3z d^3w \frac{8}{N_f\pi^2|y-z|^2}\frac{8}{N_f\pi^2|y-w|^2}\Big[\frac{1}{4\pi|w|}i\overleftrightarrow{\partial}^w_\mu \frac{1}{4\pi|w-z|}i\overleftrightarrow{\partial}^z_\mu \frac{1}{4\pi|z|}\Big]$$
$$= -\frac{4N_f}{(4\pi|x|)^2}\Big(\frac{16}{N_f}\Big)^2\int\frac{d^3p}{(2\pi)^3}\int\frac{d^3q}{(2\pi)^3}\frac{(p+q)^2}{p^4q^2(q-p)^2}\ , \tag{C.2}$$

where in the last line we performed Fourier transformation (B.1, B.2, B.3) to pass to the momentum space. First we perform integration over momentum p using formulas (B.5, B.6) and we obtain

$$\text{Graph } (C.1) = -\frac{4N_f}{(4\pi|x|)^2}\Big(\frac{16}{N_f}\Big)^2\int\frac{d^3q}{(2\pi)^3}\frac{1}{4|q|^3}\ . \tag{C.3}$$

The integral over q is logarithmically divergent. We regularize it by putting a UV cut-off Λ. The final result is

$$\text{Graph } (C.1) = 4\times\frac{-16\log(x^2\Lambda^2)}{\pi^2N_f}\Big(\frac{1}{4\pi|x|}\Big)^2\ . \tag{C.4}$$

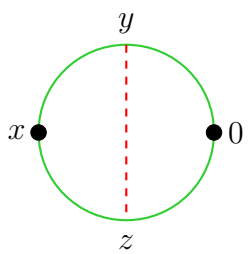

Figure C.2: Symmetry factor is 1 .

The Feynman graph (C.2) corresponds to the following expression

$$\text{Graph } (C.2) = -\int d^3y d^3z \mathrm{Tr}\Big[\frac{\not{z}-\not{y}}{4\pi|\mathrm{x}-\mathrm{y}|^3}\frac{\not{y}}{4\pi|\mathrm{y}|^3}\frac{-\not{z}}{4\pi|\mathrm{z}|^3}\frac{\not{z}-\not{x}}{4\pi|\mathrm{z}-\mathrm{x}|^3}\Big]\frac{4}{\pi^2\mathrm{N_f}|\mathrm{y}-\mathrm{z}|^2}\ . \tag{C.5}$$

Where the minus sign stands for the fermion loop. The logarithmic divergence of the integral (C.5) comes from the regions where y, z are close either to 0 or to x. We will consider the region y, z close to 0 and multiply the answer by 2, since the other region gives the same contribution.

$$\text{Graph } (C.2) = -2\Big(\frac{\not{x}}{4\pi|x|^3}\Big)^2\int d^3y d^3z \mathrm{Tr}\Big[\frac{\not{y}}{4\pi|\mathrm{y}|^3}\frac{\not{z}}{4\pi|\mathrm{z}|^3}\Big]\frac{4}{\pi^2\mathrm{N_f}|\mathrm{y}-\mathrm{z}|^2}\ . \tag{C.6}$$

Now we pass to the momentum space using (B.1, B.2, B.3, B.4).

$$\text{Graph } (C.2) = -2\Big(\frac{\not{x}}{4\pi|x|^3}\Big)^2\int\frac{d^3p}{(2\pi)^3}\mathrm{Tr}\Big[\frac{\mathrm{i}\not{p}}{\mathrm{p}^2}\frac{-\mathrm{i}\not{p}}{\mathrm{p}^2}\Big]\frac{8}{\mathrm{N_f}|\mathrm{p}|}\ . \tag{C.7}$$

This integral is logarithmically divergent. We regularize with a UV cutoff Λ .

$$\text{Graph } (C.2) = \frac{4\log x^2\Lambda^2}{\pi^2 N_f} \times 2\Big(\frac{\not{x}}{4\pi|x|^3}\Big)^2 . \tag{C.8}$$

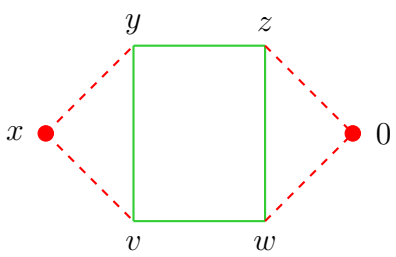

Figure C.3: Symmetry factor is 4.

Using the Feynman rules we can read the graph (C.3) as follows

$$\begin{aligned}\text{Graph } (C.3) = -4N_f \int d^3y d^3z d^3w d^3v \frac{4}{\pi^2 N_f|x-y|^2}\frac{4}{\pi^2 N_f|x-v|^2} \\ \times \mathrm{Tr}\Big[\frac{(\not{y}-\not{z})}{4\pi|\mathrm{y}-\mathrm{z}|^3}\frac{(\not{z}-\not{w})}{4\pi|\mathrm{z}-\mathrm{w}|^3}\frac{(\not{w}-\not{v})}{4\pi|\mathrm{w}-\mathrm{v}|^3}\frac{(\not{v}-\not{y})}{4\pi|\mathrm{v}-\mathrm{y}|^3}\Big]\frac{4}{\pi^2\mathrm{N_f}|\mathrm{z}^2|}\frac{4}{\pi^2\mathrm{N_f}|\mathrm{w}^2|} .\end{aligned} \tag{C.9}$$

The minus stands for the fermion (green) loop in (C.3), factor N_f comes from summing over the number of fermion flavors in the same loop, 4 is the symmetry factor of the graph. The logarithmic divergences of the integral (C.9) come from the regions where y, z, v, w are close either to 0 or to x. Let us inspect the region y, z, v, w close to 0 and multiply the answer by 2, since it is obvious that the other region gives the same logarithmic divergence.

$$\begin{aligned}\text{Graph } (C.3) =& 2 \times (-4N_f)\Big(\frac{4}{\pi^2 N_f|x^2|}\Big)^2 \int d^3y d^3z d^3w d^3v \frac{4}{\pi^2 N_f|z|^2}\frac{4}{\pi^2 N_f|w|^2} \\ &\times \mathrm{Tr}\Big[\frac{(\not{y}-\not{z})}{4\pi|\mathrm{y}-\mathrm{z}|^3}\frac{(\not{z}-\not{w})}{4\pi|\mathrm{z}-\mathrm{w}|^3}\frac{(\not{w}-\not{v})}{4\pi|\mathrm{w}-\mathrm{v}|^3}\frac{(\not{v}-\not{y})}{4\pi|\mathrm{v}-\mathrm{y}|^3}\Big] .\end{aligned} \tag{C.10}$$

Now using (B.1, B.2, B.3, B.4) we perform a Fourier transformation to the momentum space.

$$\text{Graph } (C.3) = 2\Big(\frac{4}{\pi^2 N_f|x^2|}\Big)^2 \times \frac{-8^2\cdot 4}{N_f}\int\frac{d^3p}{(2\pi)^3}\int\frac{d^3q}{(2\pi)^3}\frac{2q(p+q)}{p^2q^2(p+q)^4} . \tag{C.11}$$

First one performs integral over the momentum q

$$\text{Graph } (C.3) = 2\Big(\frac{4}{\pi^2 N_f|x^2|}\Big)^2 \times \frac{-8^2\cdot 4}{N_f}\int\frac{d^3p}{(2\pi)^3}\frac{1}{8|p|^3} . \tag{C.12}$$

The integral over p is logarithmically divergent. We regularize it by putting a UV cutoff Λ and perform integration over the p. The final answer is

$$\text{Graph } (C.3) = \frac{-8\log x^2\Lambda^2}{\pi^2 N_f} \times 2\Big(\frac{4}{\pi^2 N_f|x^2|}\Big)^2 . \tag{C.13}$$

Appendix D

Scaling dimensions of monopole operators in $\mathcal{N} = 1$ SQED

The scaling dimensions of the monopole operators $\mathfrak{M}^{2q}$ with topological charge $2q$ ($2q$ is an integer) in $\mathcal{N} = 1$ SQED, at the leading order in the large N_f expansion, have been computed in [14]. We use formula 2.59 of [14]

$$\frac{\Delta[\mathfrak{M}^{2q}]}{N_f} = \sum_{j \geq q-1/2} (2j+1)\sqrt{(j+1/2)^2 - q^2} - \widehat{\sum_{j \geq q-1/2}} (2j+1)\sqrt{(j+1/2)^2 - q^2} \ . \tag{D.1}$$

where in the first sum $j \geq q - 1/2$ runs over the values for which $(j - q)$ is a non-negative integer, while in the second sum $j \geq q - 1/2$ runs over the values for which $(j - q - 1/2)$ is a non-negative integer. Both sums are divergent, since for large values of j the expressions under the sum scale like j^2. We follow the approach of [14] to regularize the sums and extract the scaling dimensions of monopole operators. First we shift the power of the energy mode as follows

$$\Big((j+1/2)^2 - q^2\Big)^{\frac{1}{2}} \to \Big((j+1/2)^2 - q^2\Big)^{\frac{1}{2}-s} \ . \tag{D.2}$$

It is clear that by choosing large values for s one makes the sum (D.1) convergent. Next we add and subtract quantities that are divergent when $s=0$

$$\begin{aligned}\frac{\Delta[\mathfrak{M}^{2q}]}{N_f} =& \lim_{s\to 0}\sum_{j\geq q-1/2}\big[(2j+1)\big((j+1/2)^2-q^2\big)^{\frac{1}{2}-s}-2(j+1/2)^{2-2s}+q^2(1-2s)(j+1/2)^{-2s}\big]\\ &-\lim_{s\to 0}\sum_{j\geq q-1/2}\big[-2(j+1/2)^{2-2s}+q^2(1-2s)(j+1/2)^{-2s}\big]\\ &-\lim_{s\to 0}\widehat{\sum_{j\geq q-1/2}}\big[(2j+1)\big((j+1/2)^2-q^2\big)^{\frac{1}{2}-s}-2(j+1/2)^{2-2s}+q^2(1-2s)(j+1/2)^{-2s}\big]\\ &+\lim_{s\to 0}\widehat{\sum_{j\geq q-1/2}}\big[-2(j+1/2)^{2-2s}+q^2(1-2s)(j+1/2)^{-2s}\big]\ . \end{aligned} \tag{D.3}$$

Notice that the first and the third lines of (D.3) are convergent, this is true since for large values of j the expressions under sum scale like $1/j^2$. One can evaluate them in the limit $s\to 0$ numerically. The second and forth lines are divergent and one needs to regularise them using zeta functions. Finally we obtain

$$\begin{aligned}\frac{\Delta[\mathfrak{M}^{2q}]}{N_f} =& \sum_{j\geq q-1/2}\big[(2j+1)\sqrt{(j+1/2)^2-q^2}-2(j+1/2)^2+q^2\big]+\frac{q(1+2q^2)}{6}\\ &-\widehat{\sum}_{j\geq q-1/2}\big[(2j+1)\sqrt{(j+1/2)^2-q^2}-2(j+1/2)^2+q^2\big]-\frac{q(q+2)(2q-1)}{6}\ . \end{aligned} \tag{D.4}$$

Using (D.4) one evaluates scaling dimensions of monopole operators with charges $(\pm1,\pm2,\pm3,\pm4)$ as follows

$$\frac{\Delta[\mathfrak{M}^{\pm1}]}{N_f} = 0.3619 + O(1/N_f)\ , \tag{D.5}$$

$$\frac{\Delta[\mathfrak{M}^{\pm2}]}{N_f} = 0.8996 + O(1/N_f)\ , \tag{D.6}$$

$$\frac{\Delta[\mathfrak{M}^{\pm3}]}{N_f} = 1.5708 + O(1/N_f)\ , \tag{D.7}$$

$$\frac{\Delta[\mathfrak{M}^{\pm4}]}{N_f} = 2.3534 + O(1/N_f)\ . \tag{D.8}$$

Bibliography

[1] T. Senthil, A. Vishwanath, L. Balents, S. Sachdev, M.P.A. Fisher, “”Deconfined” quantum critical points,” Science 303, 1490 (2004) doi:10.1126/science.1091806 [arXiv:cond-mat/0311326 [cond-mat.str-el]].

[2] T. Senthil, L. Balents, S. Sachdev, A. Vishwanath, and M.P. A. Fisher, “Quantum criticality beyond the Landau-Ginzburg-Wilson paradigm,” Phys. Rev. B 70, 144407 doi:10.1103/PhysRevB.70.144407 [arXiv:cond-mat/0312617 [cond-mat.str-el]].

[3] O. I. Motrunich and A. Vishwanath, “Emergent photons and new transitions in the O(3) sigma model with hedgehog suppression,” Phys. Rev. B **70** (2004) 075104 doi:10.1103/PhysRevB.70.075104 [cond-mat/0311222].

[4] M. Franz, Z. Tesanovic and O. Vafek, “QED(3) theory of pairing pseudogap in cuprates. 1. From D wave superconductor to antiferromagnet via ’algebraic’ Fermi liquid,” Phys. Rev. B **66** (2002) 054535 doi:10.1103/PhysRevB.66.054535 [cond-mat/0203333].

[5] I. F. Herbut, “QED(3) theory of underdoped high temperature superconductors,” Phys. Rev. B **66** (2002) 094504 doi:10.1103/PhysRevB.66.094504 [cond-mat/0202491].

[6] S. Benvenuti and H. Khachatryan, “QED’s in 2+1 dimensions: complex fixed points and dualities,” arXiv:1812.01544 [hep-th].

[7] A. Karch and D. Tong, “Particle-Vortex Duality from 3d Bosonization,” Phys. Rev. X **6**, no. 3, 031043 (2016) doi:10.1103/PhysRevX.6.031043 [arXiv:1606.01893 [hep-th]].

[8] C. Wang, A. Nahum, M. A. Metlitski, C. Xu and T. Senthil, “Deconfined quantum critical points: symmetries and dualities,” Phys. Rev. X **7**, no. 3, 031051 (2017) doi:10.1103/PhysRevX.7.031051 [arXiv:1703.02426 [cond-mat.str-el]].

[9] I. R. Klebanov, S. S. Pufu, S. Sachdev and B. R. Safdi, “Entanglement Entropy of 3-d Conformal Gauge Theories with Many Flavors,” JHEP **1205**, 036 (2012) doi:10.1007/JHEP05(2012)036 [arXiv:1112.5342 [hep-th]].

[10] S. S. Pufu, "Anomalous dimensions of monopole operators in three-dimensional quantum electrodynamics," Phys. Rev. D **89**, no. 6, 065016 (2014) doi:10.1103/PhysRevD.89.065016 [arXiv:1303.6125 [hep-th]].

[11] E. Dyer, M. Mezei, S. S. Pufu and S. Sachdev, "Scaling dimensions of monopole operators in the $\mathbb{CP}^{N_b-1}$ theory in 2 + 1 dimensions," JHEP **1506**, 037 (2015) Erratum: [JHEP **1603**, 111 (2016)] doi:10.1007/JHEP03(2016)111, 10.1007/JHEP06(2015)037 [arXiv:1504.00368 [hep-th]].

[12] K. Diab, L. Fei, S. Giombi, I. R. Klebanov and G. Tarnopolsky, "On C_J and C_T in the Gross-Neveu and O(N) models," J. Phys. A **49**, no. 40, 405402 (2016) doi:10.1088/1751-8113/49/40/405402 [arXiv:1601.07198 [hep-th]].

[13] S. Giombi, G. Tarnopolsky and I. R. Klebanov, "On C_J and C_T in Conformal QED," JHEP **1608**, 156 (2016) doi:10.1007/JHEP08(2016)156 [arXiv:1602.01076 [hep-th]].

[14] S. M. Chester, L. V. Iliesiu, M. Mezei and S. S. Pufu, "Monopole Operators in $U(1)$ Chern-Simons-Matter Theories," JHEP **1805**, 157 (2018) doi:10.1007/JHEP05(2018)157 [arXiv:1710.00654 [hep-th]].

[15] G. Murthy and S. Sachdev, "Action of Hedgehog Instantons in the Disordered Phase of the (2+1)-dimensional CP^{N-1} Model," Nucl. Phys. B **344**, 557 (1990). doi:10.1016/0550-3213(90)90670-9

[16] V. Borokhov, A. Kapustin and X. k. Wu, "Topological disorder operators in three-dimensional conformal field theory," JHEP **0211**, 049 (2002) doi:10.1088/1126-6708/2002/11/049 [hep-th/0206054].

[17] D. Gaiotto, Z. Komargodski and J. Wu, "Curious Aspects of Three-Dimensional $\mathcal{N} = 1$ SCFTs," JHEP **1808**, 004 (2018) doi:10.1007/JHEP08(2018)004 [arXiv:1804.02018 [hep-th]].

[18] F. Benini and S. Benvenuti, "$N = 1$ QED in 2+1 dimensions: Dualities and enhanced symmetries," arXiv:1804.05707 [hep-th].

[19] A. N. Vasil'ev, Y. M. Pismak and Y. R. Khonkonen, "Simple Method of Calculating the Critical Indices in the $1/N$ Expansion," Theor. Math. Phys. **46** (1981) 104 [Teor. Mat. Fiz. **46** (1981) 157]. doi:10.1007/BF01030844

[20] J. Zinn-Justin, "Quantum Field Theory and Critical Phenomena." Oxford : Clarendon Press,(1996) 1008 p

[21] R. D. Pisarski, "Chiral Symmetry Breaking in Three-Dimensional Electrodynamics," Phys. Rev. D **29**, 2423 (1984). doi:10.1103/PhysRevD.29.2423

[22] T. Appelquist, D. Nash and L. C. R. Wijewardhana, "Critical Behavior in (2+1)-Dimensional QED," Phys. Rev. Lett. **60** (1988) 2575. doi:10.1103/PhysRevLett.60.2575

[23] D. Nash, "Higher Order Corrections in (2+1)-Dimensional QED," Phys. Rev. Lett. **62** (1989) 3024. doi:10.1103/PhysRevLett.62.3024

[24] K. I. Kubota and H. Terao, "Dynamical symmetry breaking in QED(3) from the Wilson RG point of view," Prog. Theor. Phys. **105** (2001) 809 doi:10.1143/PTP.105.809 [hep-ph/0101073].

[25] K. Kaveh and I. F. Herbut, "Chiral symmetry breaking in QED(3) in presence of irrelevant interactions: A Renormalization group study," Phys. Rev. B **71**, 184519 (2005) doi:10.1103/PhysRevB.71.184519 [cond-mat/0411594].

[26] V. P. Gusynin and P. K. Pyatkovskiy, "Critical number of fermions in three-dimensional QED," Phys. Rev. D **94**, no. 12, 125009 (2016) doi:10.1103/PhysRevD.94.125009 [arXiv:1607.08582 [hep-ph]].

[27] A. V. Kotikov, V. I. Shilin and S. Teber, "Critical behavior of (2+1)-dimensional QED: $1/\mathrm{N}_f$ corrections in the Landau gauge," Phys. Rev. D **94** (2016) no.5, 056009 Erratum: [Phys. Rev. D **99** (2019) no.11, 119901] doi:10.1103/PhysRevD.99.119901, 10.1103/PhysRevD.94.056009 [arXiv:1605.01911 [hep-th]].

[28] A. V. Kotikov and S. Teber, "Critical behavior of $(2+1)$-dimensional QED: $1/N_f$ corrections in an arbitrary nonlocal gauge," Phys. Rev. D **94** (2016) no.11, 114011 doi:10.1103/PhysRevD.94.114011 [arXiv:1609.06912 [hep-th]].

[29] A. V. Kotikov and S. Teber, "Addendum to "Critical behaviour of $(2+1)$-dimensional QED: $1/N_f$-corrections in an arbitrary non-local gauge"," arXiv:1902.03790 [hep-th].

[30] I. F. Herbut, "Chiral symmetry breaking in three-dimensional quantum electrodynamics as fixed point annihilation," Phys. Rev. D **94**, no. 2, 025036 (2016) doi:10.1103/PhysRevD.94.025036 [arXiv:1605.09482 [hep-th]].

[31] S. Giombi, I. R. Klebanov and G. Tarnopolsky, "Conformal QED_d, F-Theorem and the ϵ Expansion," J. Phys. A **49**, no. 13, 135403 (2016) doi:10.1088/1751-8113/49/13/135403 [arXiv:1508.06354 [hep-th]].

[32] L. Di Pietro, Z. Komargodski, I. Shamir and E. Stamou, "Quantum Electrodynamics in d=3 from the ϵ-Expansion," Phys. Rev. Lett. **116**, no. 13, 131601 (2016) doi:10.1103/PhysRevLett.116.131601 [arXiv:1508.06278 [hep-th]].

[33] L. Di Pietro and E. Stamou, "Scaling dimensions in QED_3 from the ϵ-expansion," JHEP **1712**, 054 (2017) doi:10.1007/JHEP12(2017)054 [arXiv:1708.03740 [hep-th]].

[34] J. Lou, A.W. Sandvik and N. Kawashima, "Antiferromagnetic to valence-bond-soild transitions in two-dimensional SU(N) Heisenberg models with multi-spin interactions," Phys. Rev. B 80, 180414(R) doi:10.1103/PhysRevB.80.180414 [arXiv:0908.0740 [cond-mat.str-el]].

[35] R. K. Kaul and A. W. Sandvik, "Lattice Model for the SU(N) Nèel to Valence-Bond Solid Quantum Phase Transition at Large N," Phys. Rev. Lett. **108**, no. 13, 137201 (2012) doi:10.1103/PhysRevLett.108.137201 [arXiv:1110.4130 [cond-mat.str-el]].

[36] J. D'Emidio and R. K. Kaul, "New easy-plane $\mathbb{CP}^{N-1}$ fixed points," Phys. Rev. Lett. **118**, no. 18, 187202 (2017) doi:10.1103/PhysRevLett.118.187202 [arXiv:1610.07702 [cond-mat.str-el]].

[37] X. F. Zhang, Y. C. He, S. Eggert, R. Moessner and F. Pollmann, "Continuous Easy-Plane Deconfined Phase Transition on the Kagome Lattice," Phys. Rev. Lett. **120**, no. 11, 115702 (2018) doi:10.1103/PhysRevLett.120.115702 [arXiv:1706.05414 [cond-mat.str-el]].

[38] N. Karthik and R. Narayanan, "Scale-invariance of parity-invariant three-dimensional QED," Phys. Rev. D **94**, no. 6, 065026 (2016) doi:10.1103/PhysRevD.94.065026 [arXiv:1606.04109 [hep-th]].

[39] Y. Nakayama and T. Ohtsuki, "Conformal Bootstrap Dashing Hopes of Emergent Symmetry," Phys. Rev. Lett. **117**, no. 13, 131601 (2016) doi:10.1103/PhysRevLett.117.131601 [arXiv:1602.07295 [cond-mat.str-el]].

[40] D. Simmons-Duffin, unpublished.

[41] L. Iliesiu, talk at Simons Center for Geometry and Physics: "The Nèel-VBA quantum phase transition and the conformal bootstrap", 2018-11-05.

[42] D. Poland, S. Rychkov and A. Vichi, "The Conformal Bootstrap: Theory, Numerical Techniques, and Applications," arXiv:1805.04405 [hep-th].

[43] Z. Li, "Solving QED_3 with Conformal Bootstrap," arXiv:1812.09281 [hep-th].

[44] D. B. Kaplan, J. W. Lee, D. T. Son and M. A. Stephanov, "Conformality Lost," Phys. Rev. D **80** (2009) 125005 doi:10.1103/PhysRevD.80.125005 [arXiv:0905.4752 [hep-th]].

[45] S. Gukov, "RG Flows and Bifurcations," Nucl. Phys. B **919** (2017) 583 doi:10.1016/j.nuclphysb.2017.03.025 [arXiv:1608.06638 [hep-th]].

[46] V. Gorbenko, S. Rychkov and B. Zan, "Walking, Weak first-order transitions, and Complex CFTs," JHEP **1810**, 108 (2018) doi:10.1007/JHEP10(2018)108 [arXiv:1807.11512 [hep-th]].

[47] J. March-Russell, "On the possibility of second order phase transitions in spontaneously broken gauge theories," Phys. Lett. B **296**, 364 (1992) doi:10.1016/0370-2693(92)91333-5 [hep-ph/9208215].

[48] A. Nahum, J. T. Chalker, P. Serna, M. Ortuno and A. M. Somoza, "Deconfined Quantum Criticality, Scaling Violations, and Classical Loop Models," Phys. Rev. X **5**, no. 4, 041048 (2015) doi:10.1103/PhysRevX.5.041048 [arXiv:1506.06798 [cond-mat.str-el]].

[49] A. Nahum, P. Serna, J. T. Chalker, M. Ortuno and A. M. Somoza, "Emergent SO(5) Symmetry at the Nèel to Valence-Bond-Solid Transition," Phys. Rev. Lett. **115**, no. 26, 267203 (2015) doi:10.1103/PhysRevLett.115.267203 [arXiv:1508.06668 [cond-mat.str-el]].

[50] P. Serna and A. Nahum, "Emergence and spontaneous breaking of approximate $O(4)$ symmetry at a weakly first-order deconfined phase transition," arXiv:1805.03759 [cond-mat.str-el].

[51] F. S. Nogueira and A. Sudbo, "Deconfined Quantum Criticality and Conformal Phase Transition in Two-Dimensional Antiferromagnets," EPL **104**, no. 5, 56004 (2013) doi:10.1209/0295-5075/104/56004 [arXiv:1304.4938 [cond-mat.str-el]].

[52] F. Gehring, H. Gies and L. Janssen, "Fixed-point structure of low-dimensional relativistic fermion field theories: Universality classes and emergent symmetry," Phys. Rev. D **92** (2015) no.8, 085046 doi:10.1103/PhysRevD.92.085046 [arXiv:1506.07570 [hep-th]].

[53] Z. Komargodski and N. Seiberg, "A symmetry breaking scenario for QCD_3," JHEP **1801**, 109 (2018) doi:10.1007/JHEP01(2018)109 [arXiv:1706.08755 [hep-th]].

[54] J. Gomis, Z. Komargodski and N. Seiberg, "Phases Of Adjoint QCD_3 And Dualities," SciPost Phys. **5**, 007 (2018) doi:10.21468/SciPostPhys.5.1.007 [arXiv:1710.03258 [hep-th]].

[55] C. Choi, D. Delmastro, J. Gomis and Z. Komargodski, "Dynamics of QCD_3 with Rank-Two Quarks And Duality," arXiv:1810.07720 [hep-th].

[56] B. I. Halperin, T. C. Lubensky and S. K. Ma, "First order phase transitions in superconductors and smectic A liquid crystals," Phys. Rev. Lett. **32** (1974) 292. doi:10.1103/PhysRevLett.32.292

[57] R. Folk, S. Kolnberger "Critical fluctuations in superconductors," Phys. Rev. B **41**, 4083 (1990) doi.org/10.1103/PhysRevB.41.4083

[58] R. Folk, Yu. Holovatch "On the critical fluctuations in superconductors." J. Phys. A: Math. Gen. **29** 3409 (1996) doi:10.1088/0305-4470/29/13/014

[59] R. Folk, Yu. Holovatch " Critical fluctuations in normal-to-superconducting transition," (1998) arXiv:cond-mat/9807421

[60] B. Ihrig, N. Zerf, P. Marquard, I. F. Herbut and M. M. Scherer, "Abelian Higgs model at four loops, fixed-point collision and deconfined criticality," arXiv:1907.08140 [cond-mat.str-el].

[61] P. I. Fomin, V. P. Gusynin and V. A. Miransky, "Vacuum Instability of Massless Electrodynamics and the Gell-mann-low Eigenvalue Condition for the Bare Coupling Constant," Phys. Lett. **78B** (1978) 136. doi:10.1016/0370-2693(78)90366-0

[62] P. I. Fomin, V. P. Gusynin, V. A. Miransky and Y. A. Sitenko, "Dynamical Symmetry Breaking and Particle Mass Generation in Gauge Field Theories," Riv. Nuovo Cim. **6N5** (1983) 1.

[63] V. A. Miransky and K. Yamawaki, "Conformal phase transition in gauge theories," Phys. Rev. D **55** (1997) 5051 Erratum: [Phys. Rev. D **56** (1997) 3768] doi:10.1103/PhysRevD.56.3768, 10.1103/PhysRevD.55.5051 [hep-th/9611142].

[64] I. Herbut, "A Modern Approach to Critical Phenomena," Cambridge University Press, (2007) doi.org/10.1017/CBO9780511755521

[65] L. Fei, S. Giombi and I. R. Klebanov, "Critical $O(N)$ models in $6-\epsilon$ dimensions," Phys. Rev. D **90** (2014) no.2, 025018 doi:10.1103/PhysRevD.90.025018 [arXiv:1404.1094 [hep-th]].

[66] R. Percacci and G. P. Vacca, "Are there scaling solutions in the $O(N)$-models for large N in $d > 4$?," Phys. Rev. D **90** (2014) 107702 doi:10.1103/PhysRevD.90.107702 [arXiv:1405.6622 [hep-th]].

[67] L. Fei, S. Giombi, I. R. Klebanov and G. Tarnopolsky, "Three loop analysis of the critical $O(N)$ models in $6-\epsilon$ dimensions," Phys. Rev. D **91** (2015) no.4, 045011 doi:10.1103/PhysRevD.91.045011 [arXiv:1411.1099 [hep-th]].

[68] J. A. Gracey, "Four loop renormalization of ϕ^3 theory in six dimensions," Phys. Rev. D **92** (2015) no.2, 025012 doi:10.1103/PhysRevD.92.025012 [arXiv:1506.03357 [hep-th]].

[69] S. M. Chester, S. S. Pufu and R. Yacoby, "Bootstrapping $O(N)$ vector models in $4 < d < 6$," Phys. Rev. D **91** (2015) no.8, 086014 doi:10.1103/PhysRevD.91.086014 [arXiv:1412.7746 [hep-th]].

[70] I. F. Herbut and L. Janssen, "Critical $O(2)$ and $O(3)$ ϕ^4 theories near six dimensions," Phys. Rev. D **93** (2016) no.8, 085005 doi:10.1103/PhysRevD.93.085005 [arXiv:1510.05691 [hep-th]].

[71] J. A. Gracey, "Six dimensional QCD at two loops," Phys. Rev. D **93** (2016) no.2, 025025 doi:10.1103/PhysRevD.93.025025 [arXiv:1512.04443 [hep-th]].

[72] J. A. Gracey, I. F. Herbut and D. Roscher, "Tensor $O(N)$ model near six dimensions: fixed points and conformal windows from four loops," Phys. Rev. D **98** (2018) no.9, 096014 doi:10.1103/PhysRevD.98.096014 [arXiv:1810.05721 [hep-th]].

[73] A.N. Vasil'ev, M.Yu. Nalimov, "The CP^{N-1} model: Calculation of anomalous dimensions and the mixing matrices in the order 1/N," Theor. Math. Phys. (1983) 56: 643. https://doi.org/10.1007/BF01027537

[74] S. Hikami, "Renormalization Group Functions of CP^{N-1} Nonlinear Sigma Model and N Component Scalar QED Model," Prog. Theor. Phys. **62** (1979) 226. doi:10.1143/PTP.62.226

[75] R. K. Kaul and S. Sachdev, "Quantum criticality of U(1) gauge theories with fermionic and bosonic matter in two spatial dimensions," Phys. Rev. B **77**, 155105 (2008) doi:10.1103/PhysRevB.77.155105 [arXiv:0801.0723 [cond-mat.str-el]].

[76] L. Janssen and Y. C. He, "Critical behavior of the QED_3-Gross-Neveu model: Duality and deconfined criticality," Phys. Rev. B **96**, no. 20, 205113 (2017) doi:10.1103/PhysRevB.96.205113 [arXiv:1708.02256 [cond-mat.str-el]].

[77] B. Ihrig, L. Janssen, L. N. Mihaila and M. M. Scherer, "Deconfined criticality from the QED_3-Gross-Neveu model at three loops," Phys. Rev. B **98**, no. 11, 115163 (2018) doi:10.1103/PhysRevB.98.115163 [arXiv:1807.04958 [cond-mat.str-el]].

[78] N. Zerf, P. Marquard, R. Boyack and J. Maciejko, "Critical behavior of the QED_3-Gross-Neveu-Yukawa model at four loops," Phys. Rev. B **98**, no. 16, 165125 (2018) doi:10.1103/PhysRevB.98.165125 [arXiv:1808.00549 [cond-mat.str-el]].

[79] J. Braun, H. Gies, L. Janssen and D. Roscher, "Phase structure of many-flavor QED_3," Phys. Rev. D **90**, no. 3, 036002 (2014) doi:10.1103/PhysRevD.90.036002 [arXiv:1404.1362 [hep-ph]].

[80] C. Xu, "Renormalization group studies on four-fermion interaction instabilities on algebraic spin liquids," Phys. Rev. B 78, 054432 doi:10.1103/PhysRevB.78.054432 [arXiv:0803.0794 [hep-th]].

[81] S. M. Chester and S. S. Pufu, "Anomalous dimensions of scalar operators in QED_3," JHEP **1608**, 069 (2016) doi:10.1007/JHEP08(2016)069 [arXiv:1603.05582 [hep-th]].

[82] W. Rantner and X. G. Wen, "Spin correlations in the algebraic spin liquid: Implications for high-Tc superconductors," Phys. Rev. B **66** (2002) 144501. doi:10.1103/PhysRevB.66.144501

[83] M. Hermele, T. Senthil and M. P. A. Fisher, "Algebraic spin liquid as the mother of many competing orders," Phys. Rev. B **72** (2005) no.10, 104404 doi:10.1103/PhysRevB.72.104404 [cond-mat/0502215 [cond-mat.str-el]].

[84] Michael Hermele, T. Senthil, and Matthew P. A. Fisher Phys. Rev. B 76, 149906

[85] R. Boyack, A. Rayyan and J. Maciejko, "Deconfined criticality in the QED_3-Gross-Neveu-Yukawa model: the $1/N$ expansion revisited," arXiv:1812.02720 [cond-mat.str-el].

[86] J. A. Gracey, "Gauged Nambu-Jona-Lasinio model at O(1/N) with and without a Chern-Simons term," Mod. Phys. Lett. A **8**, 2205 (1993) doi:10.1142/S0217732393001938 [hep-th/9306105].

[87] J. A. Gracey, "Critical point analysis of various fermionic field theories in the large N expansion," J. Phys. A **25** (1992) L109.

[88] J. A. Gracey, "Gauge independent critical exponents for QED coupled to a four fermi interaction with and without a Chern-Simons term," Annals Phys. **224** (1993) 275 doi:10.1006/aphy.1993.1047 [hep-th/9301113].

[89] J. A. Gracey, "Fermion bilinear operator critical exponents at $O(1/N^2)$ in the QED-Gross-Neveu universality class," Phys. Rev. D **98**, no. 8, 085012 (2018) doi:10.1103/PhysRevD.98.085012 [arXiv:1808.07697 [hep-th]].

[90] J. A. Gracey, "Electron mass anomalous dimension at O(1/(Nf(2)) in quantum electrodynamics," Phys. Lett. B **317** (1993) 415 doi:10.1016/0370-2693(93)91017-H [hep-th/9309092].

[91] S. J. Gates, M. T. Grisaru, M. Rocek and W. Siegel, "Superspace Or One Thousand and One Lessons in Supersymmetry," Front. Phys. **58** (1983) 1 [hep-th/0108200].

[92] K. A. Intriligator and N. Seiberg, "Mirror symmetry in three-dimensional gauge theories," Phys. Lett. B **387** (1996) 513 doi:10.1016/0370-2693(96)01088-X [hep-th/9607207].

[93] A. Kapustin and M. J. Strassler, "On mirror symmetry in three-dimensional Abelian gauge theories," JHEP **9904** (1999) 021 doi:10.1088/1126-6708/1999/04/021 [hep-th/9902033].

[94] M. Gremm and E. Katz, "Mirror symmetry for N=1 QED in three-dimensions," JHEP **0002** (2000) 008 doi:10.1088/1126-6708/2000/02/008 [hep-th/9906020].

[95] J. A. Gracey, "Critical Exponents for the Supersymmetric σ Model," J. Phys. A **23** (1990) 2183.

[96] F. Benini and S. Benvenuti, "$\mathcal{N} = 1$ dualities in 2+1 dimensions," JHEP **1811** (2018) 197 doi:10.1007/JHEP11(2018)197 [arXiv:1803.01784 [hep-th]].

[97] F. Kos, D. Poland, D. Simmons-Duffin and A. Vichi, "Precision Islands in the Ising and $O(N)$ Models," JHEP **1608** (2016) 036 doi:10.1007/JHEP08(2016)036 [arXiv:1603.04436 [hep-th]].

[98] P. Calabrese, A. Pelissetto and E. Vicari, "Multicritical phenomena in O(n(1)) + O(n(2)) symmetric theories," Phys. Rev. B **67**, 054505 (2003) doi:10.1103/PhysRevB.67.054505 [cond-mat/0209580].

[99] K. Chen, Y. Huang, Y. Deng, A. B. Kuklov, N. V. Prokof'ev and B. V. Svistunov, "Deconfined criticality flow in the Heisenberg model with ring-exchange interactions," Phys. Rev. Lett. **110** (2013) no.18, 185701 doi:10.1103/PhysRevLett.110.185701 [arXiv:1301.3136 [cond-mat.str-el]].

[100] S. Benvenuti and H. Khachatryan, "Easy-plane QED_3's in the large N_f limit," JHEP **1905** (2019) 214 doi:10.1007/JHEP05(2019)214 [arXiv:1902.05767 [hep-th]].

[101] O. Aharony, S. Jain and S. Minwalla, "Flows, Fixed Points and Duality in Chern-Simons-matter theories," JHEP **1812** (2018) 058 doi:10.1007/JHEP12(2018)058 [arXiv:1808.03317 [hep-th]].

[102] A. Dey, I. Halder, S. Jain, L. Janagal, S. Minwalla and N. Prabhakar, "Duality and an exact Landau-Ginzburg potential for quasi-bosonic Chern-Simons-Matter theories," JHEP **1811**, 020 (2018) doi:10.1007/JHEP11(2018)020 [arXiv:1808.04415 [hep-th]].

[103] A. N. Vasil'ev and M. Y. Nalimov, "Analog of Dimensional Regularization for Calculation of the Renormalization Group Functions in the 1/n Expansion for Arbitrary Dimension of Space," Theor. Math. Phys. **55** (1983) 423 [Teor. Mat. Fiz. **55** (1983) 163]. doi:10.1007/BF01015800

[104] A. A. Vladimirov, "Method for Computing Renormalization Group Functions in Dimensional Renormalization Scheme," Theor. Math. Phys. **43** (1980) 417 [Teor. Mat. Fiz. **43** (1980) 210]. doi:10.1007/BF01018394

[105] A. N. Vasil'ev, "The field theoretic renormalization group in critical behavior theory and stochastic dynamics," Boca Raton, USA: Chapman and Hall/CRC (2004) 681 p

[106] M. E. Machacek and M. T. Vaughn, "Two Loop Renormalization Group Equations in a General Quantum Field Theory. 1. Wave Function Renormalization," Nucl. Phys. B **222** (1983) 83. doi:10.1016/0550-3213(83)90610-7

[107] M. E. Machacek and M. T. Vaughn, "Two Loop Renormalization Group Equations in a General Quantum Field Theory. 3. Scalar Quartic Couplings," Nucl. Phys. B **249** (1985) 70. doi:10.1016/0550-3213(85)90040-9

Acknowledgements

I would like to thank my supervisor Francesco Benini for useful advice and support. I also acknowledge many useful discussions we had, which helped me to better understand various concepts and ideas in physics. I would like to thank Sergio Benvenuti, for introducing me into the research field of the present thesis and for close collaboration. I was very happy to work with him. I also thank to Vladimir Bashmakov for the interesting project we are working on together. I learnt a lot from discussions with him.

I would like to thank my thesis referees Silviu Pufu and Sofian Teber for careful reading of the manuscript, for useful questions and suggestions.

I would like to thank my friends Rodrigo de Leon Ardon, Riccardo Bergamin, Alessandro Davoli, Marco Gorghetto, Carlos Nieto Guerrero, Paolo Milan, Ui Ri Mun, Mihael Petac, Elena Venturini, Jiaxin Wang.

Finally, I would like to express my gratitude to my family for their love, encouragement and support. These years would have been much harder without your help.